Late Holocene changes in sea-surface conditions in the North Water Polynya, northern Baffin Bay, using organic-walled dinoflagellate cysts

by

Kelsey Amber Koerner

Bachelors of Earth Sciences (Hons.), 2018

A Thesis Submitted in Partial Fulfillment
of the Requirements for the Degree of

Master of Science

in the Graduate Academic Unit of Earth Sciences

Supervisor: A. Limoges, Ph.D., Department of Earth Sciences

Supervisory committee:
N. Van Nieuwenhove, Ph.D., Department of Earth Sciences
D. Keighley, Ph.D., Department of Earth Sciences

Examining Board:
C. McFarlane, Ph.D., Department of Earth Sciences
L. Cwynar, Ph.D., Department of Biology, UNB

This thesis is accepted by the
Dean of Graduate Studies

THE UNIVERSITY OF NEW BRUNSWICK

August, 2020

©Kelsey Amber Koerner, 2020

Abstract

The North Water (NOW) polynya, located in northern Baffin Bay, is the largest recurrent polynya in the Arctic. This area of open water or low sea-ice concentrations in a region otherwise characterized by high sea-ice concentrations fosters primary production that helps sustain a large and diverse food web and provides resources to the surrounding human communities. The NOW owes its formation to i) the presence of ice arches in Nares Strait that define its northern boundary, ii) strong northerly winds that blow newly formed sea ice southward out of the polynya region, and iii) the upwelling of relatively warm water masses. Due to recent climate warming and Arctic amplification, the factors promoting the formation of the polynya are changing rapidly. This is notably evident from the recent observed instability of the Nares Strait ice arches. This thesis aims to understand the long-term sea-surface variability of the NOW polynya using dinoflagellate cyst (dinocyst) assemblages from a marine record spanning the last ca. 3800 years, and also compares the natural variability of the polynya's dinocyst composition and fluxes to recent (last ca. 60 years) changes.

Our results infer relatively gradual changes to the NOW polynya between ca. 3800 and 156 years BP associated with a general sea-surface cooling trend. However, between ca. 1965 and 2015 there is a shift to higher contributions of autotrophic taxa and one to two orders of magnitude higher dinoflagellate cyst fluxes, suggesting a rapid shift to more stratified and open water conditions as a result of increased cryospheric melt associated with Arctic amplification. Climate projections in the Arctic indicate continued cryospheric melt into the future, which will continue to impact the polynya and its formation factors, likely leading to a seasonally open gateway between the Artic and northern Baffin Bay.

Acknowledgements

This thesis was not possible without the collaborative effort of many hard-working people in Canada and Europe. Dr. Audrey Limoges, thank you for your guidance and consistent support over the last two years. Dr. Nicolas Van Nieuwenhove, thank you for all the laughs in the lab and additional help with the ever complex dinocyst taxonomy. Dr. Sofia Ribeiro, thank you for the "long-distance" discussions and helpful comments throughout this project. To my lab-mates Josh Evans and Liam MacNeil, thank you for all the conversations (paleoenvironmental or not) and help over the last two years. Everyone wishes for a great research group and we are lucky enough to have it.

To the Department of Earth Sciences at UNB, thank you for all the memories. You have become my second family and taught me a lot about the world both in academia and in life. I also want to thank my parents Michele Koerner and Allan Dietrich, my friends and family for your patience and support. Finally, I want to thank Brandon Walzak, your steadfast patience, support, and advice was a major pillar during these last two years.

Table of Contents

Abstract ..... **ii**

Acknowledgements ..... **iii**

Table of Contents ..... **iv**

List of Tables ..... **vii**

List of Figures ..... **viii**

List of Abbreviations ..... **x**

Chapter 1. Introduction **1**

1.1 Arctic Climate 1

1.2 Arctic Sea Ice 1

1.3 Atmospheric Forcing 3

1.3.1 The North Atlantic and Arctic Oscillations 4

1.3.2 Atmosphere-ocean forcing 4

1.4 Arctic Ocean Circulation 6

1.5 The North Water (NOW) Polynya 7

1.5.1 Regional Setting and Formation 7

1.5.2 Oceanography of the NOW 9

1.5.3 Primary Production and Ecosystem Services in the NOW 11

1.6 Arctic Holocene Climate Variability 12

1.7 Dinoflagellates and the Modern Analogue Technique 14

1.7.1 Dinoflagellates and Dinoflagellate cysts (Dinocysts) 14

1.7.2 The Modern Analogue Technique 16

1.8 Previous Work and Thesis Objectives 18

1.9 Statement of Contributions to Research and Writing 19

1.10 References 21

Chapter 2. Late Holocene sea-surface changes in the North Water Polynya (northern Baffin Bay) inferred from organic-walled dinoflagellate cyst records 35

2.1 Abstract 36

2.2 Introduction 37

2.3 Oceanographic Setting 41

2.4 Methods 42

2.4.1 Geochronology 42

2.4.2 Dinoflagellate Cysts 44

2.4.3 Modern Analogue Technique 45

2.4.4 Modern Analogue Index 46

2.5 Results 48

2.6 Discussion 57

2.6.1 MAT Indices 57

2.6.2 Late Holocene changes in sea surface conditions in the NOW 59

2.6.3 The NOW and recent climate changes 67

2.7 Conclusions 68

2.8 Acknowledgements 69

2.9 References 70

Chapter 3. Discussion and Conclusions 86

3.1 Discussion 86

3.2 Issues and Future Work 87

3.3 References 89

Appendix I: Additional Statistical Analysis and Palynomorph Counts 90

I-I STATCOUNTS 90

I-II Principal component analysis 90

I-III Dinocyst Counts 92

I-IV Palynomorphs Counted 128

I-V MAT Summer Reconstructions 132

I-VI References 134

Curriculum Vitae

List of Tables

Table 2.1 The main (> 1%) dinocyst taxa observed in this study. 50

Table I-1 The principal components (PC) and their associated eigenvalue and percent variance. 91

Table I-2 Raw Dinocyst Counts from AMD15-Casq1-BC4 and AMD15-Casq1. All ages are in Years BP. 92

Table I-3 Counted Lycopodium clavatum *marker grains, foraminiferal linings and specimens of* Halodinium *spp. in BC4 and Casq1* 128

List of Figures

Figure 1.1 A map of the Arctic showing the average sea-ice extent between 1979 to 2000 for September and March (Serreze et al., 2007). 2

Figure 1.2 Surface (light grey) and deep (black) ocean currents in the Arctic Ocean (modified from Jones, 2001). 3

Figure 1.3 Map showing a simplified representation of the surface circulation in the Arctic Ocean during positive and negative Arctic Oscillation (AO) phases, respectively (modified after Steele et al., 2004 and Georgiadis et al., 2020). 5

Figure 1.4 Map showing the main surface ocean currents and location of the NOW polynya (Satellite image from EOSDIS Worldview). 8

Figure 1.5 The dinoflagellate life cycle. From Bravo & Figueroa (2014). 15

Figure 1.6 Dinocyst taxa and their relative sensitivity to oxidation (from de Vernal & Marret, 2007; Zonneveld et al., 2008) 16

Figure 1.7 The current distribution of MAT analogues (n = 1968) (de Vernal et al., 2020). 17

Figure 2.1 Map of Baffin Bay with the main oceanic currents and satellite images of the NOW (left) and NEW (right) polynyas from EOSDIS Worldview 38

Figure 2.2 a) Box core plan view showing the coring locations of AMD15-Casq1-BC1 (brown) and AMD15-Casq1-BC4 (grey) b) *Composite age model for core AMD15-Casq1 including BC4.* 43

Figure 2.3 The locations of the MAT analogues (in red) based on the dinocyst assemblages from AMD15-Casq1 and BC4. 47

Figure 2.4 Micrographs of selected organic-walled microfossils observed in the sediment core AMD15-Casq1 51

Figure 2.5 Micrographs of selected cysts produced by autotrophic dinoflagellates observed in the sediment core AMD15-Casq1..... 52

Figure 2.6 Relative abundances of the main taxa counted in our marine records, also showing the Bray-Curtis Similarity Index for the assemblages...... 53

Figure 2.7 Fluxes of the main dinocyst taxa and palynomorphs counted in our marine records 54

Figure 2.8 Evolution of the MAT index 5-point moving average in Casq1 and BC4..... 55

*Figure 2.9 The MAT index 5-point moving average, A/H ratio, total dinocyst fluxes, cold water taxa (*Islandinium minutum, Islandinium*?* cezare, Echinidinium karaense*) (Head et al., 2001), and Agassiz* $\delta^{18}O$ *temperature reconstruction (Lecavalier et al., 2017)*..... 61

Figure I-1 The broken stick model, where the intersection between the red and blue curves indicates the number of meaningful components. 91

Figure I-2 MAT reconstructed sea-surface salinity through time 132

Figure I-3 MAT reconstructed sea-surface temperature through time.. 132

Figure I-4 MAT reconstructed sea ice concentration through time 133

List of Abbreviations

A = Autotroph

AMS = Accelerator Mass Spectrometry

AO = Arctic Oscillation

BC = Baffin Current

BCE = Before Common Era

BP = Before Present (1950)

CASQ = Calypso Square

CCGS = Canadian Coast Guard Ship

CE = Common Era

CRS = Constant Rate of Supply

DA = Dark Ages

EGC = East Greenland Current

EOSDIS = Earth Observing System Data and Information System

H = Heterotroph

HCl = Hydrochloric acid

HF = Hydrofluoric acid

IC = Irminger Current

LC = Labrador Current

LIA = Little Ice Age

MAT = Modern Analogue Technique

MCA = Medieval Climate Anomaly

NAO = North Atlantic Oscillation

NEW = Northeast Water Polynya

NOW = North Water Polynya

PCA = Principal Component Analysis

PSU = Practical Salinity Unit

RWP = Roman Warm Period

TPD = Transpolar Drift Stream

UNB = University of New Brunswick

UPGMA = Unweighted Pair Group Average

WGC = West Greenland Current

Chapter 1. Introduction

1.1 Arctic Climate

The Arctic is sensitive to climate variations and is currently warming twice as fast as the global average rate (IPCC, 2014) induced by a phenomenon known as Arctic amplification (Screen & Simmonds, 2010). This unprecedented change over the last ca. 50 years already has global impacts (e.g., decreased sea-ice minimum, sea-level rise, increased storm frequency, etc.) but the future extent and severity of the changes are difficult to predict. To help understand how the Arctic will respond to future climate changes, it is valuable to (1) understand the Arctic's response to past climatic changes, (2) identify potential past analogues, and (3) discriminate between the natural variability and human-influenced (anthropogenic) changes. The main factors controlling the local and regional Arctic climate will now be discussed.

1.2 Arctic Sea Ice

Arctic sea ice is a defining feature of the Arctic Ocean. The maximum extent of Arctic sea-ice generally occurs around March, while the minimum is typically reached in September (Serreze et al., 2007; Fig. 1.1). The sea ice is an important regulator of climate in the Arctic through increased albedo that reflects solar radiation back to the atmosphere (Curry et al., 1995), reduction of ocean-atmosphere exchange of heat and gases (Kurtz et al., 2011), and through brine rejections that act as carbon sink and facilitate deep-water formation (Nguyen et al., 2009).

In the last 40 years, the sea-ice minimum extent has decreased rapidly (Serreze et al., 2007; Fig. 1.1), with extensive impacts on Arctic and global climate (e.g., IPCC, 2014). During the summer, ice and meltwater are exported from the Arctic Ocean via Fram Strait along eastern Greenland, through the Canadian Arctic Archipelago, and Nares Strait into northern Baffin Bay (Fig. 1.2). Northern Baffin Bay is the location of the study site for this thesis, so the increased export of Arctic freshwater into northern Baffin Bay has important ecological and climate implications for the region, which are discussed further in section 1.5.

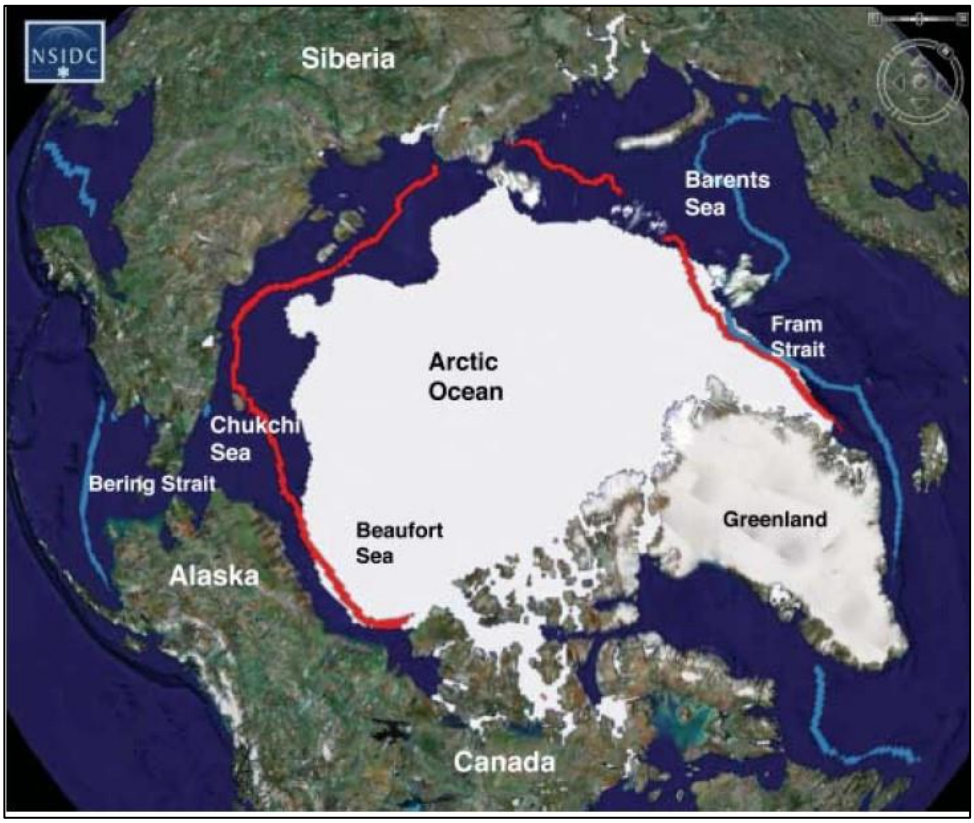


Figure 1.1 A map of the Arctic showing the average sea-ice extent for September 2005 (in white). The red line represents the median September sea-ice extent between 1979 to 2000, and the blue line represents the median March sea-ice extent for the same interval (Serreze et al., 2007).

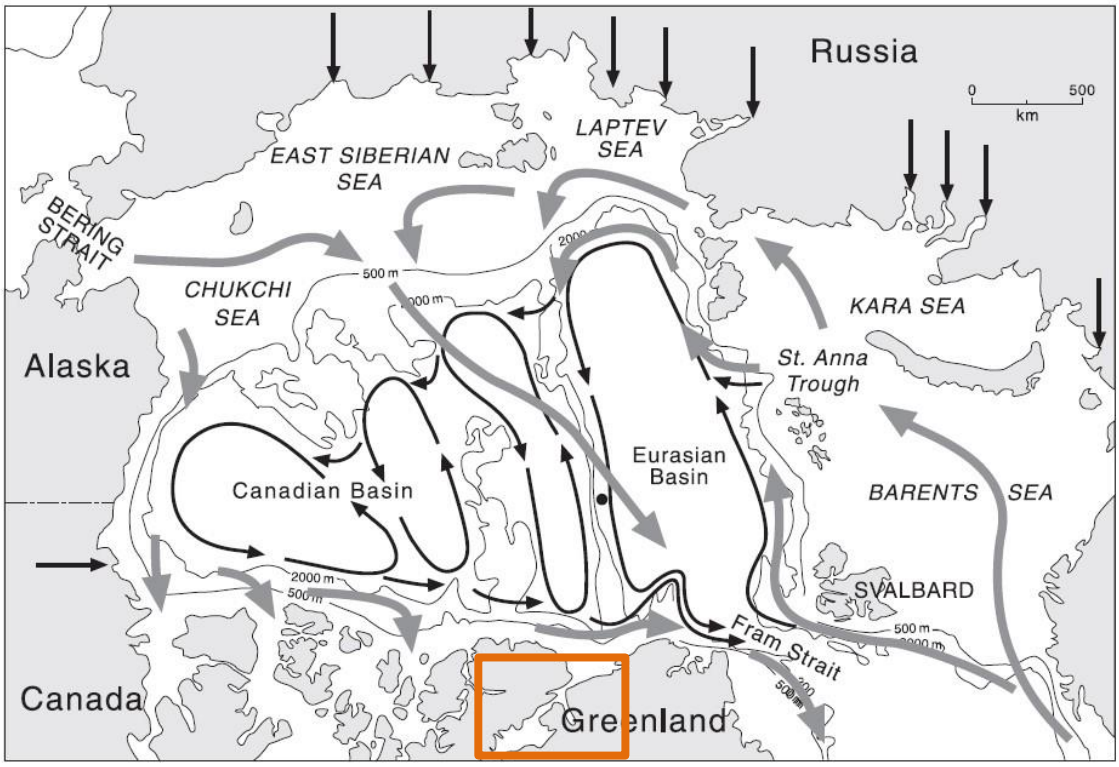


Figure 1.2 Surface (light grey) and deep (black) ocean currents in the Arctic Ocean. River input is illustrated by black arrows and the orange box shows the location of Nares Strait (modified from Jones, 2001).

1.3 Atmospheric Forcing

Atmospheric forcing influences both the temperature (e.g., Deser et al., 2010) and the movement, thickness, and breakup of sea ice at the sea-surface (Ding et al., 2017; Luo et al., 2017; Petty et al., 2016; Rigor et al., 2002). Heat fluxes at the surface of the oceans also influence the Arctic atmosphere directly through the formation of clouds via evaporation and feedback mechanisms (Schweiger et al., 2008; Screen & Simmonds, 2010) and indirectly through carbon sequestration via the biological pump. Two main atmospheric patterns that influence the Arctic and North Atlantic regions are the Arctic Oscillation (AO) and the North Atlantic Oscillation (NAO). Both circulation patterns have important impacts on sea-ice conditions and sea-surface temperatures.

1.3.1 The North Atlantic and Arctic Oscillations

The North Atlantic Oscillation (NAO) and highly correlated Arctic Oscillation (AO) reflect atmospheric circulation patterns in the Northern Hemisphere. The NAO index is a regional measure of sea-surface pressure difference between the Icelandic Low (Iceland) and Azores High (Spain) that result in changes to wind and storm tracks, which have more important effects during wintertime. It has a quasi-periodicities of ca. 20, 50 to 70, and ca. 170 to 300 years (Hurrell et al., 2001). A negative NAO phase causes warmer winter temperatures in northern Greenland and Canada, and cooler and drier winters in Europe and the eastern United States (Hurrell & Deser, 2010). The opposite is observed during a positive NAO phase. The AO refers to the atmospheric circulation for the Northern Hemisphere, from the north pole to ~45ºN. During a positive AO phase there are strong upper level winds that trap cold air masses in the Arctic and during a negative AO phase the weak pressure allows for cold Arctic air to move further south (Thompson & Wallace, 1998; Rigor et al., 2002; Darby et al., 2012). The AO can affect the strength of the Beaufort Gyre and Transpolar Drift Stream (see below; Fig. 1.3), two sea-surface currents that modulate the movement, buildup, and export of (multiyear) sea-ice and freshwater within and out of the Arctic Ocean (Steele et al., 2004).

1.3.2 Atmosphere-ocean forcing

The Beaufort Gyre is a dominant anti-cyclonic circulation pattern in the western Arctic Ocean, close to the Canadian and Alaskan coastlines (Fig. 1.3). Relatively fresh Pacific-sourced waters moving through the Bering Strait and river output from Canada and Alaska contribute to the Beaufort Gyre. The anti-cyclonic circulation of the Beaufort

Gyre restricts these water masses to the western Arctic, and therefore surface conditions are fresher than on the eastern side (Giles et al., 2012; Steele et al, 2004). The Transpolar Drift Stream refers to the ocean current that transports sea ice from the Eurasian to Makarov Basin towards Fram Strait (Fig. 1.2, 1.3).

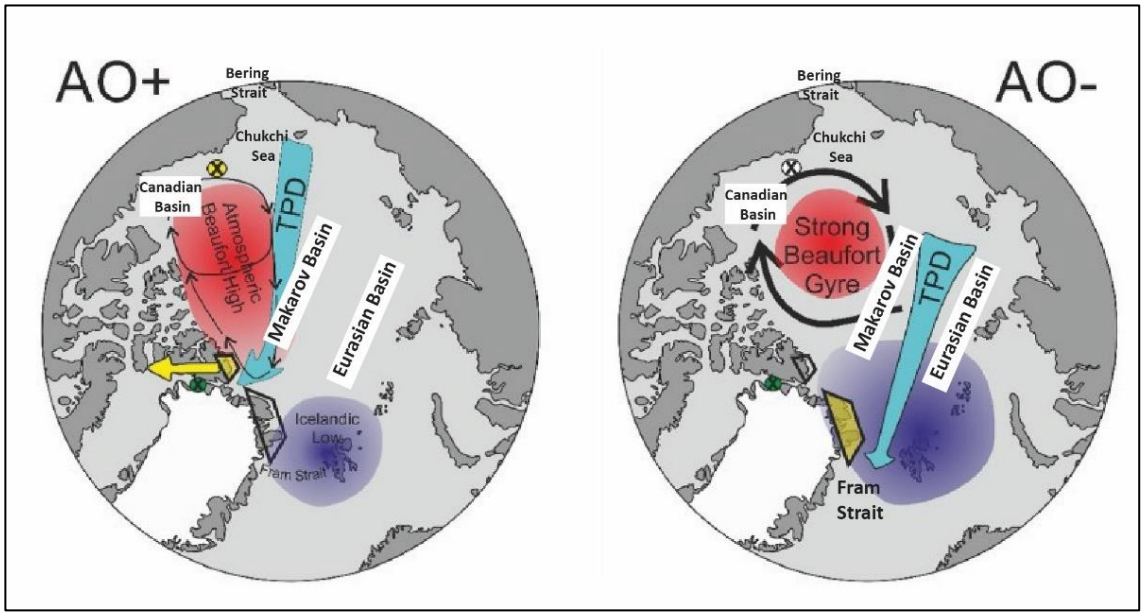


Figure 1.3 Map showing a simplified representation of the surface circulation in the Arctic Ocean during positive and negative Arctic Oscillation (AO) phases, respectively. Abbreviation: TPD: Transpolar Drift (modified after Steele et al., 2004 and Georgiadis et al., 2020).

During a negative phase of (AO-), the Transpolar Drift Stream follows a more direct route from the eastern Arctic toward Fram Strait (Fig. 1.3), where sea ice is exported out of the Arctic and transported southward by the East Greenland Current. The Beaufort Gyre circulation is strong, facilitating the buildup of multiyear ice in the Canadian Basin while freshwater input from Canada is restricted to within the Beaufort Gyre (Steele et al., 2004). During a positive phase of the (AO+), a weak Beaufort Gyre is associated with generally thinner Arctic Ocean sea ice and earlier ice melt. The Transpolar Drift Stream

can veer to the west, entraining more of the freshwater from the Beaufort Gyre and Pacific water from the Chukchi Sea (Mysak, 2001; Steele et al., 2004; Fig. 1.3). Consequently, during AO+, freshwater exports are promoted through the different Arctic Ocean gateways (i.e., Fram Strait, Nares Strait, and the Canadian Arctic Archipelago).

1.4 Arctic Ocean Circulation

Nutrient-rich (N, P, Si) and relatively fresh (< 33 psu) Pacific waters (Swift et al., 1997) enter through the Bering Strait in the western Arctic (Torres-Valdés et al., 2013), and relatively warm (> 0 ºC) (McLaughlin et al., 1996), saline (> 34 psu) Atlantic waters (Swift et al., 1997) enter through eastern Fram Strait and across the Barents Sea in the eastern Arctic (Schauer et al., 2002; Fig. 1.2).

In addition, minor N, P, and Si input into the Arctic Ocean comes from river run-off (Tremblay et al., 2015; Fig. 1.2). Export from the Arctic Ocean is in the form of surface meltwater and modified Atlantic- and Pacific-sourced waters at depth. Most of the export from the Arctic Ocean is through the Canadian Arctic Archipelago (via Jones and Lancaster Sounds), Nares Strait, and Fram Strait (Fig. 1.2). This export of freshwater and sea ice into the North Atlantic can influence the North Atlantic deep-water formation by freshening the surface waters and thereby reducing the density of the surface waters, slowing down their vertical sinking to the bottom of the water column (Otterå et al, 2003; Gregory et al., 2003; Smith & Gregory, 2009).

The eastern Arctic is characterized by a surface layer of relatively fresh surface mixed water (i.e., Polar Mixed Layer) that is 5 to 10 m thick and is separated from the Atlantic water by a strong halocline (Rudels et al., 1996). This cold halocline acts as a

barrier between the relatively warm Atlantic waters and the surface water, which helps deter the melt of sea ice (Rudels et al., 1996). At 400 m depth, beneath the Atlantic water, is a dense, cold, highly saline water mass that follows the seafloor bathymetry (Jones, 2001).

The western Arctic is also characterized by a thin, fresh, surface mixed layer. Beneath this layer are Pacific waters that can be subdivided into Pacific Summer (50 to100 m) and Pacific Winter (~100 to 150 m) waters, with Atlantic waters underneath (~200 to 400 m; Rudels et al., 1996; Rudels et al., 2013). At the bottom of the water column are highly saline and cold waters, which are slightly warmer than in the eastern Arctic (Jones, 2001).

The western Arctic waters are exported from the Arctic through the Canadian Arctic Archipelago and Nares Strait (Fig. 1.2, 1.4). The southward flow is predominantly a result of sea-level difference between the Lincoln Sea (Arctic Ocean) (high) and Baffin Bay (low), and the northerly winds that drive sea ice and surface waters towards northern Baffin Bay at an average rate of 10 to 15 cm s^{-1} (Melling et al., 2001; Münchow & Melling, 2008).

1.5 The North Water (NOW) Polynya

1.5.1 Regional Setting and Formation

The North Water (NOW) polynya is located in northern Baffin Bay between Greenland and Ellesmere Island (Fig. 1.4). A polynya is an area of reduced or low sea-ice concentrations in a region that is normally characterized by high sea-ice concentrations.

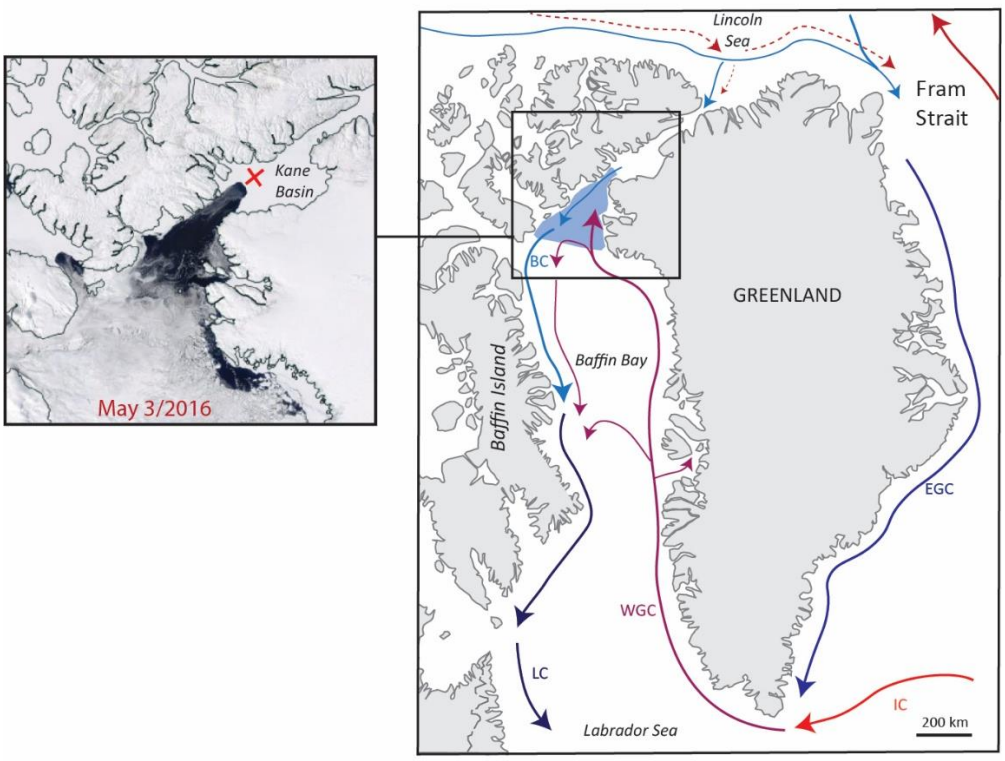


Figure 1.4 Map showing the main surface ocean currents and location of the NOW polynya. The blue arrows represent cold and fresh surface water masses, the red and purple arrows represent Atlantic -influenced or -sourced (sub)surface water masses. The blue shaded area is the average spring (May) extent of open water of the NOW. The red cross on the satellite image from May 2016 indicates the edge of the Kane Basin ice arch (Satellite image from EOSDIS Worldview).

The NOW polynya generally forms in early March until June when it connects with the open water of Baffin Bay and stops being a polynya in the strict sense (Melling et al., 2001). The formation of the NOW relies on both physical and oceanographic factors.

First, an ice arch consolidated at the northern margin of the polynya in Kane Basin (Rasmussen et al., 2010) prevents free-floating ice from drifting into the region of the polynya. This ice arch relies heavily on cohesion of multi-year sea ice, and shallow bathymetry (100 to 300 m; Tang et al., 2004) that allows for grounding of ice (Dumont et

al, 2009). The ice arch does not always form at the same location and can vary in longitude depending on interannual variations in other environmental factors such as the sea-ice thickness, properties of the southward moving Baffin Current and strength of the northerly winds through Nares Strait (Georgiadis et al., 2020).

The formation of the NOW is also facilitated by strong orographically channeled northerly winds that push newly formed sea ice southward of the NOW region. The northerly winds also contribute to a westward movement of the surface water within the NOW region, resulting from Ekman transport (Melling et al., 2001, Yao & Tang, 2003).

The last factor that can contribute to the maintenance of the polynya is the advection of relatively warm water by the West Greenland Current (WGC) that upwells in the eastern region of the NOW with the facilitation of northerly winds (Bâcle et al., 2002). The upwelling along with the heat of the current can restrict the formation of new sea ice. However, the NOW is considered predominately a latent heat polynya (Bâcle et al., 2002; Melling et al., 2001; Maqueda et al., 2004).

1.5.2 Oceanography of the NOW

Two main currents influence the NOW. The first is the WGC, a relatively warm and saline subsurface current that carries a mix of relatively fresh Arctic-sourced water from the East Greenland Current and relatively warm, saline Atlantic-sourced water from the Irminger Current. Furthermore, the WGC is an important source of nitrate and a minor source of silicate into the NOW region (Tremblay et al., 2002). The depth of the WGC varies temporally and seasonally throughout the polynya and ranges between 300 and 500 m (Bâcle et al., 2002). There are two main branches of the WGC: one follows the coast,

is slightly fresher and warmer and flows northward into the polynya. The other is a slightly more saline and cooler branch that is observed in the central region of the NOW (Melling et al., 2001; Fig. 1.4). The penetration of the northward branch is highly reliant on wind forcing (Dumont et al., 2010). The WGC is most prominent in the southeastern region of the polynya and becomes progressively cooler and less saline as it mixes with the cooler freshwater outflow from the northern portion of the polynya (Melling et al., 2001).

The second current, called the Baffin Current (BC), carries glacial meltwater and fresh, cool, nutrient-rich (P, Si; Tremblay et al., 2002) surface waters and drift ice originating from the Arctic Ocean. The BC flows southward along the western side of the NOW region (Fig. 1.4) where it makes up the upper 300 m of the water column, excluding the top 20 m surface layer which is influenced by solar radiation and slightly warmer (Melling et al., 2001). The BC funnels through Nares Strait and can influence two-thirds of the surface conditions within Baffin Bay (Bâcle et al., 2002; Melling et al., 2001). This southward flow also has an important influence on vertical mixing in the water column as freshwater reduces the salinity at the sea surface, thereby potentially reducing subsequent dense brine formation. The continuous formation of sea ice during the spring in the polynya (i.e., ice factory) results in dense salt rejections (brines) that sink to the bottom of the water column. In addition to contributing to the mixing of the water column, brine formation in the polynya is hypothesized to influence the ocean circulation in northern Baffin Bay, notably through its influence on the northward penetration of the WGC (Jackson et al., In Review).

1.5.3 Primary Production and Ecosystem Services in the NOW

In the Arctic, primary production is largely limited by light and nutrient availability. Light availability is mainly controlled by the seasonal variations in irradiance and sea-ice properties, which can reduce the amount and quality of light penetrating into the water column (Nicolaus et al., 2012). Nutrient availability is influenced by the advection of nutrients by different water masses and mixing processes (i.e., nutrient recycling within the water column). Primary production in the NOW is dominated by diatoms, and to a lesser extent, autotrophic dinoflagellates (Lovejoy et al., 2002). In the NOW, the early exposure to light, the advection of nutrient-rich water masses, and the upwelling of the WGC result in earlier and longer phytoplankton growth seasons and thus enhanced net primary production (Marchese et al., 2017). Furthermore, the bloom initiation is more concentrated towards the eastern portion of the NOW, suggesting that the WGC plays a role in local productivity dynamics (Marchese et al., 2017). Blooms in the NOW typically peak in May and remain highly active until the end of June, with a steady decrease of activity into September (Marchese et al., 2017). Tremblay et al. (2002) measured the size and extent of Arctic phytoplankton blooms and concluded that the NOW polynya blooms were an order of magnitude larger than those elsewhere in Baffin Bay, confirming the key role of the NOW for the regional biological productivity.

The NOW sustains a large and diverse food web (Heide-Jørgensen et al., 2013, 2016). It acts as a refuge for many large mammals such as seals, belugas, narwhals, and walruses (Heide-Jørgensen et al., 2016). Accordingly, it has provided subsistence resources for the local human communities over thousands of years (Hastrup et al., 2018). Peripheral to the NOW, northwest Greenland is home to the largest community of little

auks in the Arctic (Davidson et al., 2018). The little auk communities are dependent on the NOW polynya for food resources and the colonies respond to changes in the polynya (Davidson et al., 2018). There is also evidence of intervals of human abandonment in northwest Greenland, which may be related to changes in the ecosystem services provided by the NOW polynya (Hastrup et al., 2018; Ribeiro et al., In Review). The impact of continued climate changes on the primary production of the NOW could have a large influence on the entire NOW ecosystem.

1.6 Arctic Holocene Climate Variability

The Holocene epoch encompasses the last ca. 11,650 years and is preceded by the Pleistocene, which is characterized by glacial-interglacial periods where the glaciation covered up to 30 % of the Earth. The Holocene can be subdivided into three major climatic phases: 1) the Early Holocene notably characterized by the deglaciation of the Laurentide and Fennoscandian Ice Sheets and retreat of the Greenland Ice Sheet established from the previous Pleistocene interval formally referred to as the Greenlandian stage (ca. 11,000 to 8,200 years BP; Carlson et al., 2007, 2008, 2014; Funder et al., 2011; Stroeven et al., 2016; Walker et al., 2019), 2) the Holocene Thermal Maximum corresponding to the interval of temperature maxima formally referred to as the Northgrippian stage (ca. 8,200 to 3,500 years BP; Kaufman et al., 2004; Renssen et al., 2012; Walker et al., 2019), and 3) the Neoglacial period formally referred to as the Meghalayan stage (ca. 4,200 to 200 years BP; Porter & Denton, 1967; Walker et al., 2019). It is however important to note that there is major diachroneity in the timing of Holocene temperature changes across the

high latitudes of the Northern Hemisphere, reflecting varying local environmental context and response time (Nicolle et al., 2018; Briner et al., 2016).

The Neoglacial corresponds to an overall cooling trend in the Arctic (latitudes > 66ºN) related to decreased summer insolation in the Northern Hemisphere (Berger & Loutre, 1991) and refers to a period of glacial advances that extended up to the 19th century (Porter & Denton, 1967). The lower summer insolation is related to a higher angle in Earth's axial tilt (obliquity ~23.26º) and more circular shape of the Earth's orbit (eccentricity) (Berger, 1978; Berger & Loutre, 1991). This cooling trend is documented in both terrestrial (e.g., Lecavalier et al., 2017) and marine records (e.g., Briner et al., 2016 and references therein) of the North Atlantic region, although important climate oscillations are also recorded during this interval. For example, the Roman Warm Period refers to a relatively warm period between 210 BCE to 450 CE when temperatures were similar to modern day (ca. 1961 to 1990 CE equivalents; Ljungqvist, 2010). The Dark Ages Cold Period (450 to 900 CE) refers to a relatively cold period documented predominately in the North Atlantic and Europe thought to be related to low solar activity (i.e., sunspots, solar minimum) and increased volcanic activity (Helama et al., 2017). The Medieval Climate Anomaly is a relatively warm period that varied in duration at North Atlantic sites between 800 to 1550 CE (Nicolle et al., 2018). It corresponds to a period of low volcanic activity and solar irradiance and as such, has also been referred to as the Medieval Quiet Period (Bradley et al., 2016). The Little Ice Age is a cold period that is documented in diverse paleoenvironmental and historical records between 1200 and 1900 CE (Auger et al., 2019; Fischer et al., 1998). Finally, the last century was characterized by a warming trend, largely associated with human-induced increases in atmospheric

greenhouse-gas concentrations (e.g., Nicolle et al., 2018: Briner et al., 2016), and the term *Anthropocene* has been suggested for this interval, but its time boundaries are still debated (Lewis & Maslin, 2015; Walker et al., 2019).

1.7 Dinoflagellates and the Modern Analogue Technique

1.7.1 Dinoflagellates and Dinoflagellate cysts (Dinocysts)

Dinoflagellates are ubiquitous, eukaryotic single-celled organisms (Fensome et al., 1996) with a distribution that extends to freshwater and marine systems. They move using a transverse flagellum that wraps around the dinoflagellates body, and a longitudinal flagellum that acts as a whip-like projection (Fensome et al., 1996). Dinoflagellates can be autotrophic (photosynthetic), heterotrophic (micrograzers) or mixotrophic (perform both trophic strategies), and they dominate the upper portions of the water column (Schnepf & Elbrächter, 1992; Jeong et al., 2010). As a part of their complex life cycle, many dinoflagellates form a protective coating around their cell content referred to as a cyst (Fig. 1.5; Evitt, 1985). Encystment is hypothesized to be triggered by stress or unfavorable environmental conditions (most commonly changes in sea-surface temperature and nutrient availability) and notably represents a mechanism to preserve genetic diversity and facilitate dispersion (Bravo & Figueroa, 2014).

Dinoflagellates can form four types of dinocysts; these are pellicle and resting cysts that can be produced during both the haploid (asexual) or diploid (sexual) phases (Fig. 1.5; Fensome et al., 1996). The pellicle cysts feature a thin membrane that does not preserve in sediment. However, while a small portion of dinoflagellates produce calcareous resting cysts that can preserve in sediment (Zonneveld et al., 1999), the

majority of the resting cysts are made of a highly refractive organic material called dinosporin (carbohydrate-based polymer (Versteegh et al., 2012)) that has a high preservation potential.

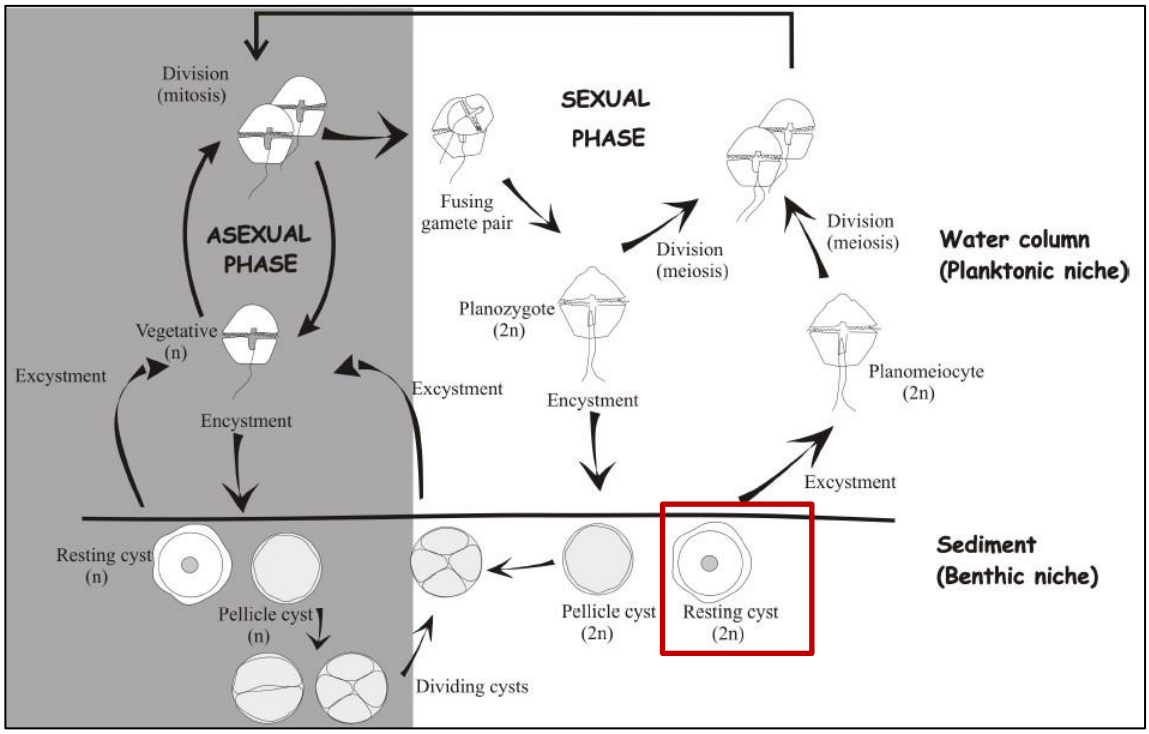


Figure 1.5 The dinoflagellate life cycle where the grey section represents the haploid phase and the white represents the diploid phase. The red box highlights the stage of dinoflagellate life cycle analyzed in this study: the benthic resting cysts. From Bravo & Figueroa (2014).

It has been estimated that between 15-20% of dinoflagellate species produce organic-walled resting cysts, providing a fragmentary record of past dinoflagellate populations in sediment records (Dale, 1976; Versteegh & Blokker, 2004). Unlike diatoms or foraminifera, organic-walled dinoflagellate cysts (dinocysts) are not subject to dissolution from Si- or $CaCO_3$-undersaturated waters. However, some dinocyst taxa are subject to oxidation during diagenesis (Zonneveld et al., 2008) (Fig. 1.6).

Sensitivity to oxygen	Organic-walled cysts
Extremely sensitive	Cysts from *Protoperidinium* species *Echinidinium* species
Moderately sensitive	*Lingulodinium machaerophorum* *Operculodinium centrocarpum* *Pyxidinopsis reticulata* *Spiniferites* species (*S. bentorii, S. mirabilis, S. pachydermus, S. ramosus*) *Nematosphaeropsis labyrinthus*
Resistant	*Impagidinium species (I. aculeatum, I. paradoxum, I. patulum, I. plicatum, I. Sphaericum)* *Operculodinium israelianum* Cysts of *Pentapharsodinium dalei* *Polysphaeridium zoharyi*

Figure 1.6 Dinocyst taxa and their relative sensitivity to oxidation (from de Vernal & Marret, 2007; Zonneveld et al., 2008)

1.7.2 The Modern Analogue Technique

The Modern Analogue Technique (MAT) is a statistical technique that compares the species composition of modern fossil assemblages with known environmental parameters to past, or downcore, fossil assemblages. The MAT was first used by Hutson (1980), looking at the Agulhas Current in the southern Indian Ocean in the Pleistocene using planktonic foraminifera. The MAT for dinocysts was first developed and then expanded by de Vernal et al. (1994, 2001, 2005, 2013a, 2013b, 2019) to the current database that includes 1968 sites distributed across the Northern Hemisphere (de Vernal et al., 2020; Fig. 1.7). The MAT relies on the assumption that similar dinocyst assemblages occur in similar environmental conditions through time and that the sea-surface conditions influence the composition of dinocyst assemblages present (de Vernal et al., 2001). The use of MAT is also dependent on the database being large enough to represent both modern and ancient environmental conditions such that comparisons between past and present can be made.

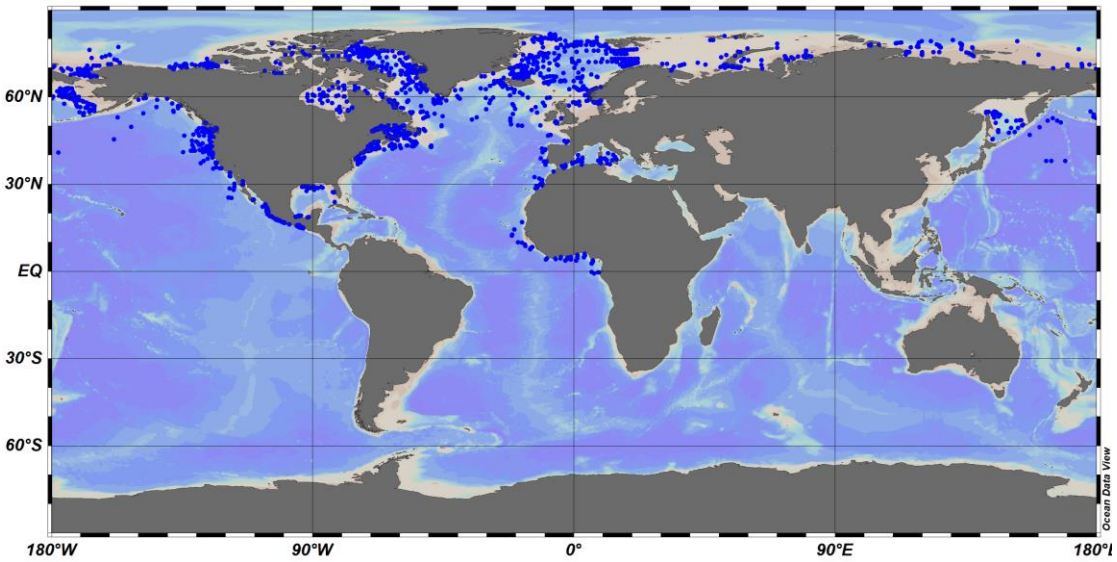


Figure 1.7 The current distribution of MAT analogues (n = 1968) (de Vernal et al., 2020). This database was used in creating the MAT index used in this paper (see section 2.4.4).

In paleoenvironmental studies, the MAT compares downcore dinocyst assemblages to modern assemblages from surface sediment samples. The MAT has been used to reconstruct sea-surface parameters (temperature, salinity, sea-ice concentration, and productivity) and has been used as an additional statistical exploratory tool to aid in regional paleoenvironmental studies (e.g., Allan et al., 2018; Caron et al., 2019).

The sea-surface parameters associated with the modern analogues are collected from satellite data, where the sea-surface temperature, salinity, dissolved oxygen, and nutrients are taken from the World Ocean Atlas 2013 (WOA13, https://www.nodc.noaa.gov/OC5/woa13/woa13data.html). The spatial resolution for the measurements is one to a quarter of a degree for temperature and salinity, and one degree for dissolved oxygen, nitrate, and phosphate. The sea-ice concentration is collected from the National Snow and Ice Data Centre (Walsh et al., 2015) at a quarter of a degree resolution, where sea-ice concentration refers to an area with > 50% sea-ice presence. Both parameters use an average monthly value from 1955 to 2012 (de Vernal et al., 2020).

These sea-surface parameters are then associated with the surface samples collected from a particular location, and the analogues are defined.

By using the MAT, quantitative environmental information can be inferred from dinocyst assemblages preserved in sediment archives. However, there are some shortcomings that need to be noted when using the MAT: (1) there has been increased taxonomic understanding and expansion of cyst species diversity and microscopy technology since initial development of the modern database to which assemblages counted today are compared, (2) the time span represented by the surface samples used in the database is variable, and (3) the fact that some of the reconstructed parameters might not exert a large influence on the dinocyst assemblage composition and their reconstructed values simply follow that of the selected analogue.

Efforts to mitigate the issues mentioned above have been achieved through standardization of sample processing (de Vernal et al., 2020) and taxonomic identification within the scientific community (Van Nieuwenhove et al., 2020). Also, when possible, the surface samples used in the analogue database are dated radiometrically.

In this study we exploited the potential of the MAT without directly using reconstructed values, but instead we developed an index based on the location of the MAT analogues to infer information about changes in the NOW polynya dynamics through time.

1.8 Previous Work and Thesis Objectives

The NOW polynya has been the subject of paleoenvironmental studies using dinocysts to understand changes in sea-surface conditions during the last few centuries

(Hamel et al., 2002; Cormier et al., 2016) and throughout the Holocene (Levac et al., 2001; Mudie et al., 2005;2006; Knudsen et al., 2008). However, the short timescale study cannot be used to place recent changes (i.e., human influenced) in the context of the natural variability of the system, and the long-term studies lack a high-resolution approach or contain hiatuses.

More recently, Jackson et al. (In Review) studied changes in the benthic foraminiferal assemblages at one site located in the central region of the NOW (same sediment archive as this study) and another at the periphery of the polynya, where they link polynya activity, brine production, and northward penetration of the WGC into the NOW. However, this study looks at bottom water conditions, leaving an incomplete picture of the long-term evolution at the polynya's sea-surface conditions during the Holocene.

To address these research gaps, this project aims at understanding changes in sea-surface dynamics of the NOW polynya during the last ca. 3800 years using dinocyst assemblages preserved in a 5.43 m long marine sediment core and a 24.5 cm long marine box core. Both qualitative (dinocyst fluxes and assemblage composition) and quantitative (statistical analysis and MAT) approaches are used to infer paleoenvironmental information. This study is the first to propose the use of MAT-based indices as a complementary approach to reconstruct past environmental changes.

1.9 Statement of Contributions to Research and Writing

The research was designed within the framework of a collaboration between Drs. Audrey Limoges and Sofia Ribeiro. Chapter 2 of this thesis is in the form of a paper that

is intended to be submitted to the peer-reviewed journal Palaeogeography, Palaeoclimatology, Palaeoecology. I counted the dinocysts with Drs. Audrey Limoges (AMD15-Casq1 and AMD15-Casq1-BC4) and Thomas Richerol (AMD15-Casq1-BC4). The age model used here was developed by Ribeiro et al. (In Review). Palynological preparations were completed at Ghent University for core AMD15-Casq1 and by Thomas Richerol at UQAR for core AMD15-Casq1-BC4. Analysis and interpretation of the data were conducted by myself, with suggestions and comments from Drs. Audrey Limoges, Nicolas Van Nieuwenhove and Sofia Ribeiro. The MAT index described in Chapter 2 was developed by Drs. Audrey Limoges, Nicolas Van Nieuwenhove and myself. All chapters of this thesis were written by me, with guidance and comments from Drs. Audrey Limoges, Nicolas Van Nieuwenhove and David Keighley.

1.10 References

Allan, E., Vernal, A. de, Knudsen, M.F., Hillaire-Marcel, C., Moros, M., Ribeiro, S., Ouellet-Bernier, M.-M., Seidenkrantz, M.-S., 2018. Late Holocene Sea Surface Instabilities in the Disko Bugt Area, West Greenland, in Phase With δ18O Oscillations at Camp Century. Paleoceanography and Paleoclimatology 33, 227–243. https://doi.org/10.1002/2017PA003289

Auger, J.D., Mayewski, P.A., Maasch, K.A., Schuenemann, K.C., Carleton, A.M., Birkel, S.D., Saros, J.E., 2019. 2000 years of North Atlantic-Arctic climate. Quaternary Science Reviews 216, 1–17. https://doi.org/10.1016/j.quascirev.2019.05.020

Bâcle, J., Carmack, E.C., Ingram, R.G., 2002. Water column structure and circulation under the North Water during spring transition: April–July 1998. Deep Sea Research Part II: Topical Studies in Oceanography, The International North Water Polynya Study 49, 4907–4925. https://doi.org/10.1016/S0967-0645(02)00170-4

Berger, A., Loutre, M.F., 1991. Insolation values for the climate of the last 10 million years. Quaternary Science Reviews 10, 297–317. https://doi.org/10.1016/0277-3791(91)90033-Q

Berger, A., 1978. Long-Term Variations of Daily Insolation and Quaternary Climatic Changes. Journal of Atmospheric Science. 35, 2362–2367. https://doi.org/10.1175/1520-0469(1978)035<2362:LTVODI>2.0.CO;2

Bradley, R.S., Wanner, H., Diaz, H.F., 2016. The Medieval Quiet Period. The Holocene 26, 990–993. https://doi.org/10.1177/0959683615622552

Bravo, I., Figueroa, R.I., 2014. Towards an Ecological Understanding of Dinoflagellate Cyst Functions. Microorganisms 2, 11–32. https://doi.org/10.3390/microorganisms2010011

Briner, J.P., McKay, N.P., Axford, Y., Bennike, O., Bradley, R.S., de Vernal, A., Fisher, D., Francus, P., Fréchette, B., Gajewski, K., Jennings, A., Kaufman, D.S., Miller, G., Rouston, C., Wagner, B., 2016. Holocene climate change in Arctic Canada and Greenland. Quaternary Science Reviews, Special Issue: PAST Gateways (Palaeo-Arctic Spatial and Temporal Gateways) 147, 340–364. https://doi.org/10.1016/j.quascirev.2016.02.010

Carlson, A.E., Clark, P.U., Raisbeck, G.M., Brook, E.J., 2007. Rapid Holocene Deglaciation of the Labrador Sector of the Laurentide Ice Sheet. Journal of Climate 20, 5126–5133. https://doi.org/10.1175/JCLI4273.1

Carlson, A.E., LeGrande, A.N., Oppo, D.W., Came, R.E., Schmidt, G.A., Anslow, F.S., Licciardi, J.M., Obbink, E.A., 2008. Rapid early Holocene deglaciation of the Laurentide ice sheet. Nature Geoscience 1, 620–624. https://doi.org/10.1038/ngeo285

Carlson, A.E., Winsor, K., Ullman, D.J., Brook, E.J., Rood, D.H., Axford, Y., LeGrande, A.N., Anslow, F.S., Sinclair, G., 2014. Earliest Holocene south Greenland ice sheet retreat within its late Holocene extent. Geophysical Research Letters 41, 5514–5521. https://doi.org/10.1002/2014GL060800

Caron, M., Rochon, A., Montero-Serrano, J.-C., St-Onge, G., 2019. Evolution of sea-surface conditions on the northwestern Greenland margin during the Holocene. Journal of Quaternary Science 34, 569–580. https://doi.org/10.1002/jqs.3146

Cormier, M.-A., Rochon, A., de Vernal, A., Gélinas, Y., 2016. Multi-proxy study of primary production and paleoceanographical conditions in northern Baffin Bay during the last centuries. Marine Micropaleontology 127, 1–10. https://doi.org/10.1016/j.marmicro.2016.07.001

Curry, J.A., Schramm, J.L., Ebert, E.E., 1995. Sea Ice-Albedo Climate Feedback Mechanism. Journal of Climate 8, 240–247. https://doi.org/10.1175/1520-0442(1995)008<0240:SIACFM>2.0.CO;2

Dale, B., 1976. Cyst formation, sedimentation, and preservation: Factors affecting dinoflagellate assemblages in recent sediments from trondheimsfjord, Norway. Review of Palaeobotany and Palynology 22, 39–60. https://doi.org/10.1016/0034-6667(76)90010-5

Darby, D.A., Ortiz, J.D., Grosch, C.E., Lund, S.P., 2012. 1,500-year cycle in the Arctic Oscillation identified in Holocene Arctic sea-ice drift. Nature Geoscience; London 5, 897–900. http://dx.doi.org.proxy.hil.unb.ca/10.1038/ngeo1629

Davidson, T.A., Wetterich, S., Johansen, K.L., Grønnow, B., Windirsch, T., Jeppesen, E., Syväranta, J., Olsen, J., González-Bergonzoni, I., Strunk, A., Larsen, N.K., Meyer, H., Søndergaard, J., Dietz, R., Eulears, I., Mosbech, A., 2018. The history of seabird colonies and the North Water ecosystem: Contributions from palaeoecological and archaeological evidence. Ambio 47, 175–192. https://doi.org/10.1007/s13280-018-1031-1

de Vernal, A., Turon, J. L., & Guiot, J. (1994). Dinoflagellate cyst distribution in high latitude environments and development of transfer function for the reconstruction of sea-surface temperature, salinity and seasonality. Canadian Journal of Earth Sciences, 31, 48-62.

de Vernal, A., Henry, M., Matthiessen, J., Mudie, P.J., Rochon, A., Boessenkool, K.P., Eynaud, F., GrØsfjeld, K., Guiot, J., Hamel, D., Harland, R., Head, M.J., Kunz-Pirrung, M., Levac, E., Loucheur, V., Peyron, O., Pospelova, V., Radi, T., Turon, J.-L., Voronina, E., 2001. Dinoflagellate cyst assemblages as tracers of sea-surface conditions in the northern North Atlantic, Arctic and sub-Arctic seas: the new ‘n = 677’ data base and its application for quantitative palaeoceanographic reconstruction. Journal of Quaternary Science 16, 681–698. https://doi.org/10.1002/jqs.659

de Vernal, A., Eynaud, F., Henry, M., Hillaire-Marcel, C., Londeix, L., Mangin, S., Matthiessen, J., Marret, F., Radi, T., Rochon, A., Solignac, S., Turon, J.-L., 2005. Reconstruction of sea-surface conditions at middle to high latitudes of the Northern Hemisphere during the Last Glacial Maximum (LGM) based on dinoflagellate cyst assemblages. Quaternary Science Reviews, Multiproxy Approach for the Reconstruction of the Glacial Ocean surface 24, 897–924. https://doi.org/10.1016/j.quascirev.2004.06.014

de Vernal, A., Marret, F., 2007. Chapter Nine. Organic Walled Dinoflagellate Cysts: Tracers of Sea-Surface Conditions, in: Hillaire–Marcel, C., De Vernal, A. (Eds.), Developments in Marine Geology, Proxies in Late Cenozoic Paleoceanography. Elsevier, pp. 523–563. https://doi.org/10.1016/S1572-5480(07)01018-4

de Vernal, A., Hillaire-Marcel, C., Rochon, A., Fréchette, B., Henry, M., Solignac, S., Bonnet, S., 2013a. Dinocyst-based reconstructions of sea ice cover concentration during the Holocene in the Arctic Ocean, the northern North Atlantic Ocean and its adjacent seas. Quaternary Science Reviews, Sea Ice in the Paleoclimate System: the Challenge of Reconstructing Sea Ice from Proxies 79, 111–121. https://doi.org/10.1016/j.quascirev.2013.07.006

de Vernal, A., Rochon, A., Fréchette, B., Henry, M., Radi, T., Solignac, S., 2013b. Reconstructing past sea ice cover of the Northern Hemisphere from dinocyst assemblages: status of the approach. Quaternary Science Reviews, Sea Ice in the Paleoclimate System: the Challenge of Reconstructing Sea Ice from Proxies 79, 122–134. https://doi.org/10.1016/j.quascirev.2013.06.022

de Vernal, A., Radi, T., Zaragosi, S., Van Nieuwenhove, N., Rochon, A., Allan, E., De Schepper, S., Eynaud, F., Head, M.J., Limoges, A., Londeix, L., Marret, F., Matthiessen, J., Penaud, A., Pospelova, V., Price, A., Richerol, T., 2020. Distribution of common modern dinoflagellate cyst taxa in surface sediments of the Northern Hemisphere in

relation to environmental parameters: The new n=1968 database. Marine Micropaleontology 101796. https://doi.org/10.1016/j.marmicro.2019.101796

Deser, C., Alexander, M.A., Xie, S.-P., Phillips, A.S., 2010. Sea Surface Temperature Variability: Patterns and Mechanisms. Annual Review of Marine Science 2, 115–143. https://doi.org/10.1146/annurev-marine-120408-151453

Ding, Q., Schweiger, A., L'Heureux, M., Battisti, D.S., Po-Chedley, S., Johnson, N.C., Blanchard-Wrigglesworth, E., Harnos, K., Zhang, Q., Eastman, R., Steig, E.J., 2017. Influence of high-latitude atmospheric circulation changes on summertime Arctic sea ice. Nature Climate Change 7, 289–295. https://doi.org/10.1038/nclimate3241

Dumont, D., Gratton, Y., Arbetter, T.E., 2009. Modeling the Dynamics of the North Water Polynya Ice Bridge. Journal of Physical Oceanography 39, 1448–1461. https://doi.org/10.1175/2008JPO3965.1

Dumont, D., Gratton, Y., Arbetter, T.E., 2010. Modeling Wind-Driven Circulation and Landfast Ice-Edge Processes during Polynya Events in Northern Baffin Bay. Journal of Physical Oceanography. 40, 1356–1372. https://doi.org/10.1175/2010JPO4292.1

Evitt, W.R., 1985. Sporopollenin Dinoflagellate Cysts: Their Morphology and Interpretation. American Association of Stratigraphic Palynologists Foundation. 1-325. Dallas, Tex.

Fensome, R.A., MacRae, R.A., Moldowan, J.M., Taylor, F.J.R., Williams, G.L., 1996. The early Mesozoic radiation of dinoflagellates. Paleobiology 22, 329–338. https://doi.org/10.1017/S0094837300016316

Fischer, H., Werner, M., Wagenbach, D., Schwager, M., Thorsteinnson, T., Wilhelms, F., Kipfstuhl, J., Sommer, S., 1998. Little Ice Age clearly recorded in northern Greenland ice cores. Geophysical Research Letters 25, 1749–1752. https://doi.org/10.1029/98GL01177

Funder, S., Kjeldsen, K.K., Kjær, K.H., Ó Cofaigh, C., 2011. Chapter 50 - The Greenland Ice Sheet During the Past 300,000 Years: A Review, in: Ehlers, J., Gibbard, P.L., Hughes, P.D. (Eds.), Developments in Quaternary Sciences, Quaternary Glaciations - Extent and Chronology. Elsevier, pp. 699–713. https://doi.org/10.1016/B978-0-444-53447-7.00050-7

Georgiadis, E., Giraudeau, J., Jennings, A., Limoges, A., Jackson, R., Ribeiro, S., Massé, G., 2020. Local and regional controls on Holocene sea ice dynamics and oceanography in Nares Strait, Northwest Greenland. Marine Geology 422, 106115. https://doi.org/10.1016/j.margeo.2020.106115

Giles, K.A., Laxon, S.W., Ridout, A.L., Wingham, D.J., Bacon, S., 2012. Western Arctic Ocean freshwater storage increased by wind-driven spin-up of the Beaufort Gyre. Nature Geoscience 5, 194–197. https://doi.org/10.1038/ngeo1379

Gregory, J.M., Saenko, O.A., Weaver, A.J., 2003. The role of the Atlantic freshwater balance in the hysteresis of the meridional overturning circulation. Climate Dynamics 21, 707–717. https://doi.org/10.1007/s00382-003-0359-8

Hamel, D., Vernal, A. de, Gosselin, M., Hillaire-Marcel, C., 2002. Organic-walled microfossils and geochemical tracers: sedimentary indicators of productivity changes in the North Water and northern Baffin Bay during the last centuries. Deep Sea Research Part II: Topical Studies in Oceanography, The International North Water Polynya Study 49, 5277–5295. https://doi.org/10.1016/S0967-0645(02)00190-X

Hastrup, K., Mosbech, A., Grønnow, B., 2018. Introducing the North Water: Histories of exploration, ice dynamics, living resources, and human settlement in the Thule Region. Ambio 47, 162–174. https://doi.org/10.1007/s13280-018-1030-2

Heide-Jørgensen, M.P., Burt, L.M., Hansen, R.G., Nielsen, N.H., Rasmussen, M., Fossette, S., Stern, H., 2013. The Significance of the North Water Polynya to Arctic Top Predators. Ambio 42, 596–610. https://doi.org/10.1007/s13280-012-0357-3

Heide-Jørgensen, M.P., Sinding, M.-H.S., Nielsen, N.H., Rosing-Asvid, A., Hansen, R.G., 2016. Large numbers of marine mammals winter in the North Water polynya. Polar Biology 39, 1605–1614. https://doi.org/10.1007/s00300-015-1885-7

Helama, S., Jones, P.D., Briffa, K.R., 2017. Dark Ages Cold Period: A literature review and directions for future research. The Holocene. 27, 1600–1606. https://doi.org/10.1177/0959683617693898

Hurrell, J.W., Deser, C., 2010. North Atlantic climate variability: The role of the North Atlantic Oscillation. Journal of Marine Systems, Impact of climate variability on marine ecosystems: A comparative approach 79, 231–244. https://doi.org/10.1016/j.jmarsys.2009.11.002

Hurrell, J.W., Kushnir, Y., Visbeck, M., 2001. The North Atlantic Oscillation. Science 291, 603–605. https://doi.org/10.1126/science.1058761

Hutson, W.H., 1980. The Agulhas Current During the Late Pleistocene: Analysis of Modern Faunal Analogs. Science 207, 64–66. https://doi.org/10.1126/science.207.4426.64

IPCC, 2014. Climate Change 2014: Synthesis Report. Contribution of Working Groups I, II and III to the Fifth Assessment Report of the Intergovernmental Panel on Climate

Change [Core Writing Team, R.K. Pachauri and L.A. Meyer (eds.)]. IPCC, Geneva, Switzerland, pp. 1-151.

Jackson, R., Bang, A., Limoges, A., Georgiadis, E., Olsen, S., Tallberg, P., Andersen, T., Mikkelsen, N., Giraudeau, J., Massé, G., Ribeiro, S., submitted. North Water Polynya dynamics mediate Holocene Atlantic water influence in northern Baffin Bay. In Review. Scientific Reports.

Jeong, H.J., Yoo, Y.D., Kim, J.S., Seong, K.A., Kang, N.S., Kim, T.H., 2010. Growth, feeding and ecological roles of the mixotrophic and heterotrophic dinoflagellates in marine planktonic food webs. Ocean Science Journal. 45, 65–91. https://doi.org/10.1007/s12601-010-0007-2

Jones, E.P., 2001. Circulation in the Arctic Ocean. Polar Research 20, 139–146. https://doi.org/10.1111/j.1751-8369.2001.tb00049.x

Kaufman, D.S., Ager, T.A., Anderson, N.J., Anderson, P.M., Andrews, J.T., Bartlein, P.J., Brubaker, L.B., Coats, L.L., Cwynar, L.C., Duvall, M.L., Dyke, A.S., Edwards, M.E., Eisner, W.R., Gajewski, K., Geirsdóttir, A., Hu, F.S., Jennings, A.E., Kaplan, M.R., Kerwin, M.W., Lozhkin, A.V., MacDonald, G.M., Miller, G.H., Mock, C.J., Oswald, W.W., Otto-Bliesner, B.L., Porinchu, D.F., Rühland, K., Smol, J.P., Steig, E.J., Wolfe, B.B., 2004. Holocene thermal maximum in the western Arctic (0–180°W). Quaternary Science Reviews 23, 529–560. https://doi.org/10.1016/j.quascirev.2003.09.007

Knudsen, K.L., Stabell, B., Seidenkrantz, M.-S., Eiríksson, J., Blake, W., 2008. Deglacial and Holocene conditions in northernmost Baffin Bay: sediments, foraminifera, diatoms and stable isotopes. Boreas 37, 346–376. https://doi.org/10.1111/j.1502-3885.2008.00035.x

Kurtz, N.T., Markus, T., Farrell, S.L., Worthen, D.L., Boisvert, L.N., 2011. Observations of recent Arctic sea ice volume loss and its impact on ocean-atmosphere energy exchange and ice production. Journal of Geophysical Research: Oceans 116 C04015 https://doi.org/10.1029/2010JC006235

Lecavalier, B.S., Fisher, D.A., Milne, G.A., Vinther, B.M., Tarasov, L., Huybrechts, P., Lacelle, D., Main, B., Zheng, J., Bourgeois, J., Dyke, A.S., 2017. High Arctic Holocene temperature record from the Agassiz ice cap and Greenland ice sheet evolution. PNAS 114, 5952–5957. https://doi.org/10.1073/pnas.1616287114

Lewis, S.L., Maslin, M.A., 2015. Defining the Anthropocene. Nature 519, 171–180. https://doi.org/10.1038/nature14258

Levac, E., Vernal, A.D., Blake, W., Jr., 2001. Sea-surface conditions in northernmost Baffin Bay during the Holocene: palynological evidence. Journal of Quaternary Science 16, 353–363. https://doi.org/10.1002/jqs.614

Ljungqvist, F.C., 2010. A new reconstruction of temperature variability in the extra-tropical northern hemisphere during the last two millennia. Geografiska Annaler: Series A, Physical Geography 92, 339–351. https://doi.org/10.1111/j.1468-0459.2010.00399.x

Lovejoy, C., Legendre, L., Price, N.M., 2002. Prolonged diatom blooms and microbial food web dynamics: experimental results from an Arctic polynya. Aquatic Microbial Ecology 29, 267–278. https://doi.org/10.3354/ame029267

Luo, B., Luo, D., Wu, L., Zhong, L., Simmonds, I., 2017. Atmospheric circulation patterns which promote winter Arctic sea ice decline. Environmental Research Letters. 12, 054017. https://doi.org/10.1088/1748-9326/aa69d0

Maqueda, M.A.M., Willmott, A.J., Biggs, N.R.T., 2004. Polynya dynamics: a review of observations and modeling. Reviews of Geophysics. 42. RG1004. https://doi.org/10.1029/2002RG000116

Marchese, C., Albouy, C., Tremblay, J.-É., Dumont, D., D'Ortenzio, F., Vissault, S., Bélanger, S., 2017. Changes in phytoplankton bloom phenology over the North Water (NOW) polynya: a response to changing environmental conditions. Polar Biology 40, 1721–1737. https://doi.org/10.1007/s00300-017-2095-2

McLaughlin, F.A., Carmack, E.C., Macdonald, R.W., Bishop, J.K.B., 1996. Physical and geochemical properties across the Atlantic/Pacific water mass front in the southern Canadian Basin. Journal of Geophysical Research: Oceans 101, 1183–1197. https://doi.org/10.1029/95JC02634

Melling, H., Gratton, Y., Ingram, G., 2001. Ocean circulation within the North Water polynya of Baffin Bay. Atmosphere-Ocean 39, 301–325. https://doi.org/10.1080/07055900.2001.9649683

Mudie, P.J., Rochon, A., Levac, E., 2005. Decadal-scale sea ice changes in the Canadian Arctic and their impacts on humans during the past 4,000 years. Environmental Archaeology 10, 113–126. https://doi.org/10.1179/env.2005.10.2.113

Mudie, P.J., Rochon, A., Prins, M.A., Soenarjo, D., Troelstra, S.R., Levac, E., 2006. Late Pleistocene-Holocene Marine Geology of Nares Strait region: paleoceanography from foraminifera and dinoflagellate cysts, sedimentology and stable isotopes. Polarforschung (Bremerhaven) 74, 169–183.

Münchow, A., Melling, H., 2008. Ocean current observations from Nares Strait to the west of Greenland: Interannual to tidal variability and forcing. Journal of Marine Research 66, 801–833. https://doi.org/10.1357/002224008788064612

Mysak, L.A., 2001. Patterns of Arctic Circulation. Science 293, 1269–1270. https://doi.org/10.1126/science.1064217

Nguyen, A.T., Menemenlis, D., Kwok, R., 2009. Improved modeling of the Arctic halocline with a subgrid-scale brine rejection parameterization. Journal of Geophysical Research: Oceans 114. C11014 https://doi.org/10.1029/2008JC005121

Nicolaus, M., Katlein, C., Maslanik, J., Hendricks, S., 2012. Changes in Arctic sea ice result in increasing light transmittance and absorption. Geophysical Research Letters 39. L24501. https://doi.org/10.1029/2012GL053738

Nicolle, M., Debret, M., Massei, N., Colin, C., deVernal, A., Divine, D., Werner, J., Hormes, A., Korhola, A., Linderholm, H.W., 2018. Climate variability in the subarctic area for the last 2 millennia. Climate of the Past 14, 101–116. https://doi.org/10.5194/cp-14-101-2018

Otterå, O.H., Drange, H., Bentsen, M., Kvamstø, N.G., Jiang, D., 2003. The sensitivity of the present-day Atlantic meridional overturning circulation to freshwater forcing. Geophysical Research Letters 30, 171898. https://doi.org/10.1029/2003GL017578

Petty, A.A., Hutchings, J.K., Richter-Menge, J.A., Tschudi, M.A., 2016. Sea ice circulation around the Beaufort Gyre: The changing role of wind forcing and the sea ice state. Journal of Geophysical Research: Oceans 121, 3278–3296. https://doi.org/10.1002/2015JC010903

Porter, S.C., Denton, G.H., 1967. Chronology of neoglaciation in the North American Cordillera. American Journal of Science 265, 177–210. https://doi.org/10.2475/ajs.265.3.177

Rasmussen, T.A.S., Kliem, N., Kaas, E., 2010. Modelling the sea ice in the Nares Strait. Ocean Modelling 35, 161–172. https://doi.org/10.1016/j.ocemod.2010.07.003

Renssen, H., Seppä, H., Crosta, X., Goosse, H., Roche, D.M., 2012. Global characterization of the Holocene Thermal Maximum. Quaternary Science Reviews 48, 7–19. https://doi.org/10.1016/j.quascirev.2012.05.022

Ribeiro S, Limoges A, Massé G, Colgan W, Jackson R, Mikkelsen N, Johannsen KL, Georgiadis E, Weckström K, Kuijpers A, Olsen J, Olsen SM, Nissen M, Strunk A, Wetterich S, Syvaranta J, Henderson ACG, Mackay H, Taipale S, Jeppesen E, Larsen NK, Crosta X, Giraudeau J, Holm L, Nuttall M, Gronnow, B, Mosbech A, Davidson TA. Vulnerability of the North Water polynya ecosystem to climate change. In Review. Nature Climate Change

Rigor, I.G., Wallace, J.M., Colony, R.L., 2002. Response of Sea Ice to the Arctic Oscillation. Journal of Climate 15, 2648–2663. https://doi.org/10.1175/1520-0442(2002)015<2648:ROSITT>2.0.CO;2

Rudels, B., Anderson, L.G., Jones, E.P., 1996. Formation and evolution of the surface mixed layer and halocline of the Arctic Ocean. Journal of Geophysical Research: Oceans 101, 8807–8821. https://doi.org/10.1029/96JC00143

Rudels, B., Jones, E.P., Anderson, L.G., Kattner, G., 2013. On the Intermediate Depth Waters of the Arctic Ocean, in: The Polar Oceans and Their Role in Shaping the Global Environment. American Geophysical Union (AGU), pp. 33–46. https://doi.org/10.1029/GM085p0033

Schauer, U., Loeng, H., Rudels, B., Ozhigin, V.K., Dieck, W., 2002. Atlantic Water flow through the Barents and Kara Seas. Deep Sea Research Part I: Oceanographic Research Papers 49, 2281–2298. https://doi.org/10.1016/S0967-0637(02)00125-5

Schnepf, E., Elbrächter, M., 1992. Nutritional strategies in dinoflagellates: A review with emphasis on cell biological aspects. European Journal of Protistology 28, 3–24. https://doi.org/10.1016/S0932-4739(11)80315-9

Schweiger, A.J., Lindsay, R.W., Vavrus, S., Francis, J.A., 2008. Relationships between Arctic Sea Ice and Clouds during Autumn. Journal of Climate 21, 4799–4810. https://doi.org/10.1175/2008JCLI2156.1

Screen, J.A., Simmonds, I., 2010. The central role of diminishing sea ice in recent Arctic temperature amplification. Nature 464, 1334–1337. https://doi.org/10.1038/nature09051

Serreze, M.C., Holland, M.M., Stroeve, J., 2007. Perspectives on the Arctic's Shrinking Sea-Ice Cover. Science 315, 1533–1536. https://doi.org/10.1126/science.1139426

Smith, R.S., Gregory, J.M., 2009. A study of the sensitivity of ocean overturning circulation and climate to freshwater input in different regions of the North Atlantic. Geophysical Research Letters 36, C3. https://doi.org/10.1029/2009GL038607

Steele, M., Morison, J., Ermold, W., Rigor, I., Ortmeyer, M., Shimada, K., 2004. Circulation of summer Pacific halocline water in the Arctic Ocean. Journal of Geophysical Research: Oceans 109, C02027. https://doi.org/10.1029/2003JC002009

Stroeven, A.P., Hättestrand, C., Kleman, J., Heyman, J., Fabel, D., Fredin, O., Goodfellow, B.W., Harbor, J.M., Jansen, J.D., Olsen, L., Caffee, M.W., Fink, D., Lundqvist, J., Rosqvist, G.C., Strömberg, B., Jansson, K.N., 2016. Deglaciation of Fennoscandia. Quaternary Science Reviews, Special Issue: PAST Gateways (Palaeo-Arctic Spatial and Temporal Gateways) 147, 91–121. https://doi.org/10.1016/j.quascirev.2015.09.016

Swift, J.H., Jones, E.P., Aagaard, K., Carmack, E.C., Hingston, M., MacDonald, R.W., McLaughlin, F.A., Perkin, R.G., 1997. Waters of the Makarov and Canada basins. Deep Sea Research Part II: Topical Studies in Oceanography 44, 1503–1529. https://doi.org/10.1016/S0967-0645(97)00055-6

Tang, C.C.L., Ross, C.K., Yao, T., Petrie, B., DeTracey, B.M., Dunlap, E., 2004. The circulation, water masses and sea-ice of Baffin Bay. Progress in Oceanography 63, 183–228. https://doi.org/10.1016/j.pocean.2004.09.005

Thompson, D.W.J., Wallace, J.M., 1998. The Arctic oscillation signature in the wintertime geopotential height and temperature fields. Geophysical Research Letters 25, 9, 1297–1300. https://doi.org/10.1029/98GL00950

Torres-Valdés, S., Tsubouchi, T., Bacon, S., Naveira-Garabato, A.C., Sanders, R., McLaughlin, F.A., Petrie, B., Kattner, G., Azetsu-Scott, K., Whitledge, T.E., 2013. Export of nutrients from the Arctic Ocean. Journal of Geophysical Research: Oceans 118, 1625–1644. https://doi.org/10.1002/jgrc.20063

Tremblay, J.-É., Anderson, L.G., Matrai, P., Coupel, P., Bélanger, S., Michel, C., Reigstad, M., 2015. Global and regional drivers of nutrient supply, primary production and CO2 drawdown in the changing Arctic Ocean. Progress in Oceanography, Overarching perspectives of contemporary and future ecosystems in the Arctic Ocean 139, 171–196. https://doi.org/10.1016/j.pocean.2015.08.009

Tremblay, J.-É., Gratton, Y., Carmack, E.C., Payne, C.D., Price, N.M., 2002. Impact of the large-scale Arctic circulation and the North Water Polynya on nutrient inventories in Baffin Bay. Journal of Geophysical Research: Oceans 107, 26-1-26–14. https://doi.org/10.1029/2000JC000595

US Department of Commerce, World Ocean Atlas 2013: data access [WWW Document]. URL https://www.nodc.noaa.gov/OC5/woa13/woa13data.html (accessed 6.9.20).

Van Nieuwenhove, N., Head, M.J., Limoges, A., Pospelova, V., Mertens, K.N., Matthiessen, J., De Schepper, S., de Vernal, A., Eynaud, F., Londeix, L., Marret, F., Penaud, A., Radi, T., Rochon, A., 2020. An overview and brief description of common marine organic-walled dinoflagellate cyst taxa occurring in surface sediments of the Northern Hemisphere. Marine Micropaleontology 101814. https://doi.org/10.1016/j.marmicro.2019.101814

Versteegh, G.J.M., Blokker, P., 2004. Resistant macromolecules of extant and fossil microalgae. Phycological Research 52, 325–339. https://doi.org/10.1111/j.1440-183.2004.00361.x

Versteegh, G.J.M., Blokker, P., Bogus, K.A., Harding, I.C., Lewis, J., Oltmanns, S., Rochon, A., Zonneveld, K.A.F., 2012. Infra red spectroscopy, flash pyrolysis, thermally assisted hydrolysis and methylation (THM) in the presence of tetramethylammonium hydroxide (TMAH) of cultured and sediment-derived Lingulodinium polyedrum (Dinoflagellata) cyst walls. Organic Geochemistry 43, 92–102. https://doi.org/10.1016/j.orggeochem.2011.10.007

Walker, M., Head, M.J., Lowe, J., Berkelhammer, M., BjÖrck, S., Cheng, H., Cwynar, L.C., Fisher, D., Gkinis, V., Long, A., Newnham, R., Rasmussen, S.O., Weiss, H., 2019. Subdividing the Holocene Series/Epoch: formalization of stages/ages and subseries/subepochs, and designation of GSSPs and auxiliary stratotypes. Journal of Quaternary Science 34, 173–186. https://doi.org/10.1002/jqs.3097

Walsh, J.E., Chapman, W.L., Fetterer, F., 2015. Updated 2016. *Gridded Monthly Sea Ice Extent and Concentration, 1850 Onward, Version 1*. NSIDC: National Snow and Ice Data Center, Boulder, Colorado USA. https://doi.org/10.7265/N5833PZ5.

Worldview: Explore Your Dynamic Planet [WWW Document], https://worldview.earthdata.nasa.gov/ (accessed 6.23.20).

Yao, T., Tang, C.L., 2003. The formation and maintenance of the North Water Polynya. Atmosphere-Ocean 41, 187–201. https://doi.org/10.3137/ao.410301

Zonneveld, K.A.F., Höll, C., Janofske, D., Karwath, B., Kerntopf, B., Rühlemann, C., Willems, H., 1999. Calcareous Dinoflagellate Cysts as Paleo-Environmental Tools, in: Fischer, G., Wefer, G. (Eds.), Use of Proxies in Paleoceanography: Examples from the South Atlantic. Springer, Berlin, Heidelberg, pp. 145–164. https://doi.org/10.1007/978-3-642-58646-0_5

Zonneveld, K.A.F., Versteegh, G., Kodrans-Nsiah, M., 2008. Preservation and organic chemistry of Late Cenozoic organic-walled dinoflagellate cysts: A review. Marine Micropaleontology, Dinocysts as tracers of hydrographical conditions and productivity along the ocean margins 68, 179–197. https://doi.org/10.1016/j.marmicro.2008.01.015

Chapter 2. [1]Late Holocene sea-surface changes in the North Water Polynya (northern Baffin Bay) inferred from organic-walled dinoflagellate cyst records

[1] Koerner K, Limoges A, Van Nieuwenhove N, Richerol T, Massé G, Ribeiro S. (In Preparation for submission to *Palaeogeography, Palaeoclimatology, Palaeoecology*) Late Holocene sea-surface changes in the North Water Polynya (northern Baffin Bay) inferred from organic-walled dinoflagellate cyst records.

2.1 Abstract

The recent rapid sea-ice melt associated with climate warming has resulted in important changes to the functioning of Arctic ecosystems. In northern Baffin Bay, the formation of the North Water polynya, which is intrinsically linked to local ice conditions and ocean circulation, has become more variable in recent years. This study aims to understand the long-term response of the NOW to climate-driven changes by studying a sedimentary archive that covers the past ca. 3800 years. We analyzed dinoflagellate cysts to infer changes to the sea-surface conditions, and developed a new index based on modern analogue locations. Our results suggest a relatively stable polynya with a long open-water season between ca. 3800 to 2500 years BP, followed by a gradual sea-surface cooling and increased sea-ice influence from 2500 to 1500 years BP. At 2200 years BP there is an important shift in our modern analogue index values and *Halodinium* spp. fluxes that suggest increased freshwater and sea ice influence. From 1500 to 156 years BP, a shorter open-water season and cold conditions prevailed, whereas higher contributions of autotrophic taxa and one to two orders of magnitude increase of dinoflagellate cyst fluxes between 1965 to 2009 CE suggest a rapid shift to more open water conditions. For the uppermost part of our record (2009 to 2015 CE), the assemblages suggest more stratified waters inferred to be a result of increased input of glacial runoff and Arctic sea-ice melt into the NOW region. Arctic climate projections point to accelerated cryospheric melt in the future, which will continue to influence the NOW, pointing to a shift from a stable polynya to a seasonally open gateway between the Arctic Ocean and Baffin Bay.

2.2 Introduction

Ongoing climate change and the Arctic amplification have resulted in a rapid decline of the Arctic cryosphere (e.g., sea ice, permafrost, glaciers, and Greenland ice sheet) (Serreze et al., 2007; Rignot & Kanagaratnam, 2006) with important consequences for the Arctic freshwater budget and the oceanography of adjacent areas. Polynyas, which are areas of open water or low sea-ice concentration in regions characterized by dense sea-ice cover, are particularly sensitive to these changes in the oceanography. The formation of polynyas can be a result of horizontal divergence of ice by the prevailing winds and ocean currents (e.g., latent heat polynyas) or the advection of warm ocean water due to upwelling or tidal mixing (e.g., sensible heat polynyas) (Smith et al., 1990; Maqueda et al., 2004). Polynyas support multiple ecosystem services and can have significant physical and biological impacts at the regional scale. Their relatively open waters play a major role in ocean-atmosphere interactions (e.g., heat loss, water cycle) (Smith et al., 1990), while continuous formation of new sea ice leads to brine rejections that cause vertical mixing and deep-water formation (Schumacher et al., 1983; Smith et al., 1990; Maqueda et al., 2004). The polynya's ice-free waters can also allow the earlier development of the spring algal blooms and result in longer growing seasons that can sustain large and diverse food webs (Stirling, 1997; Marchese et al., 2017).

The North Water (NOW) polynya or *Pikialasorsuaq* is located between Greenland and Ellesmere Island in northern Baffin Bay (Fig. 2.1). The NOW can extend over an area of ~ 80,000 km^2 in early spring (early March), making it the largest recurrent coastal polynya in the Arctic. The opening and maintenance of the NOW polynya are largely associated with the formation of ice arches due to the convergence and grounding of

multiyear Arctic Ocean sea ice and glacial calved ice in the narrow sectors of Nares Strait (Dumont et al., 2009, Rasmussen et al., 2010, Georgiadis et al., 2020; Fig. 2.1).

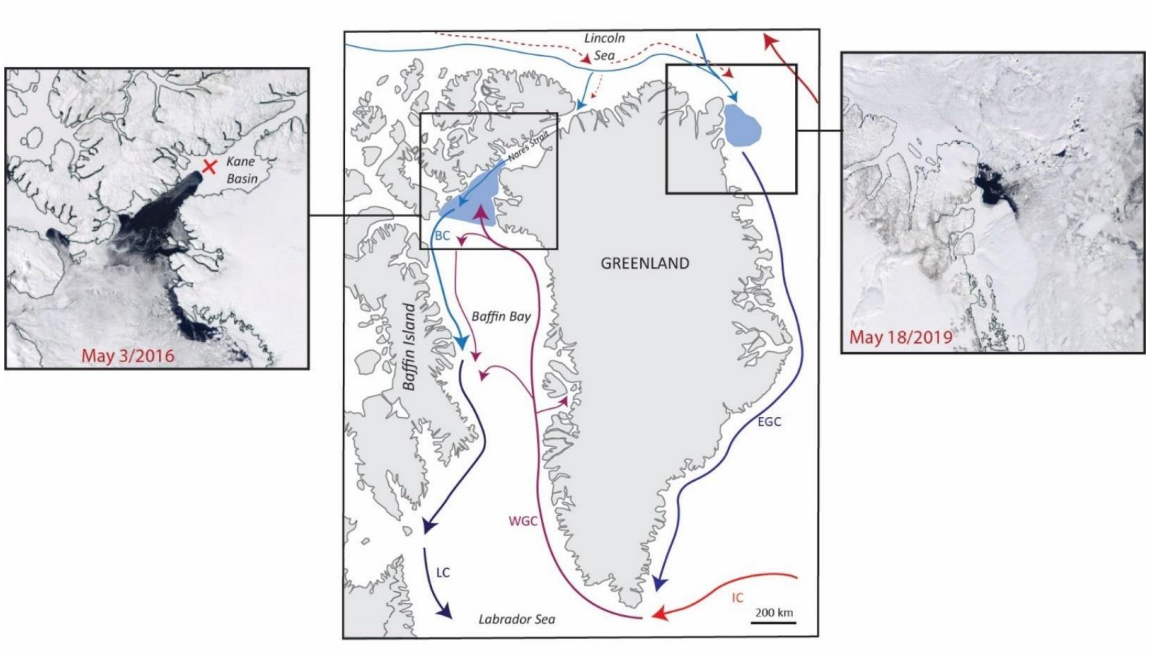


Figure 2.1 Map of Baffin Bay with the main oceanic currents and satellite images of the NOW (left) and NEW (right) polynyas from EOSDIS Worldview. Abbreviations: BC = Baffin Current, WGC = West Greenland Current, LC = Labrador Current, EGC = East Greenland Current, and IC = Irminger Current. The blue shaded areas in the central image represent the average present-day area of the NOW and NEW polynyas. The red arrows indicate relatively warm saline water originating from the North Atlantic. The red X in the satellite image to the left indicates the location of the Kane Basin ice arch.

Together with the southward flowing ocean current, the strong prevailing northerly winds contribute to the formation and cohesion of the Nares Strait ice arches (Dumont et al., 2009), and aid in sweeping newly formed sea ice southwards downwind of the ice arches (Yao & Tang, 2003; Rasmussen et al., 2010). Additionally, relatively warm subsurface waters are advected by the West Greenland Current (WGC) and to some degree contribute to the polynya's maintenance by hindering sea-ice formation, in particular in the southeastern sector, off the Northwest Greenland coast (Melling et al., 2001).

Archaeological evidence suggests that humans have relied on the NOW resources for millennia (Jeppesen et al., 2018; Hastrup et al., 2018) and these resources represent important livelihoods to local communities today. With accelerating warming, and changes in the Arctic occurring at twice the global average rate (IPCC, 2014), significant modifications to the NOW polynya dynamics can be expected. For instance, the increased Arctic warming will put the formation and stability of the ice arches in Nares Strait at risk (Vincent, 2019). As observed in 2007, a failed ice arch can result in increased Arctic Ocean sea ice outflow into the polynya region, thereby reducing the open water area and its duration (Kwok et al., 2010). The future evolution of the polynya with respect to current climate warming is difficult to predict but is certain to bring considerable changes to the composition of the dinoflagellate communities and other primary producers.

The NOW has been the subject of many oceanographic studies aimed at understanding the mechanisms driving its formation and maintenance (Barber et al., 2001; Yao & Tang, 2003; Kwok et al., 2010; Rasmussen et al., 2010; Moore & MacNeil, 2018), and at characterizing its water masses both temporally and vertically (Melling et al., 2001; Bâcle et al., 2002; Lobb et al., 2003; Tang et al., 2004; Münchow et al., 2015). In addition, paleoenvironmental studies have investigated the NOW's response to past climate variability, both in a local (Jackson et al., In Review; Ribeiro et al., In Review; Levac et al., 2001) and regional context (Cormier et al., 2016; St-Onge & St-Onge, 2014; Knudsen et al., 2008; Mudie et al., 2006). Recent paleoenvironmental studies have examined the relationship between keystone species (e.g., Little Auk) and human presence in the light of the NOW polynya dynamics, indicating the importance of the NOW to the ecosystems of northwestern Greenland and Canada (Ribeiro et al., In Review) and the impact of the

polynya in modulating ocean heat transport in the region (Jackson et al., In Review). However, our understanding of the long-term evolution of the NOW polynya is still incomplete due to the low resolution or hiatuses in the existing records.

To address this gap, this study presents high-resolution analysis of organic-walled dinoflagellate cyst (dinocyst) assemblages from a 5.43 m long marine sediment core and corresponding 24.5 cm box core collected from the seafloor of the central region of the NOW polynya. The complete core record spans the last ca. 3800 years and allows the reconstruction of the long-term evolution and sea-surface dynamics of the polynya during the Late Holocene.

Planktic dinoflagellates are single-celled eukaryotes that inhabit the upper water column, where they can be primary producers (autotrophic), micrograzers (heterotrophic) or perform a combination of both trophic strategies (mixotrophic) (Schnepf & Elbrächter, 1992; Jeong et al., 2010). An estimated 15 to 20% of dinoflagellate species produce a highly resistant organic-walled resting stage (or cyst) as part of their life cycle that can be preserved in sediment records (Dale, 1976; Head, 1996; Versteegh & Blokker, 2004). Dinoflagellates are sensitive to changes in the sea-surface conditions (temperature, salinity, sea-ice concentration) and have ecological preferences that are reflected in the composition of the dinocyst assemblages preserved in the sediments. This close relationship between dinocysts and sea-surface conditions is documented by an extensive database linking recent dinocyst assemblages and modern environmental information (de Vernal et al., 2020). This database is used to quantitatively reconstruct various parameters by applying the Modern Analogue Technique (MAT) (e.g., de Vernal et al., 2001, 2013a; 2020; Caron et al., 2019; Allan et al., 2018). The MAT can help infer trends in a selection

of sea-surface parameters, thereby providing more information about past environments (de Vernal et al., 2020). Here we developed indices based on the locations of the MAT analogues to provide a fingerprint of the polynya dynamics through time and complement our interpretation based on the assemblages.

2.3 Oceanographic Setting

The NOW polynya is influenced by two main water currents: the fresh and cold Baffin Current ($T < 0^{o}C$ and $S < 33$ psu) and the relatively warm and saline ($T > 0^{o}C$ and $S > 34$ psu) West Greenland Current (WGC; Bâcle et al., 2002; Fig. 2.1). On the western side of Baffin Bay, the dominant water mass is the Baffin Current. The Baffin Current is mainly composed of Arctic meltwater funneling through Nares Strait, Jones Sound, and Lancaster Sound in the Canadian Arctic Archipelago (Tang et al., 2004; Fig. 2.1). The Baffin Current output has a large effect on northern Baffin Bay, making up two thirds of the total surface waters (Bâcle et al., 2002; Münchow & Melling, 2008; Münchow et al., 2015). The WGC flows northward along the west Greenland margin, and originates from the confluence of the cold and fresh East Greenland Current (EGC) and the relatively warm and saline Irminger Current (IC) at the southern tip of Greenland (Hopkins, 1991; Melling et al., 2001; Fig. 2.1). Further mixing occurs between relatively fresh water hypothesized to be sourced from the Baffin Current (Rysgaard et al., 2019) and the WGC as it moves northward towards the NOW, thereby slightly diluting and cooling the WGC (Tang et al., 2004; Rysgaard et al., 2019). The depth of the WGC varies as it moves towards northern Baffin Bay due to turbulent exchange with the surface waters (Bâcle et al., 2002; Melling et al., 2001).

2.4 Methods

The marine sediment cores AMD15-Casq1 and AMD15-Casq1-BC4 were collected in 2015 using a Calypso Square (CASQ) gravity corer and box corer (BC), respectively. Both cores were collected in the central region of the NOW polynya (77°17.097'N - 74°23.214''W) at a water depth of 700 m during the ArcticNet 2015 Leg 4a expedition of the CCGS Amundsen. The AMD15-Casq1 core was subsampled onboard using u-channels and the box core was subsampled onboard at 0.5 to 1-cm intervals. All material was transported and stored at 4°C.

2.4.1 Geochronology

The box core chronology was developed using core AMD15-Casq1-BC1 (47 cm length) collected from the same box core as AMD15-Casq1-BC4 (24.5 cm length; used here for the dinocyst analysis), and is based on down-core measurements of ^{210}Pb, ^{226}Ra, and ^{137}Cs activity performed on 12 samples (2-cm resolution; Fig. 2.2a). Additionally, the uppermost 12.5 cm of AMD15-Casq1 was also analyzed for ^{210}Pb to calculate the overlap between the two sediment records and achieve a composite age-model for the complete record (Fig. 2.2a). The AMD15-Casq1 core chronology was established based on eleven radiocarbon dates obtained from bivalve shell fragments. Both the ^{210}Pb/ ^{137}Cs and radiocarbon geochronologies are presented in (Ribeiro et al., In Review; Fig. 2.2b). Accordingly, the core spans the past ca. 3800 years. Ages presented in the manuscript are the modelled means (shown both as calibrated years before present, cal years BP and calibrated years before Common Era, cal years CE/BCE). We note that there is a hiatus of 171 years between the bottom of the box core AMD15-Casq1-BC4 and the top of the gravity core AMD15-Casq1.

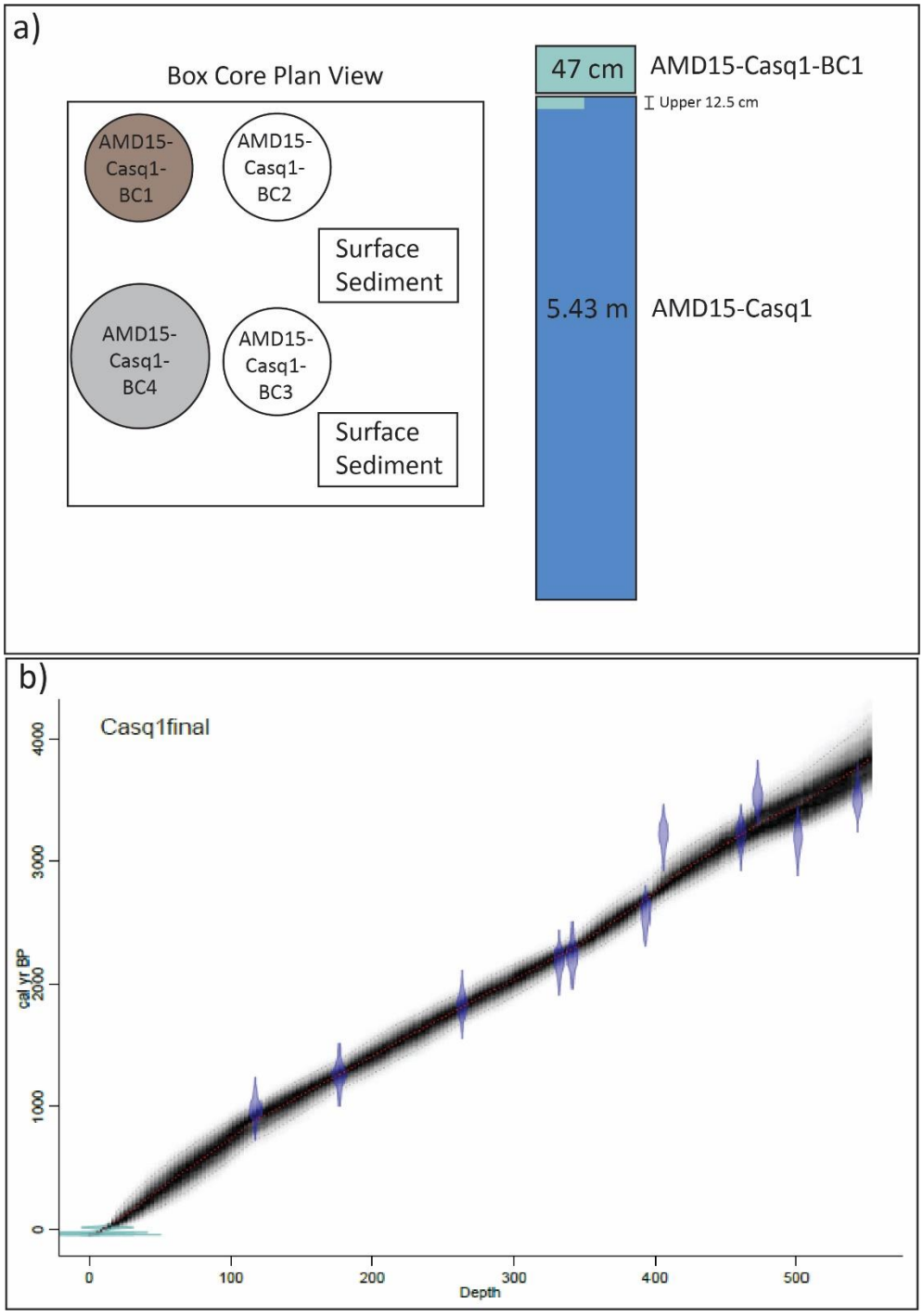


Figure 2.2 a) Box core plan view showing the coring locations of AMD15-Casq1-BC1 (brown) and AMD15-Casq1-BC4 (grey), and the core lengths of AMD15-Casq1-BC1 and AMD15-Casq1 with the geochronology used for each core: radiocarbon (blue) and ^{210}Pb (light blue) b) *Composite age model for core AMD15-Casq1 including the box core, based on 11 radiocarbon dates from the long Casq core (dark blue) and the ^{210}Pb dates retrieved for the box and Casq core (light blue).*

2.4.2 Dinoflagellate Cysts

Palynological treatments were done at Ghent University, Belgium, following the procedure described in Quaijtaal et al. (2014). The sediment samples from AMD15-Casq1 and AMD15-Casq1-BC4 were freeze-dried, weighed, and rehydrated with demineralized water. Calibrated tablets of *Lycopodium clavatum* spores were subsequently added to each sediment sample to allow later calculation of the absolute dinocyst concentrations and fluxes (Stockmarr, 1971).The sediment was treated with room temperature hydrochloric (HCl, 2N) and hydrofluoric (HF, 40%) acids to dissolve carbonates and siliceous material, respectively. The samples were rinsed with deionized water between each acid treatment. Samples were then subsequently sonicated to break up any clumps of amorphous organic material present and sieved with a 10 µm nylon mesh to remove finer particles. Residue was mixed with glycerin jelly and mounted onto microscope glass slides for observation. The dinocysts were identified using a light microscope (Olympus BX43 at the University of New Brunswick) at magnification of 400-1000x. Dinocyst assemblages were analyzed at a 5 cm sampling interval, which corresponds to a mean effective age resolution of ca. 34 years for AMD15-Casq1, and at a 0.5 cm sampling interval for the first 10 cm and then every 1 cm for the rest of AMD15-Casq1-BC4, with mean effective age resolution of ca. 2 years, based on the geochronology presented above.

A minimum of 300 and up to 1500 dinocysts were counted per slide (see Appendix 1). Fluxes were calculated by multiplying the dinocyst concentrations (cysts g^{-1}) by the mass accumulation rate (g cm^{-2} yr^{-1}). Taxonomic identifications were done following descriptions presented in Radi et al. (2013), Potvin et al. (2018), Limoges et al. (2020) and Van Nieuwenhove et al. (2020). Smooth and spiny round brown cysts were identified

respectively as “round brown” and “spiny brown” when the cyst preservation and/or orientation did not permit an identification to the species level. Below, cysts produced by autotrophic dinoflagellates will simply be referred to as “autotrophs” or “autotrophic taxa/species”, and those produced by heterotrophic dinoflagellates as “heterotrophs” or “heterotrophic taxa/species”. Note that cysts of the autotrophic *Polarella glacialis* were not included in the calculated ratios between the autotrophic and heterotrophic taxa. This decision is based on the different ecological niche occupied by the sea-ice associated *Polarella glacialis* (Montresor et al., 1999, 2003; Stoecker et al., 2000), compared to the other open-water autotrophs observed here.

Hierarchical clustering was done as part of an exploratory data analysis and used to help define stratigraphically constrained bioenvironmental zones. All taxa were included, and their relative abundances were log-transformed before analysis to account for the presence of both rare and very dominant taxa in the assemblages. The cluster analysis was calculated with the software program Past4 (Hammer et al., 2001) using a stratigraphically restricted, unweighted pair group average (UPGMA) algorithm and a Bray-Curtis similarity index. A post hoc broken-stick model was also computed using Past4 to determine whether clusters differed statistically from each other (Hammer et al, 2001).

2.4.3 Modern Analogue Technique

To extract quantitative information about changes in sea-surface conditions, the Modern Analogue Technique (MAT) developed for dinocyst assemblages was used (Guiot & de Vernal, 2007). The MAT compares the species composition of downcore dinocyst assemblages to modern assemblages from surface sediment samples collected

across the Northern Hemisphere (de Vernal et al., 2001). The modern dinocyst assemblages are then coupled with satellite data of sea-ice concentration from the National Snow and Ice Data Center (de Vernal et al., 2013a) and sea-surface temperature and salinity data from the World Atlas 2013, compiled by the National Ocean Data Center (de Vernal et al., 2013a, 2013b, 2020; Radi & de Vernal, 2008). The MAT relies on the assumption that similar dinocyst assemblages occur in similar environmental conditions through time and that the sea-surface conditions influence the composition of the dinocyst assemblages present. The most recent dataset and the one used in this study contains 1968 samples (de Vernal et al., 2020). Before running MAT, the data was log-transformed to accurately represent rare, but ecologically significant species. For each sample, the five most similar modern analogues were determined using the R software package (https://cran.r-project.org/).

2.4.4 Modern Analogue Index

Rather than solely relying on the values reconstructed by the MAT for each sea-surface parameter, we exploited the potential of the MAT by developing a new index based on the location of the five modern analogues selected for each sample. Each index and its value can be interpreted as providing a fingerprint of the sea-surface conditions at the core site at any particular time. In a first step, the locations of all selected analogues were evaluated and assigned to a particular index depending on their location. Accordingly, three indices were retained: one grouping the modern sites that occur in the modern-day North Water polynya (NOW index), those occurring in the Northeast Water polynya (NEW index) located on the shelf northeast of Greenland (Fig. 2.1), and those

occurring in a non-recurring polynya setting (Fig. 2.3). In the database, a total of 24 sites are in the NEW polynya, whereas 70 sites are distributed across the NOW polynya.

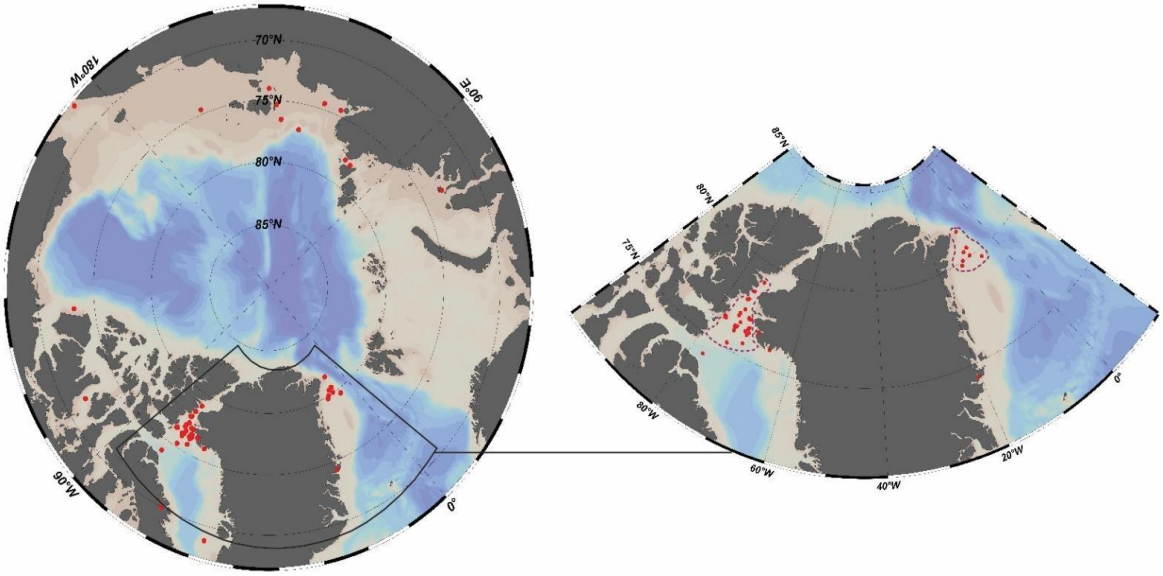


Figure 2.3 The locations of the MAT analogues (in red) based on the dinocyst assemblages from AMD15-Casq1 and BC4 with the average spring extent of the NOW and NEW polynyas in purple dotted lines. Figures completed using Ocean Data View.

In a second step, each index value for a particular core sample was calculated by summing all inverse values of the statistical distance of the modern analogue belonging to a specific domain. The statistical distance represents the degree of similarity between the sample and its selected modern analogue, with a smaller distance implying that a downcore assemblage is more similar to the modern analogue, and thus more likely to reflect similar environmental conditions (Guiot & de Vernal, 2007). A concrete example of how the index values were calculated is shown in Equation 1.

$$NOW\ index\ value = \frac{1}{Distance\ 1} + \frac{1}{Distance\ 4}$$

$$NEW\ index\ value = \frac{1}{Distance\ 2} + \frac{1}{Distance\ 3}$$

$$non\text{–}polynya\ index\ value = \frac{1}{Distance\ 5}$$

Equation 1. Example of the calculation of the MAT indices for a sample for which two modern analogue sites (1 and 4) are located within the modern day NOW, two sites (2 and 3) are located within the modern day NEW, and one site (5) is located in a non-recurring polynya setting. The distance refers to the degree of similarity between the fossil assemblage and each of the five modern assemblages, as calculated by the MAT script.

2.5 Results

Dinocyst fluxes range between ~1400 and 14500 cysts cm^{-2} yr^{-1}, with an average value of ~3700 cysts cm^{-2} yr^{-1}. The main dinocyst taxa are *Islandinium minutum* subsp. *minutum* (16 to 85%), cysts of *Pentapharsodinium dalei* (< 2 to 36%), *Brigantedinium* spp. (includes *B. simplex* and *B. cariacoense*; 1 to 35%), round brown cysts (0 to 13%), *Islandinium*? *cezare* (0 to 12%), *Echinidinium karaense* (0 to 11%), spiny brown cysts (0 to 9%), *Operculodinium centrocarpum* (includes *O. centrocarpum* with short processes and the Arctic morphotypes (de Vernal et al., 2001); 0 to 9%), spiny brown cysts with long processes (0 to 4%), *Islandinium minutum* subsp. *barbatum* (0 to 2%), *Spiniferites* spp. (< 2%), *Spiniferites elongatus* (< 2%), cf. *Islandinium brevispinosum* (< 2%), specimens similar to those identified as cysts of *Polykrikos?* sp. by Kunz-Pirrung (1998) (also reported as "Arctic morphotype"; e.g., de Vernal et al., 2001; < 2%), and cysts of *Polarella glacialis* (0 to 0.65%) (Table 2.1, Figs. 2.4, 2.5, and 2.6). Fluxes of foraminiferal

linings and the acritarch *Halodinium* spp. ranged from 36 to 6200 linings cm^{-2} yr^{-1} and 9 to 6300 specimens cm^{-2} yr^{-1}, respectively (Fig. 2.7).

Cluster analysis highlights the most important changes in the composition of the dinocyst assemblages to occur around 2500 years BP, 1500 years BP, between 156 years BP and 1965 CE, as well as around 2009 CE (Fig. 2.6). The MAT led to the identification of 66 modern analogues, mainly distributed across the Arctic (Fig. 2.3). More than half of the analogues were located within two recurrent polynyas: The NOW polynya (N = 33) and the NEW polynya (N = 7) (Fig. 2.3). Based on these results, five bioenvironmental zones were defined (Figs. 2.6, 2.7, 2.8):

Zone 1 (3822 to 2500 years BP) is characterized by the highest, but gradually decreasing relative abundances of autotrophic taxa, including *Operculodinium centrocarpum* and *Spiniferites* spp., which translates into relatively high A/H ratios. The relative abundances of *Brigantedinium* spp. are high, while the other dominant heterotrophic taxa show lower abundances compared to the rest of the core (Fig. 2.6). The cyst of *Polarella glacialis*, the only dinoflagellate that is known to go through encystment in the sea-ice matrix (e.g., Stoecker et al., 2000) and for which cysts have a potential of preservation in the sediment, is also observed within this interval (Fig. 2.6). The NOW MAT index shows the highest overall values of the core, whereas the NEW MAT index shows relatively low values during this interval (Fig. 2.8).

Zone 2 (2500 to 1500 years BP) is characterized by a decrease in the contribution of the autotrophic taxa, as expressed by low A/H ratios (Fig. 2.6). Importantly, there is an increase in the contribution of the "cold water" taxa *Islandinium minutum, Islandinium*? *cezare,* and *Echinidinium karaense* to the assemblages (Head et al., 2001).

Dinoflagellate cyst Taxa	Motile Taxon	Trophic Mode	Grouped as
Brigantedinium spp.	Peridiniaceae	H	
Brigantedinium cariacoense	*Protoperidinium avellanum*	H	*Brigantedinium* spp.
Brigantedinium simplex	*Protoperidinium conicoides*	H	
Round Brown	Unknown	H	Round Brown
Islandinium minutum subsp. *minutum*	*Protoperidinium* sp. indet	H	*Islandinium minutum*
Islandinium ? *cezare*	*Protoperidinium* sp. indet	H	*Islandinium*? *cezare*
Islandinium minutum subsp. *barbatum*		H	*Islandinium minutum* subsp. *barbatum*
Echinidinium karaense	*Diplopsalid* or *Protoperidinoid* group	H	*Echinidinium karaense*
Spiny Brown	Unknown	H	Spiny Brown
Spiny Brown Very Long Processes	Unknown	H	Spiny Brown Very Long Processes
Cyst of *Polykrikos?* sp. of Kunz-Pirrung (1998)	*Polykrikacea* group	H/A	Cyst of Polykrikos? sp. of Kunz-Pirrung (1998)
Cyst of *Polarella glacialis*	*Polarella glacialis*	A*	Cyst of *Polarella glacialis*
Cyst of *Pentapharsodinium dalei*	*Pentapharsodinium dalei*	A	*Pentapharsodinium dalei*
Operculodinium centrocarpum	*Protoceratium reticulatum*	A	
Operculodinium centrocarpum – short processes	*Protoceratium reticulatum*	A	*Operculodinium centrocarpum*
Operculodinium centrocarpum –Arctic morphotype	*Protoceratium reticulatum*	A	
Spiniferites spp.	*Gonyaulax* spp.	A	*Spiniferites* spp.
Spiniferites elongatus	*Gonyaulax elongata*	A	*Spiniferites elongatus*

*Table 2.1 The main (> 1%) dinocyst taxa observed in this study. Abbreviations: A = Autotrophic, H = Heterotrophic. *indicates that the taxa were not included in the A/H ratio (Wall & Dale, 1966; Lewis et al., 1984; Potvin et al., 2013; Claparède and Lachmann, 1859 & Ellegaard et al., 2003).*

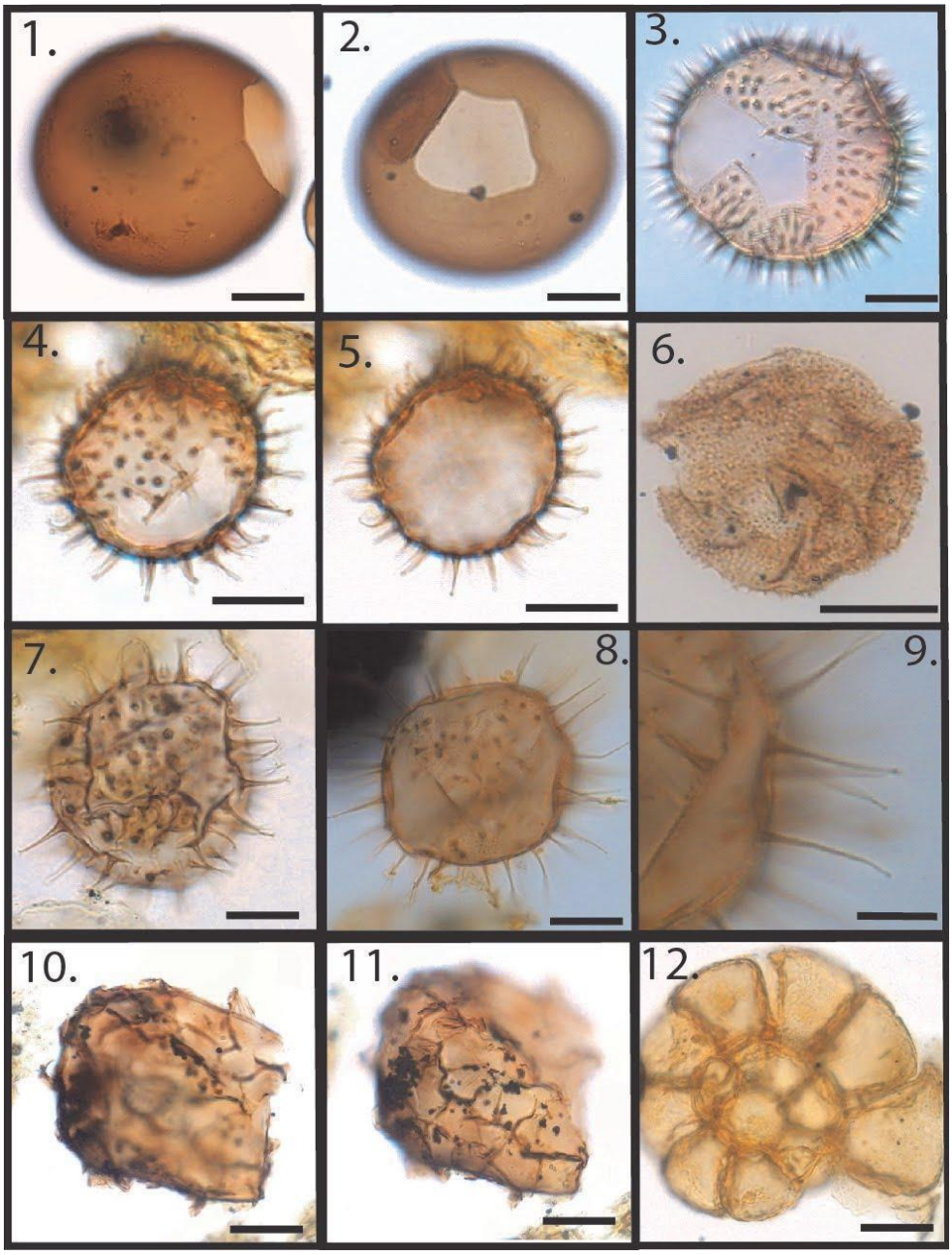


Figure 2.4 Micrographs of selected organic-walled microfossils observed in the sediment core AMD15-Casq1: 1) Brigantedinium *spp., 2)* Brigantedinium simplex, *3)* Islandinium minutum *subsp.* minutum, *4-5)* Islandinium*?* cezare, *6) cf.* Islandinium brevispinosum, *7)* Echinidinium karaense, *8)* Islandinium minutum *subsp.* barbatum, *9)* Islandinium minutum *subsp.* barbatum *showing the process termination and characteristic "barbs" on the processes, 10-11) Cyst of* Polykrikos*? sp. of Kunz-Pirrung (1998) 12) Foraminiferal lining. Scale bar: 25 µm.*

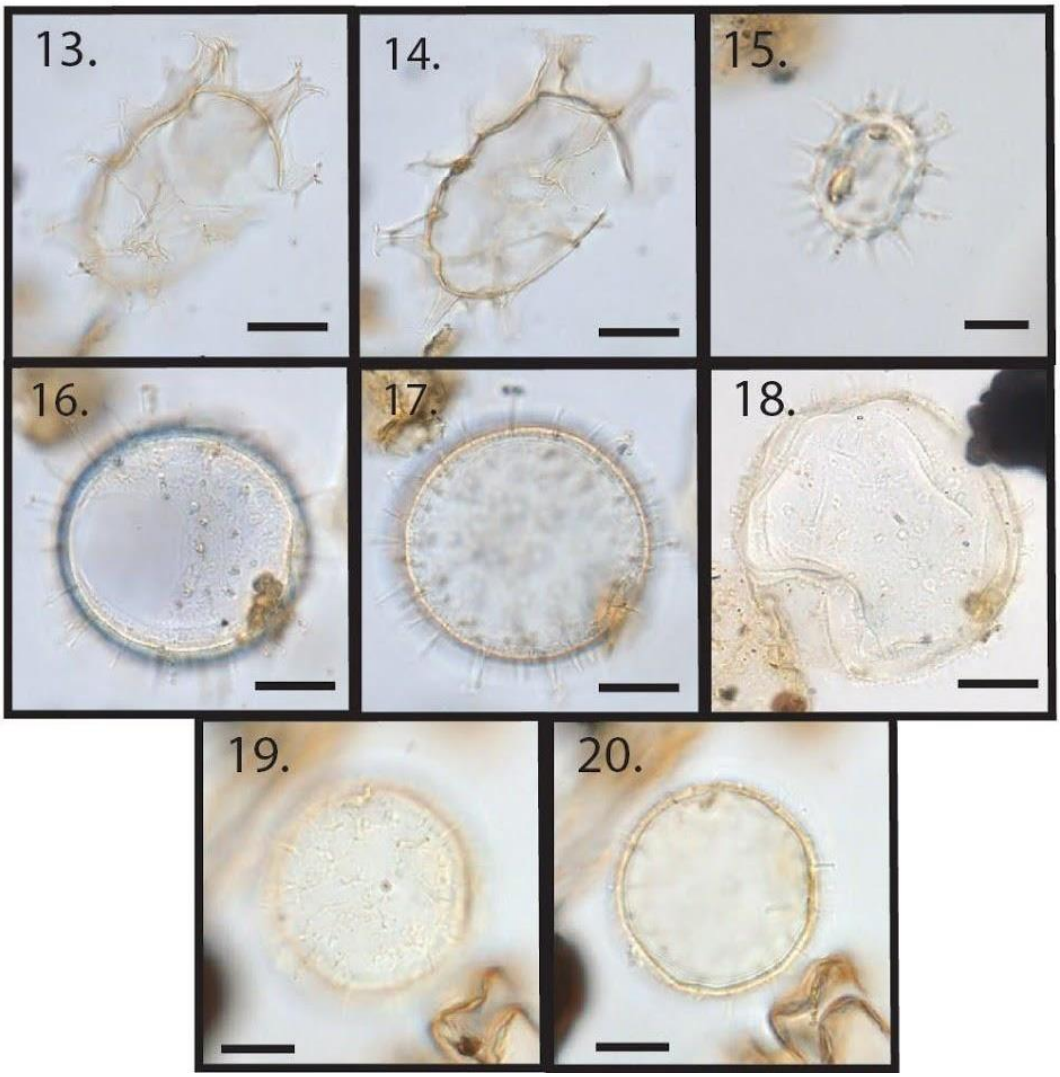


Figure 2.5 Micrographs of selected cysts produced by autotrophic dinoflagellates observed in the sediment core AMD15-Casq1. 13-14) Spiniferites elongatus, *15) cyst of* Polarella glacialis, *16-17)* Operculodinium centrocarpum, *18)* Operculodinium centrocarpum *Arctic morphotype, 19-20) cyst of* Pentapharsodinium dalei. *Scale bar: 25 µm.*

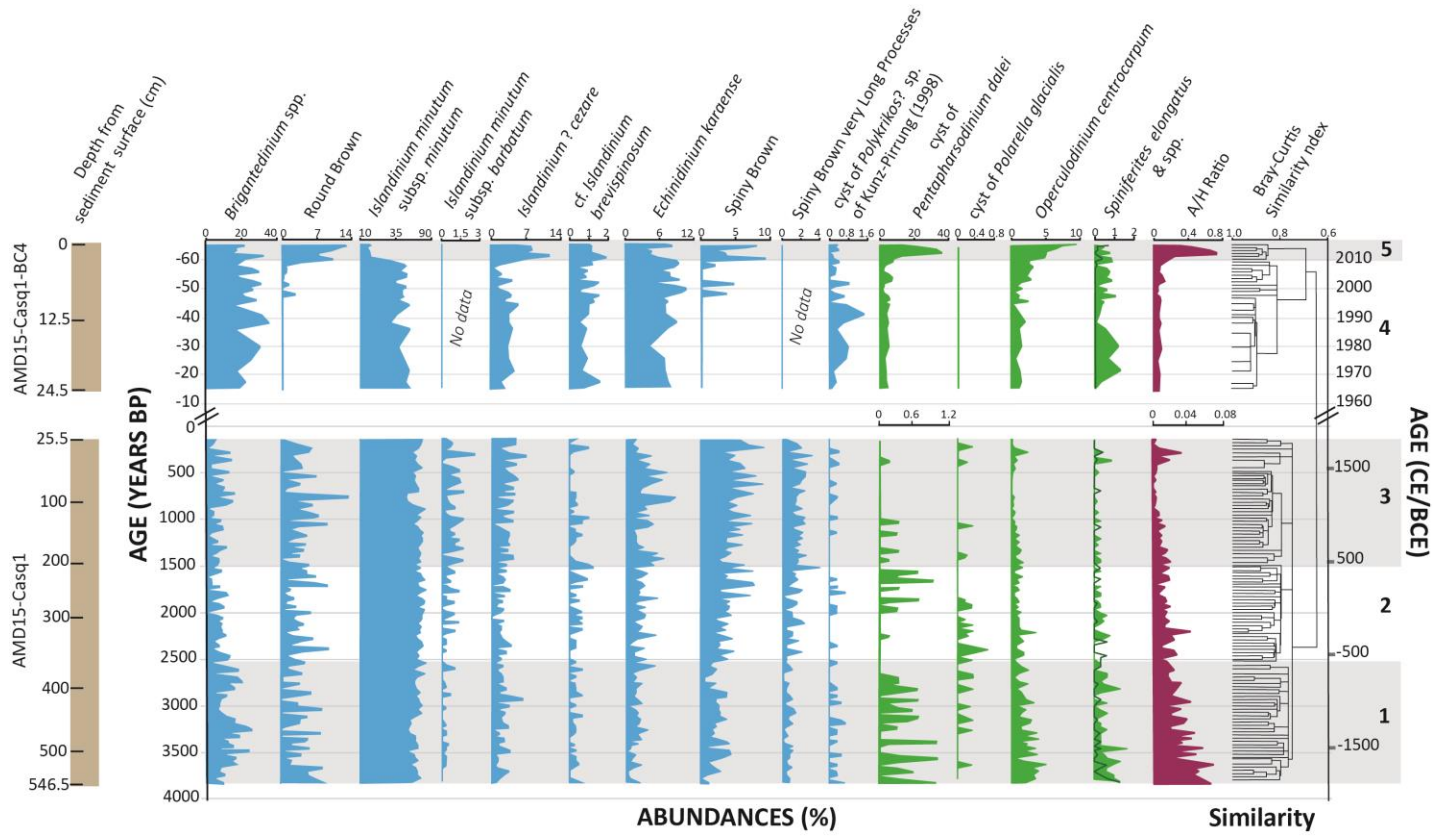


Figure 2.6 Relative abundances of the main taxa counted in our marine records, also showing the Bray-Curtis Similarity Index for the assemblages. Blue represents those taxa that are produced by heterotrophic dinoflagellates, green represents those produced by autotrophic taxa. The A/H ratio is shown in purple, where A = autotrophic taxa (excluding cysts of Polarella glacialis*) and H = heterotrophic taxa. The dark green represents* Spiniferites *spp. The gray and white and numbers 1-5 indicate the bioenvironmental zones. The brown shows the depth from seafloor surface of AMD15-Casq1 and AMD15-Casq1-BC4. Note the different scales for the X-axis of Casq1 and BC4 for the cyst of* Pentapharsodinium dalei*, the A/H ratio, and the hiatus at 1960 years CE on the y-axis. Years BP refers to Before Present = 1950.*

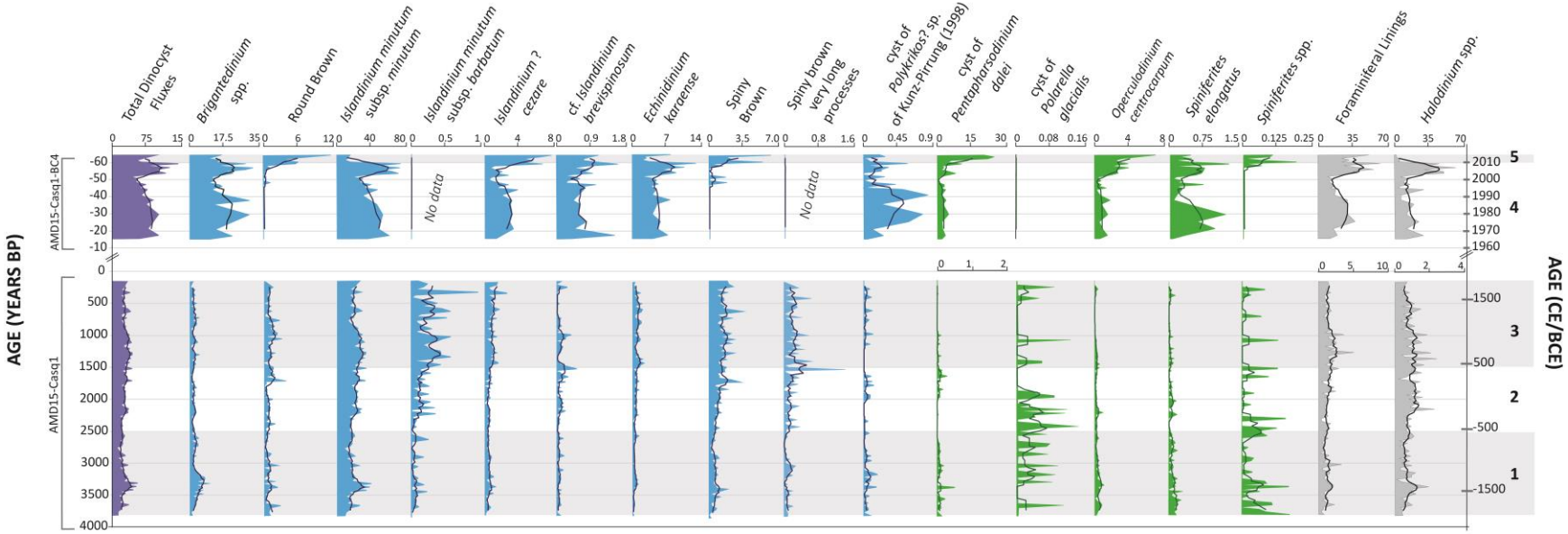


Figure 2.7 Fluxes of the main dinocyst taxa and palynomorphs counted in our marine records. The thick line represents the 5-point moving average. Purple = total dinocysts, blue = heterotrophic taxa, green = autotrophic taxa, all in 10^2 *cysts* cm^{-2} $year^{-1}$*. The grey = foraminiferal linings (*10^2 *linings* cm^{-2} $year^{-1}$*) and* Halodinium *spp. (*10^2 *specimens* cm^{-2} $year^{-1}$*). The gray and white boxes represent the bioenvironmental zones (1-5). Note the different scales for the X-axis of Casq1 and BC4 for the cyst of* Pentapharsodinium dalei*, the foraminiferal linings and* Halodinium *spp. The grey and white represent the bioenvironmental zones. Note the hiatus at 1960 years CE.*

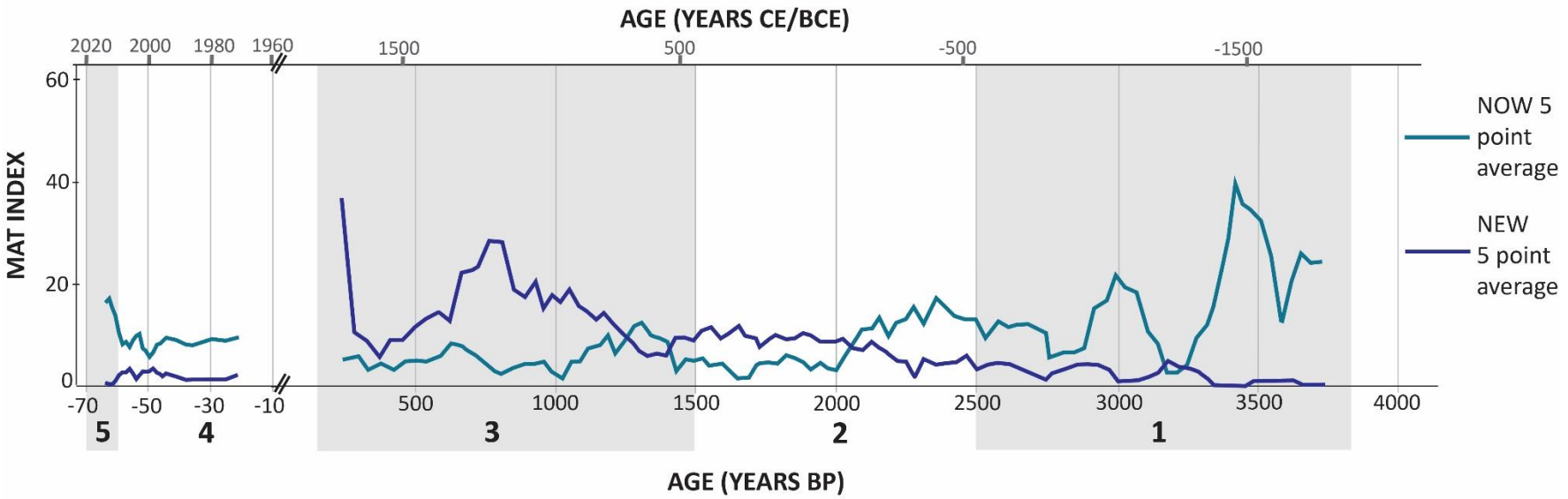


Figure 2.8 Evolution of the MAT index 5-point moving average in Casq1 and BC4, with indication of the associated bioenvironmental zones (1 to 5). A higher index value indicates a greater degree of similarity to the modern NOW or NEW conditions. Note the different time scale before and after 1960 CE, and the hiatus at 1960 years CE/-10 years BP.

The highest relative abundances of the cyst of *Polarella glacialis* are also observed within this interval (Fig. 2.6). Foraminiferal lining fluxes are at the lowest for the entire core, whereas *Halodinium* spp. fluxes increase to their highest value of AMD15-Casq1 (Fig. 2.7). Around 2200 years BP, a shift in the MAT indices takes place and the NEW values become higher than the NOW values (Fig. 2.8).

Zone 3 (1500 to 156 years BP) is characterized by relatively high abundances of *Islandinium*? c*ezare, Islandinium minutum* subsp. *minutum* and *Islandinium minutum* subsp. *barbatum* compared to the rest of the core. Autotrophic taxa are only minor contributors to the assemblages during this interval and the A/H ratio reaches its lowest value of the entire core record, followed by a small increase in values between ca. 500 to 156 years BP (Fig. 2.6). High fluxes of *Halodinium* spp. and foraminiferal linings are also observed in this zone (Fig. 2.6). The NEW MAT index reaches its highest value, whereas the NOW MAT index remains low (Fig. 2.8).

Zone 4 (1965 to 2009 years CE) shows higher abundances of autotrophic taxa expressed by higher values of the A/H ratio (Fig. 2.6). The overall fluxes of total dinocysts is one to two orders of magnitude larger in this interval than in the rest of the core. Foraminiferal linings and *Halodinium* spp. fluxes range between 990 to 6160 linings cm^{-2} yr^{-1} and 450 to 6265 specimens cm^{-2} yr^{-1} respectively, which is the highest of the entire core (Fig. 2.6). Important to note are the absence of the cyst of *Polarella glacialis* in the box core and the minor contribution (< 1%) of *Ataxiodinium choane*, *Bitectatodinium tepikiense*, *Nematosphaeropsis labyrinthus*, *Spiniferites ramosus*, *Quinquecuspis concreta, Votadinium calvum* and *Selenopemphix quanta*.

Zone 5 (2009 to 2015 years CE) shows a substantial decrease in the cold-water associated taxa *Islandinium minutum, Islandinium*? *cezare* and *Echinidinium karaense* relative to AMD15-Casq1 (Fig. 2.6), and the MAT index returns to higher NOW values (Fig. 2.8). This interval shows a substantial increase in the abundance of cysts of *Pentapharsodinium dalei* and a sharp increase in the A/H ratio (Fig. 2.6).

2.6 Discussion

Our results show that for the entire core record, the dinocyst fluxes to the seafloor are one order of magnitude larger at our study site (~1400 and 14500 cysts cm^{-2} yr^{-1}) than at other sites in northern Baffin Bay, such as Melville Bay (~50 to 390 cysts cm^{-2} yr^{-1}; Caron et al., 2019) and Kane Basin (0 to ~400 cysts cm^{-2} yr^{-1}) (Mudie et al., 2006; Caron et al., 2019; Fig. 2.7). This suggests overall persistently higher dinocyst productivity at the study site compared to other sectors of northern Baffin Bay located outside of the present-day polynya area, during the last ca. 3800 years.

2.6.1 MAT Indices

The MAT indices show a unique polynya signature for most of the record, which is reflected by the modern analogues being almost exclusively located in two recurrent polynya settings, the NOW and the NEW polynya, with a small portion of analogues plotting in known flaw or lead polynya settings (i.e., openings between landfast and pack ice, or fractures in the sea ice, respectively; Fig. 2.3).

The NEW polynya forms on the northeastern coast of Greenland between 77º–81ºN (Maqueda et al., 2004; Fig. 2.1). The NEW formation is primarily influenced by landfast ice that blocks incoming sea ice advected via the Arctic-sourced EGC from

entering the NEW polynya region (Barber & Massom, 2007), and the anticyclonic circulation which connects the southward flowing EGC and the northward flow of the Northeast Greenland Coastal Current (Budéus et al., 1997). The sea-surface waters in the NEW consist of a fresh and cool ($T < 0^{o}C$ and $S = 32.5$) water mass of 150 m in thickness that is predominately sourced from localized run off from the Greenland Ice sheet and Polar Water incorporated from an anticyclonic gyre off the coast of northeastern Greenland (Budéus & Schneider, 1995; Budéus et al., 1997). Thus, one of the differences between the NOW and the NEW polynyas is the dominance of relatively cold and fresh water in the NEW (Budéus et al., 1997; Rudels et al., 2005), as opposed to an influence of both freshwater and advection of relatively warm and saline WGC influence the NOW at the sea surface (Melling et al., 2001; Bâcle et al., 2002). In recent years, the NEW polynya recurrently opens from April/May and has a shorter open-water season than the NOW, which typically opens from early March. Therefore, we interpret swings in the MAT indices from higher/lower NOW to higher/lower NEW values to hint at changes in the polynya dynamics through time. As such, intervals of higher NEW index values may suggest colder, fresher, and relatively more contracted polynya conditions compared to intervals when the NOW index is dominant.

Considering the above, one could wonder why the highest values for the NOW index occur in the lower half of the AMD15-Casq1 core rather than closer to the surface of AMD15-Casq1-BC4. However, it is also important to consider how the taxonomic groupings were assigned in the modern reference database. While including or excluding particular morphotypes from a taxonomic unit will only marginally influence the overall assemblage composition, it will have some influence on the percentage shares of the

different taxa that make up the assemblage, thereby modulating the degree of similarity – used for calculating the index values – of a fossil sample to a modern analogue. This can be assumed to be a contributing factor for the lower NOW values in the upper part of the box core compared to the high values seen between ca. 3800 to 3000 years BP in the AMD15-casq1 core (Fig. 2.8). Furthermore, when a surface sample from a box core is also one of the analogue sites in the MAT database, it cannot be selected as an analogue location (i.e. the analogue cannot select itself). This is the case here where the surface sample from AMD15-Casq1-BC4 is included in the MAT database, and explains why the uppermost, most recently deposited analyzed sample does not have the highest NOW index value.

2.6.2 Late Holocene changes in sea surface conditions in the NOW

Based on sediment archives from lake and peat deposits along the northwest Greenland coast, Davidson et al. (2018) suggested that the inception of the NOW polynya occurred ca. 4500 years BP. Benthic foraminiferal analysis from a marine core located at the periphery of the NOW also supports this timeline (Jackson et al., In Review). Accordingly, our marine core record encompasses a time in which the NOW was supposedly recurrently forming.

AMD15-Casq1 (3822 to 156 years BP) encompasses the well-documented Neoglacial cooling, a period of decreased summer insolation in the Northern Hemisphere (Berger & Loutre, 1991) that is reflected in the $\delta^{18}O$ values from the Agassiz ice core on Ellesmere Island (Lecavalier et al., 2017; Fig. 2.9). The dinocyst assemblage record presented here also reflects a general sea-surface cooling trend from ca. 3800 towards 156

years BP indicated by increasing contributions of the cold-water taxa *Islandinium minutum, Islandinium*? *cezare* and *Echinidinium karaense* (Head et al., 2001; Fig. 2.9). This is consistent with previous observations made in the NOW region (St-Onge & St-Onge, 2014; Knudsen et al., 2008; Levac et al., 2001) and in other areas of eastern Baffin Bay such as Melville Bay (Caron et al., 2019), Disko Bay (Moros et al., 2016; Ribeiro et al., 2012; Ouellet-Bernier et al., 2014; Perner et al., 2011, 2013; Seidenkrantz et al., 2008; Andresen et al., 2011), southern Greenland (Sha et al., 2017), and off the coast of Labrador (Lochte et al., 2019).

2.6.2.1 Relatively stable NOW with prolonged open-water season (3822 to 2500 years BP)

From 3822 to 2500 years BP, we observe the highest abundances of the autotrophic taxa *Operculodinium centrocarpum, Spiniferites elongatus* and *Spiniferites* spp. (Fig. 2.6), suggesting a relatively long open-water duration in the NOW, with a well-defined summer season as preferred by these taxa (Heikkilä et al., 2014, 2016). During this interval, generally warmer air temperatures are inferred from the low Agassiz ice core $\delta^{18}O$ values (Lecavalier et al., 2017; Fig. 2.9). The NOW MAT index values are high, indicating that dinocyst assemblages during this interval were most similar to modern assemblages, and suggesting that comparable environmental conditions prevailed in the NOW (Fig. 2.8). This would be coherent with a relatively stable ice margin and long open-water season during this interval.

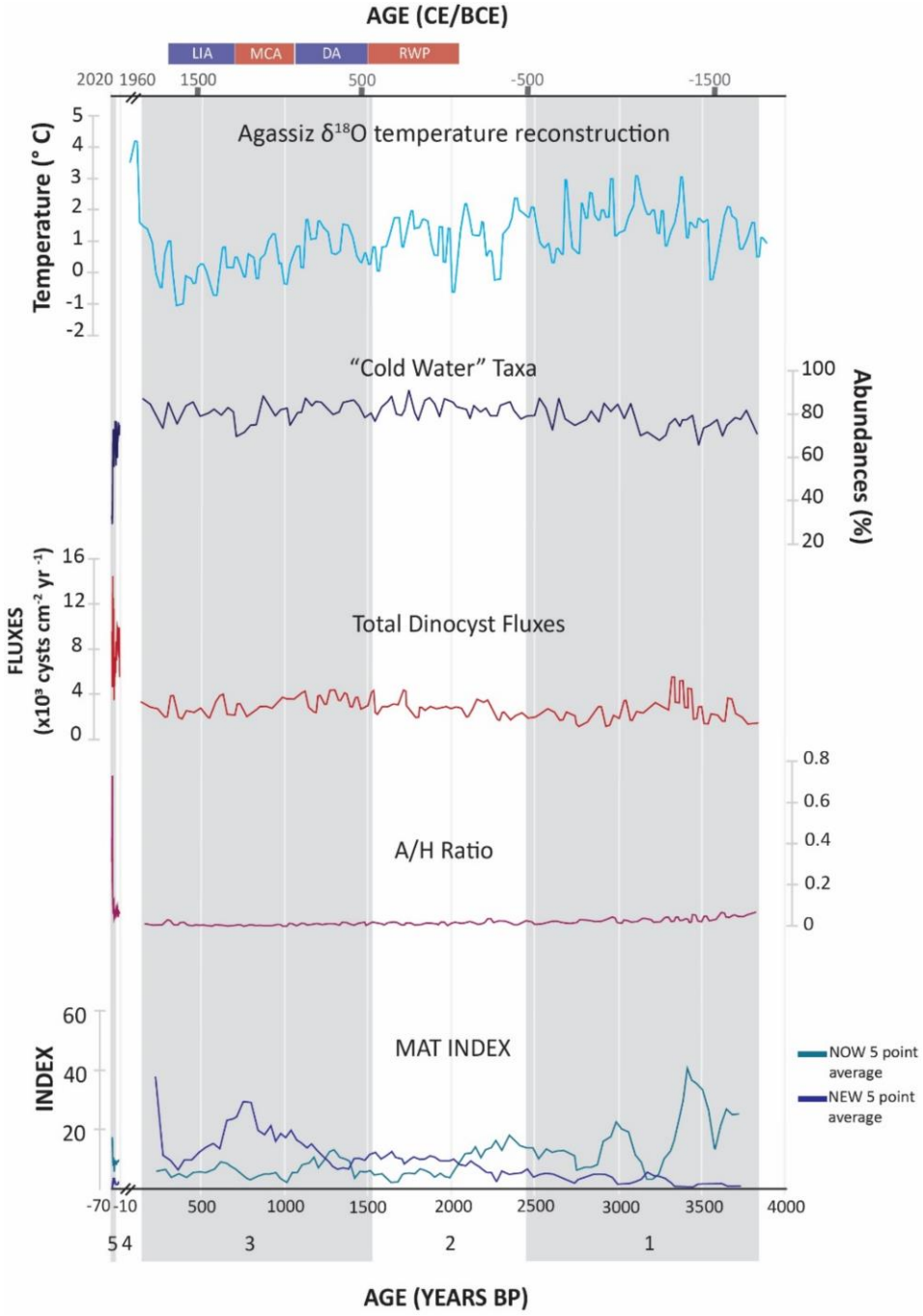


*Figure 2.9 The MAT index 5-point moving average, A/H ratio, total dinocyst fluxes, cold water taxa (*Islandinium minutum, Islandinium*?* cezare, Echinidinium karaense*) (Head et al., 2001), and Agassiz $\delta^{18}O$ temperature reconstruction (Lecavalier et al., 2017). The grey and white represent the bioenvironmental zones (1-5) that were defined based on the dinocyst assemblages. The abbreviations at the top of the graph represent: Little Ice Age (LIA), Medieval Climate Anomaly (MCA), Dark Ages Cold Period (DA) and the Roman Warm Period (RWP). Note the hiatus at 1960 years CE.*

South of the NOW in Melville Bay and Disko Bay, there is a clear regional signal of higher abundances of "warm-water" taxa (i.e., *Operculodinium centrocarpum* and *Spiniferites elongatus*) interpreted to reflect increased WGC influence along the western Greenland shelf from ca. 3400 to 2100 years BP (Caron et al., 2019) and ca. 3600 to 1500 years BP (Allan et al., 2018). Along the west Greenland shelf, diatom data suggest relatively high but decreasing primary production from ca. 4400 to 3000 years BP (Krawczyk et al., 2017; Limoges et al., submitted). We postulate that a longer open-water duration in a relatively stable NOW is likely the reason for high autotrophic abundances in this interval, rather than increased WGC influence within the NOW polynya. A longer open-water season starting relatively early in spring and lasting into fall, allows for longer sea-ice formation and thus brine production in the NOW. Indeed, benthic foraminiferal assemblages at our study site also suggest enhanced sea-ice formation within the NOW between ca. 3800 to 3000 years BP, resulting in the rejection of dense brines that may have restricted the northward penetration of the WGC (Jackson et al., In Review). Furthermore, the formation of a stable ice arch in Kane Basin was inferred to have occurred from ca. 5500 to 3000 years BP (Georgiadis et al., 2020), thereby likely restricting the export of freshwater and multiyear drift ice towards the NOW and promoting open-water conditions. Combined, the above and our data thus would suggest a prolonged open-water season and high summer dinocyst productivity until ca. 2500 years.

2.6.2.2 Surface cooling, freshening and increased sea-ice influence (2500 to 1500 years BP)

From ca. 2500 to 1500 years BP, there is a decrease in the relative abundances of the autotrophic taxa, except for cysts of *Polarella glacialis* which shows low but peak contributions during this interval (Fig. 2.6). The steady decrease in the A/H ratio could hint to a decrease in the duration of the open-water season, which may have been unfavorable to the late-season open-water bloomers *Operculodinium centrocarpum* and *Spiniferites elongatus*. This interval is also marked by an increase in the contribution of the cold-water taxa *Islandinium minutum, Islandinium*? *cezare* and *Echinidinium karaense* to the assemblages (Head et al., 2001; Fig. 2.6). Both these taxa and *Polarella glacialis* are associated with sea-ice dominated environments and have the highest cyst production during sea-ice melt or in sea-ice covered environments (Head et al., 2001; Montresor et al., 2003; Heikkilä et al., 2014, 2016). Therefore, the decrease in autotrophic dinocysts combined with the increase of *Polarella glacialis* cysts and the cold-water taxa may suggest colder sea-surface conditions, and potentially more sea ice within the polynya. This could be the result either of a polynya contraction due to harsher regional sea-ice conditions, or from the weakening of the Nares Strait ice arch, which would have allowed higher export of polar sea ice and freshwater into the region of the NOW. Interestingly, the MAT index shows a decrease in the NOW index values until ca. 2200 years BP, followed by a clear shift to high NEW index values (Fig. 2.8), reinforcing the hypothesis of increased freshwater and sea-ice influence in the NOW region after ca. 2200 cal. years BP. This is coeval with a slight increase in the abundance of *Halodinium* spp.,

a group of ciliate cysts that has been associated with freshwater influence and estuarine environments (Gurdebeke et al., 2018; Matthiessen, 2000).

Georgiadis et al. (2020) proposed that between ca. 3000 and 1500 years BP strong northerly winds blew through Nares Strait due to a positive index of the Arctic Oscillation (Darby et al., 2012), which could lead to destabilization of the Kane Basin ice arch resulting in more ice and freshwater flowing into the polynya from the Arctic Ocean. Destabilization of the Nares Strait ice arch occurred in 2007, and large amounts of sea ice were observed flowing into the NOW region (Kwok et al., 2010; Moore & MacNeil, 2018). The increased NEW index values around ca. 2200 years BP would indeed be coherent with increased ice-laden polar water throughflow in the NOW from ca. 2200 to 1500 years BP (Fig. 2.8).

2.6.2.3 Surface cooling and delayed polynya opening (1500 to 156 years BP)

From ca. 1500 to 156 years BP, there is a continued increase in the relative abundances of the cold-water taxa *Islandinium*? *cezare* and *Echinidinium karaense*, and further decrease in the autotrophic taxa, which collectively reach a minimum during this interval (Fig. 2.9). The lowest contribution of autotrophic taxa *Operculodinium centrocarpum* and *Spiniferites elongatus* to the assemblages suggest a short open-water season, likely restricted to the summer months. This change in the composition of the dinocyst assemblage translates into a steady increase and peak in the values of the NEW index centered around ca. 800 years BP, supporting an increased sea-ice influence at the study site (Fig. 2.8), that is further coherent with the presence of the cysts of *Polarella glacialis* during this interval.

The planktonic and benthic foraminiferal assemblages from our core suggest increased influence of the WGC at depth and a well-stratified water column from ca. 2200 years BP until 150 years BP (Jackson et al., In Review). Weaker brine formation in a less active or contracted polynya may have led to reduced mixing between the freshwater lens at the surface and the sub-surface WGC, resulting in a cold-water sea-surface signal, but an Atlantic-sourced water signal at depth. The dominance of cold-water associated dinocyst taxa during this interval and the associated high NEW index values are coherent with this scenario (Figs. 2.8, 2.9). Between ca. 480 to 156 years BP, our data show a small increase in the A/H ratio and the abundances of *Spiniferites elongatus* and *Operculodinium centrocarpum*. This timing aligns with the Little Ice Age (Fischer et al., 1998; Auger et al., 2019; Fig. 2.9), which was possibly associated with a brief return to a stable ice margin and more stable conditions in a contracted polynya.

2.6.2.4 Highly productive NOW (1965 CE to 2009 CE)

The transition to the mid-twentieth century is characterized by rapid and large amplitude changes in the composition of the dinocyst assemblages and fluxes of all palynomorphs. Notable is the one to two orders of magnitude higher fluxes for all palynomorphs in core AMD15-Casq1-BC4 (Fig. 2.7) compared to AMD15-Casq1 (3822 to 156 years BP), and the increase in autotrophic taxa indicating a transition to a longer open-water duration and a more productive polynya (Fig. 2.9). Interestingly, we see an increase in the abundances of "*Polykrikos?* sp. by Kunz-Pirrung (1998)" which is associated with cold-water and low saline environments in the Arctic (Kunz-Pirrung, 2001) and Hudson Bay (Heikkilä et al., 2014, 2016), and *Islandinium brevispinosum* which was first reported from shallow and nutrient-rich temperate estuarine waters of New

England (Pospelova & Head, 2002). The high fluxes of *Halodinium* spp. suggest increased terrestrial freshwater input (Matthiessen et al., 2000; Gurdebeke et al., 2018; Fig. 2.7). This interval is also marked by a strong increase in the relative abundance of the cosmopolitan *Brigantedinium* spp., which can be dominant in highly productive systems (Pospelova et al., 2008) and has notably been associated with areas influenced by river runoff where food is abundant (Richerol et al., 2008). During this interval, the dinocyst assemblages have a signature characteristic of highly productive systems, which contrasts with the previous cold and contracted polynya inferred in the preceeding bioenvironmental zone (1500 to 156 years BP). This is reinforced by the still dominant cold-water taxa that make up ~75% of the dinocyst assemblages and the return to NOW-dominated MAT index values (Fig. 2.9). Extended open-water conditions are also inferred within the Canadian Arctic Archipelago from ca. 1940 to 2000 CE (Pieńkowski et al., 2011), and increased abundances of autotrophic taxa were also observed just south of the polynya in northern Baffin Bay during the 20th century (Cormier et al., 2016).

The changes in the composition of the dinocyst assemblages seen here for the second half of the 20th century seem to be coupled strongly with a weakening and northward movement of the Nares Strait ice arch from Kane Basin up into Nares Strait in recent decades (Vincent et al., 2019; Barber et al., 2001). The weakening of the Kane Basin ice arch has in turn been linked to a reduction in thick or multi-year ice flowing through Nares Strait (Vincent et al., 2019), which is detrimental to ice arch cohesion (Moore & McNeil, 2018; Dumont et al., 2009). As such, satellite data show higher sea-ice concentrations in the NOW region from 1979 to 1996, from a less stable ice arch (Barber et al., 2001).

2.6.2.5 Surface freshening and extended open-water season (2009 to 2015 CE)

The uppermost part of our record documents a sharp increase in the contributions from autotrophic taxa, especially the cysts of *Pentapharsodinium dalei*, but also the open-water *Operculodinium centrocarpum* (Figs. 2.6, 2.7, 2.9). Large cyst production by *Pentapharsodinium dalei* has been associated with highly stratified and productive spring waters, notably resulting from riverine input associated with melt events (Heikkilä et al., 2014). The strong increase in the cysts of *Pentapharsodinium dalei* may suggest enhanced influence of terrestrially-sourced freshwater during this interval.

Since the last decade, accelerated Greenland Ice Sheet melt has been observed (Box & Decker, 2011): the Petermann Glacier, located in northwest Greenland east of Nares Strait, has notably experienced major calving in 2010 and 2012 (Münchow et al., 2014, 2016). Satellite data further show that from 1979 to 2019, the average number of days that the ice arch blocks Arctic sea ice and freshwater from entering the NOW had decreased by 2.1 days/year (Vincent, 2019). Our data therefore seem coherent with a recent progressive surface freshening associated with increased meltwater runoff and Arctic Ocean throughflow, and an overall extended open-water season that favors the growth of the autotrophic dinoflagellate species.

2.6.3 The NOW and recent climate changes

Previous studies from the NOW proposed that the margins of the polynya were more susceptible to change than the central region (Bailey et al., 2013, Hamel et al., 2002). Here, we also note marked changes in the central area of the polynya during the last decade, a time that was not covered by the previous studies. As such, the large amplitude changes in the dinocyst composition and production recorded here suggest that the

formation dynamics and sea-surface conditions of the NOW polynya responded sensitively to the recent Arctic climate warming. Furthermore, the pace at which these changes occurred does not find any close analogue in the last ca. 3800 years covered by our core record. With the predicted continued warming and associated impact on the cryosphere, it can be expected that the NOW polynya will enter a new state and transition from a unique Arctic biological oasis to a seasonally open gateway between the Arctic Ocean and Baffin Bay.

2.7 Conclusions

This study offers a high-resolution record of changes in sea-surface conditions during the Late Holocene, in the central region of the NOW. It is the first study of its kind to use an approach based on the development of MAT indices to infer complementary information on long-term environmental changes. It is also one of a few studies to report the preservation of cysts of *Polarella glacialis* in sediment cores spanning several millennia.

Our data suggest that the period from 3822 to 2500 years BP was characterized by a long open-water duration and a stable polynya, expressed by high abundances of open-water dinocysts and high NOW index values. The interval from 2500 to 1500 years BP was marked by a surface cooling and freshening, indicated by a progressive increase in cold water taxa and a general increase of the NEW index values. From 1500 to 156 years BP, there was continued sea-surface cooling marked by a shorter open-water season. While our data document relatively gradual changes in the NOW polynya between ca. 3800 to 156 years BP, a marked change in both the composition and the magnitude of the dinocyst fluxes (one to two orders magnitude higher) towards the top of our record likely

reflects the rapid Arctic warming that occurred over the last century. The increase in the autotrophic taxa, largely steered by the cysts of *Pentapharsodinium dalei*, suggests stratified springtime waters during the period from 2009 to 2015 years CE. The recent warming in the Arctic has resulted in changes to controlling factors in the formation of the NOW polynya, such as the weakening of the Nares Strait ice arches and increased terrestrial freshwater input from the Greenland Ice Sheet into the region, which is expected to continue to increase with rising atmospheric greenhouse gas concentrations.

Finally, the development of a MAT index proved to be successful in this study, where changes in polynya dynamics could be inferred based on the analogue locations. Future work could be directed to developing a larger database of analogue locations within the NOW, NEW and other polynyas in the Arctic to have a better representation of polynya settings.

2.8 Acknowledgements

Core AMD15-Casq1 was collected in the frame of the GreenEdge project funded by ANR and the Total Foundation. Ship-time was funded by the ERC STG ICEPROXY project. The project received financial support from the Villum Foundation, Denmark (grant VKR023454 to SR) and was funded by ArcticNet and an NSERC-DG (grant RGPIN-2018-03984) to AL.

2.9 References

Allan, E., de Vernal, A., Knudsen, M.F., Hillaire-Marcel, C., Moros, M., Ribeiro, S., Ouellet-Bernier, M.-M., Seidenkrantz, M.-S., 2018. Late Holocene Sea Surface Instabilities in the Disko Bugt Area, West Greenland, in Phase With δ18O Oscillations at Camp Century. Paleoceanography and Paleoclimatology 33, 227–243. https://doi.org/10.1002/2017PA003289

Andresen, C.S., McCarthy, D.J., Valdemar Dylmer, C., Seidenkrantz, M.-S., Kuijpers, A., Lloyd, J.M., 2011. Interaction between subsurface ocean waters and calving of the Jakobshavn Isbræ during the late Holocene. The Holocene 21, 211–224. https://doi.org/10.1177/0959683610378877

Auger, J.D., Mayewski, P.A., Maasch, K.A., Schuenemann, K.C., Carleton, A.M., Birkel, S.D., Saros, J.E., 2019. 2000 years of North Atlantic-Arctic climate. Quaternary Science Reviews 216, 1–17. https://doi.org/10.1016/j.quascirev.2019.05.020

Bâcle, J., Carmack, E.C., Ingram, R.G., 2002. Water column structure and circulation under the North Water during spring transition: April–July 1998. Deep Sea Research Part II: Topical Studies in Oceanography, The International North Water Polynya Study 49, 4907–4925. https://doi.org/10.1016/S0967-0645(02)00170-4

Bailey, J.N.-L., Macdonald, R.W., Sanei, H., Outridge, P.M., Johannessen, S.C., Hochheim, K., Barber, D., Stern, G.A., 2013. Change at the margin of the North Water Polynya, Baffin Bay, inferred from organic matter records in dated sediment cores. Marine Geology 341, 1–13. https://doi.org/10.1016/j.margeo.2013.04.017

Barber, D.G., Hanesiak, J.M., Chan, W., Piwowar, J., 2001. Sea-ice and meteorological conditions in Northern Baffin Bay and the North Water polynya between 1979 and 1996. Atmosphere-Ocean 39, 343–359. https://doi.org/10.1080/07055900.2001.9649685

Barber, D.G., Massom, R.A., 2007. Chapter 1 The Role of Sea Ice in Arctic and Antarctic Polynyas, in: Smith, W.O., Barber, D.G. (Eds.), Elsevier Oceanography Series, Polynyas: Windows to the World. Elsevier, pp. 1–54. https://doi.org/10.1016/S0422-9894(06)74001-6

Berger, A., Loutre, M.F., 1991. Insolation values for the climate of the last 10 million years. Quaternary Science Reviews 10, 297–317. https://doi.org/10.1016/0277-3791(91)90033-Q

Box, J.E., Decker, D.T., 2011. Greenland marine-terminating glacier area changes: 2000–2010. Annals of Glaciology 52, 91–98. https://doi.org/10.3189/172756411799096312

Budéus, G., Schneider, W., 1995. On the hydrography of the Northeast Water Polynya. Journal of Geophysical Research: Oceans 100, 4287–4299. https://doi.org/10.1029/94JC02024

Budéus, G., Schneider, W., Kattner, G., 1997. Distribution and exchange of water masses in the Northeast Water polynya (Greenland Sea). Journal of Marine Systems 10, 123–138. https://doi.org/10.1016/S0924-7963(96)00074-7

Caron, M., Rochon, A., Montero-Serrano, J.-C., St-Onge, G., 2019. Evolution of sea-surface conditions on the northwestern Greenland margin during the Holocene. Journal of Quaternary Science 34, 569–580. https://doi.org/10.1002/jqs.3146

Claparède, E., Lachmann, J., 1859. Etudes sur les Infusoires et les rhizopodes. Memoires de l'Institut national genevois 6, 261–482.

Cormier, M.-A., Rochon, A., de Vernal, A., Gélinas, Y., 2016. Multi-proxy study of primary production and paleoceanographical conditions in northern Baffin Bay during the last centuries. Marine Micropaleontology 127, 1–10. https://doi.org/10.1016/j.marmicro.2016.07.001

Dale, B., 1976. Cyst formation, sedimentation, and preservation: Factors affecting dinoflagellate assemblages in recent sediments from trondheimsfjord, Norway. Review of Palaeobotany and Palynology 22, 39–60. https://doi.org/10.1016/0034-6667(76)90010-5

Darby, D.A., Ortiz, J.D., Grosch, C.E., Lund, S.P., 2012. 1,500-year cycle in the Arctic Oscillation identified in Holocene Arctic sea-ice drift. Nature Geoscience; London 5, 897–900. http://dx.doi.org.proxy.hil.unb.ca/10.1038/ngeo1629

Davidson, T.A., Wetterich, S., Johansen, K.L., Grønnow, B., Windirsch, T., Jeppesen, E., Syväranta, J., Olsen, J., González-Bergonzoni, I., Strunk, A., Larsen, N.K., Meyer, H., Søndergaard, J., Dietz, R., Eulears, I., Mosbech, A., 2018. The history of seabird colonies and the North Water ecosystem: Contributions from palaeoecological and archaeological evidence. Ambio 47, 175–192. https://doi.org/10.1007/s13280-018-1031-1

de Vernal, A., Henry, M., Matthiessen, J., Mudie, P.J., Rochon, A., Boessenkool, K.P., Eynaud, F., GrØsfjeld, K., Guiot, J., Hamel, D., Harland, R., Head, M.J., Kunz-Pirrung, M., Levac, E., Loucheur, V., Peyron, O., Pospelova, V., Radi, T., Turon, J.-L., Voronina, E., 2001. Dinoflagellate cyst assemblages as tracers of sea-surface conditions in the northern North Atlantic, Arctic and sub-Arctic seas: the new ‘n = 677’ data base and its application for quantitative palaeoceanographic reconstruction. Journal of Quaternary Science 16, 681–698. https://doi.org/10.1002/jqs.659

de Vernal, A., Hillaire-Marcel, C., Rochon, A., Fréchette, B., Henry, M., Solignac, S., Bonnet, S., 2013a. Dinocyst-based reconstructions of sea ice cover concentration during the Holocene in the Arctic Ocean, the northern North Atlantic Ocean and its adjacent seas. Quaternary Science Reviews, Sea Ice in the Paleoclimate System: the Challenge of Reconstructing Sea Ice from Proxies 79, 111–121. https://doi.org/10.1016/j.quascirev.2013.07.006

de Vernal, A., Rochon, A., Fréchette, B., Henry, M., Radi, T., Solignac, S., 2013b. Reconstructing past sea ice cover of the Northern Hemisphere from dinocyst assemblages: status of the approach. Quaternary Science Reviews, Sea Ice in the Paleoclimate System: the Challenge of Reconstructing Sea Ice from Proxies 79, 122–134. https://doi.org/10.1016/j.quascirev.2013.06.022

de Vernal, A., Radi, T., Zaragosi, S., Van Nieuwenhove, N., Rochon, A., Allan, E., De Schepper, S., Eynaud, F., Head, M.J., Limoges, A., Londeix, L., Marret, F., Matthiessen, J., Penaud, A., Pospelova, V., Price, A., Richerol, T., 2020. Distribution of common modern dinoflagellate cyst taxa in surface sediments of the Northern Hemisphere in relation to environmental parameters: The new n=1968 database. Marine Micropaleontology 101796. https://doi.org/10.1016/j.marmicro.2019.101796

Dumont, D., Gratton, Y., Arbetter, T.E., 2009. Modeling the Dynamics of the North Water Polynya Ice Bridge. Journal of Physical Oceanography. 39, 1448–1461. https://doi.org/10.1175/2008JPO3965.1

Ellegaard, M., Daugbjerg, N., Rochon, A., Lewis, J., Harding, I., 2003. Morphological and LSU rDNA sequence variation within the *Gonyaulax spinifera-Spiniferites* group (Dinophyceae) and proposal of *G. elongata* comb. nov. and *G. membranacea* comb. nov. Phycologia 42, 151–164. https://doi.org/10.2216/i0031-8884-42-2-151.1

Fischer, H., Werner, M., Wagenbach, D., Schwager, M., Thorsteinnson, T., Wilhelms, F., Kipfstuhl, J., Sommer, S., 1998. Little Ice Age clearly recorded in northern Greenland ice cores. Geophysical Research Letters 25, 1749–1752. https://doi.org/10.1029/98GL01177

Georgiadis, E., Giraudeau, J., Jennings, A., Limoges, A., Jackson, R., Ribeiro, S., Massé, G., 2020. Local and regional controls on Holocene sea ice dynamics and oceanography in Nares Strait, Northwest Greenland. Marine Geology 422, 106115. https://doi.org/10.1016/j.margeo.2020.106115

Guiot, J., de Vernal, A., 2007. Chapter Thirteen Transfer Functions: Methods for Quantitative Paleoceanography Based on Microfossils, in: Hillaire–Marcel, C., de Vernal, A. (Eds.), Developments in Marine Geology, Proxies in Late Cenozoic Paleoceanography. Elsevier, pp. 523–563. https://doi.org/10.1016/S1572-5480(07)01018-4

Gurdebeke, P.R., Mertens, K.N., Takano, Y., Yamaguchi, A., Bogus, K., Dunthorn, M., Matsuoka, K., Vrielinck, H., Louwye, S., 2018. The affiliation of *Hexasterias problematica* and *Halodinium verrucatum* sp. nov. to ciliate cysts based on molecular phylogeny and cyst wall composition. European Journal of Protistology 66, 115–135. https://doi.org/10.1016/j.ejop.2018.09.002

Hamel, D., de Vernal, A., Gosselin, M., Hillaire-Marcel, C., 2002. Organic-walled microfossils and geochemical tracers: sedimentary indicators of productivity changes in the North Water and northern Baffin Bay during the last centuries. Deep Sea Research Part II: Topical Studies in Oceanography, The International North Water Polynya Study 49, 5277–5295. https://doi.org/10.1016/S0967-0645(02)00190-X

Hammer, Ø., Harper, D.A.T., Ryan, P.D., 2001. Past: Paleontological Statistics Software Package for Education and Data Analysis 9.

Hastrup, K., Mosbech, A., Grønnow, B., 2018. Introducing the North Water: Histories of exploration, ice dynamics, living resources, and human settlement in the Thule Region. Ambio 47, 162–174. https://doi.org/10.1007/s13280-018-1030-2

Head, M.J., 1996. Modern dinoflagellate cysts and their biological affinities. J., McGregor, D.C. (Eds.), Jansonius, Palynology: principles and applications, vol. 3. American Association of Stratigraphic Palynologists Foundation, 1197–1248.

Head, M.J., Harland, R., Matthiessen, J., 2001. Cold marine indicators of the late Quaternary: the new dinoflagellate cyst genus *Islandinium* and related morphotypes. Journal of Quaternary Science 16, 621–636. https://doi.org/10.1002/jqs.657

Heikkilä, M., Pospelova, V., Forest, A., Stern, G.A., Fortier, L., Macdonald, R.W., 2016. Dinoflagellate cyst production over an annual cycle in seasonally ice-covered Hudson Bay. Marine Micropaleontology 125, 1–24. https://doi.org/10.1016/j.marmicro.2016.02.005

Heikkilä, M., Pospelova, V., Hochheim, K.P., Kuzyk, Z.Z.A., Stern, G.A., Barber, D.G., Macdonald, R.W., 2014. Surface sediment dinoflagellate cysts from the Hudson Bay system and their relation to freshwater and nutrient cycling. Marine Micropaleontology 106, 79–109. https://doi.org/10.1016/j.marmicro.2013.12.002

Hopkins, T.S., 1991. The GIN Sea—A synthesis of its physical oceanography and literature review 1972–1985. Earth-Science Reviews 30, 175–318. https://doi.org/10.1016/0012-8252(91)90001-V

IPCC, 2014: Climate Change 2014: Synthesis Report. Contribution of Working Groups I, II and III to the Fifth Assessment Report of the Intergovernmental Panel on Climate Change [Core Writing Team, R.K. Pachauri and L.A. Meyer (eds.)]. IPCC, Geneva, Switzerland, pp.1-151.

Jackson, R., Bang, A., Limoges, A., Georgiadis, E., Olsen, S., Tallberg, P., Andersen, T., Mikkelsen, N., Giraudeau, J., Massé, G., Ribeiro, S.,. North Water Polynya dynamics mediate Holocene Atlantic water influence in northern Baffin Bay. In Review. Scientific Reports.

Jeong, H.J., Yoo, Y.D., Kim, J.S., Seong, K.A., Kang, N.S., Kim, T.H., 2010. Growth, feeding and ecological roles of the mixotrophic and heterotrophic dinoflagellates in marine planktonic food webs. Ocean Science Journal. 45, 65–91. https://doi.org/10.1007/s12601-010-0007-2

Jeppesen, E., Appelt, M., Hastrup, K., Grønnow, B., Mosbech, A., Smol, J.P., Davidson, T.A., 2018. Living in an oasis: Rapid transformations, resilience, and resistance in the North Water Area societies and ecosystems. Ambio 47, 296–309. https://doi.org/10.1007/s13280-018-1034-y

Knudsen, K.L., Stabell, B., Seidenkrantz, M.-S., Eiríksson, J., Blake, W., 2008. Deglacial and Holocene conditions in northernmost Baffin Bay: sediments, foraminifera, diatoms and stable isotopes. Boreas 37, 346–376. https://doi.org/10.1111/j.1502-3885.2008.00035.x

Krawczyk, D.W., Witkowski, A., Moros, M., Lloyd, J.M., Høyer, J.L., Miettinen, A., Kuijpers, A., 2017. Quantitative reconstruction of Holocene sea ice and sea surface temperature off West Greenland from the first regional diatom data set. Paleoceanography 32, 18–40. https://doi.org/10.1002/2016PA003003

Kunz-Pirrung, M., 1998. Rekonstruktion der Oberflachenwassermassen der ostlichen Laptevsee im Holozan anhand von aquatischen Palynomorphen. Berichte Polarforschung. 281, 1–117.

Kunz-Pirrung, M., 2001. Dinoflagellate cyst assemblages in surface sediments of the Laptev Sea region (Arctic Ocean) and their relationship to hydrographic conditions. Journal of Quaternary Science 16, 637–649. https://doi.org/10.1002/jqs.647

Kwok, R., Pedersen, L.T., Gudmandsen, P., Pang, S.S., 2010. Large sea ice outflow into the Nares Strait in 2007. Geophysical Research Letters 37, L03502. https://doi.org/10.1029/2009GL041872

Lecavalier, B.S., Fisher, D.A., Milne, G.A., Vinther, B.M., Tarasov, L., Huybrechts, P., Lacelle, D., Main, B., Zheng, J., Bourgeois, J., Dyke, A.S., 2017. High Arctic Holocene temperature record from the Agassiz ice cap and Greenland ice sheet evolution.

Proceedings of the National Academy of Sciences 114, 5952–5957. https://doi.org/10.1073/pnas.1616287114

Levac, E., Vernal, A.D., Blake, W., Jr., 2001. Sea-surface conditions in northernmost Baffin Bay during the Holocene: palynological evidence. Journal of Quaternary Science 16, 353–363. https://doi.org/10.1002/jqs.614

Lewis, J., Dodge, J.D., Tett, P., 1984. Cyst-theca relationships in some Protoperidinium species (Peridiniales) from Scottish sea lochs. Journal of Micropalaeontology 3, 25–34. https://doi.org/10.1144/jm.3.2.25

Limoges A., Weckström K., Ribeiro S., Georgiadis E., Hansen K., Martinez P., Seidenkrantz M-S., Giraudeau J., Crosta X., Massé G.. Nine thousand years of primary production and sea-ice changes on the Northwest Greenland shelf driven by coupled ocean-atmosphere forcing. Submitted to Global Change Biology (May 2020).

Limoges, A., Van Nieuwenhove, N., Mertens, K.N., Head, M.J., Pospelova, V., Rochon, A., 2020. A review of rare or not well known extant marine organic-walled dinoflagellate cyst taxa of the orders Gonyaulacales and Suessiales from the Northern Hemisphere. In Press Marine Micropaleontology.

Lobb, J., Carmack, E.C., Ingram, R.G., Weaver, A.J., 2003. Structure and mixing across an Arctic/Atlantic front in northern Baffin Bay. Geophysical Research Letters 30, 1833. https://doi.org/10.1029/2003GL017755

Lochte, A.A., Repschläger, J., Seidenkrantz, M.-S., Kienast, M., Blanz, T., Schneider, R.R., 2019. Holocene water mass changes in the Labrador Current. The Holocene 29, 676–690. https://doi.org/10.1177/0959683618824752

Marchese, C., Albouy, C., Tremblay, J.-É., Dumont, D., D'Ortenzio, F., Vissault, S., Bélanger, S., 2017. Changes in phytoplankton bloom phenology over the North Water

(NOW) polynya: a response to changing environmental conditions. Polar Biology 40, 1721–1737. https://doi.org/10.1007/s00300-017-2095-2

Maqueda, M.A.M., Willmott, A.J., Biggs, N.R.T., 2004. Polynya dynamics: a review of observations and modeling. Reviews of Geophysics. 42. RG1004. https://doi.org/10.1029/2002RG000116

Matthiessen, J., Kunz-Pirrung, M., Mudie, P.J., 2000. Freshwater chlorophycean algae in recent marine sediments of the Beaufort, Laptev and Kara Seas (Arctic Ocean) as indicators of river runoff. International Journal of Earth Sciences 89, 470–485. https://doi.org/10.1007/s005310000127

Melling, H., Gratton, Y., Ingram, G., 2001. Ocean circulation within the North Water polynya of Baffin Bay. Atmosphere-Ocean 39, 301–325. https://doi.org/10.1080/07055900.2001.9649683

Montresor, M., Lovejoy, C., Orsini, L., Procaccini, G., Roy, S., 2003. Bipolar distribution of the cyst-forming dinoflagellate *Polarella glacialis*. Polar Biol 26, 186–194. https://doi.org/10.1007/s00300-002-0473-9

Montresor, M., Procaccini, G., Stoecker, D.K., 1999. *Polarella Glacialis*, Gen. Nov., Sp. Nov. (dinophyceae): *Suessiaceae* Are Still Alive! Journal of Phycology 35, 186–197. https://doi.org/10.1046/j.1529-8817.1999.3510186.x

Moore, G.W.K., McNeil, K., 2018. The Early Collapse of the 2017 Lincoln Sea Ice Arch in Response to Anomalous Sea Ice and Wind Forcing. Geophysical Research Letters 45, 8343–8351. https://doi.org/10.1029/2018GL078428

Moros, M., Lloyd, J.M., Perner, K., Krawczyk, D., Blanz, T., de Vernal, A., Ouellet-Bernier, M.-M., Kuijpers, A., Jennings, A.E., Witkowski, A., Schneider, R., Jansen, E., 2016. Surface and sub-surface multi-proxy reconstruction of middle to late Holocene

palaeoceanographic changes in Disko Bugt, West Greenland. Quaternary Science Reviews 132, 146–160. https://doi.org/10.1016/j.quascirev.2015.11.017

Mudie, P.J., Rochon, A., Prins, M.A., Soenarjo, D., Troelstra, S.R., Levac, E., 2006. Late Pleistocene-Holocene Marine Geology of Nares Strait region: paleoceanography from foraminifera and dinoflagellate cysts, sedimentology and stable isotopes. Polarforschung (Bremerhaven) 74, 169–183.

Münchow, A., Melling, H., 2008. Ocean current observations from Nares Strait to the west of Greenland: Interannual to tidal variability and forcing. Journal of Marine Research 66, 801–833. https://doi.org/10.1357/002224008788064612

Münchow, A., Padman, L., Fricker, H.A., 2014. Interannual changes of the floating ice shelf of Petermann Gletscher, North Greenland, from 2000 to 2012. Journal of Glaciology 60, 489–499. https://doi.org/10.3189/2014JoG13J135

Münchow, A., Falkner, K.K., Melling, H., 2015. Baffin Island and West Greenland Current Systems in northern Baffin Bay. Progress in Oceanography, Oceanography of the Arctic and North Atlantic Basins 132, 305–317. https://doi.org/10.1016/j.pocean.2014.04.001

Münchow, A., Padman, L., Washam, P., Nicholls, K.W., 2016. The Ice Shelf of Petermann Gletscher, North Greenland, and its Connection to the Arctic and Atlantic Oceans. Oceanography 29, 84–95.

Ouellet-Bernier, M.-M., de Vernal, A., Hillaire-Marcel, C., Moros, M., 2014. Paleoceanographic changes in the Disko Bugt area, West Greenland, during the Holocene. The Holocene 24, 1573–1583. https://doi.org/10.1177/0959683614544060

Perner, K., Moros, M., Jennings, A., Lloyd, J., Knudsen, K., 2013. Holocene palaeoceanographic evolution off West Greenland. The Holocene 23, 374–387. https://doi.org/10.1177/0959683612460785

Perner, K., Moros, M., Lloyd, J.M., Kuijpers, A., Telford, R.J., Harff, J., 2011. Centennial scale benthic foraminiferal record of late Holocene oceanographic variability in Disko Bugt, West Greenland. Quaternary Science Reviews 30, 2815–2826. https://doi.org/10.1016/j.quascirev.2011.06.018

Pieńkowski, A.J., Mudie, P.J., England, J.H., Smith, J.N., Furze, M.F.A., 2011. Late Holocene environmental conditions in Coronation Gulf, southwestern Canadian Arctic Archipelago: evidence from dinoflagellate cysts, other non-pollen palynomorphs, and pollen. Journal of Quaternary Science 26, 839–853. https://doi.org/10.1002/jqs.1503

Pospelova, V., de Vernal, A., Pedersen, T.F., 2008. Distribution of dinoflagellate cysts in surface sediments from the northeastern Pacific Ocean (43–25°N) in relation to sea-surface temperature, salinity, productivity and coastal upwelling. Marine Micropaleontology, Dinocysts as tracers of hydrographical conditions and productivity along the ocean margins 68, 21–48. https://doi.org/10.1016/j.marmicro.2008.01.008

Pospelova, V., Head, M.J., 2002. Islandinium Brevispinosum Sp. Nov. (dinoflagellata), a New Organic-Walled Dinoflagellate Cyst from Modern Estuarine Sediments of New England (usa)1. Journal of Phycology 38, 593–601. https://doi.org/10.1046/j.1529-8817.2002.01206.x

Potvin, É., Kim, S.-Y., Yang, E.J., Head, M.J., Kim, H., Nam, S.-I., Yim, J.H., Kang, S.-H., 2018. *Islandinium minutum* subsp. *barbatum* subsp. nov. (Dinoflagellata), a New Organic-Walled Dinoflagellate Cyst from the Western Arctic: Morphology, Phylogenetic Position Based on SSU rDNA and LSU rDNA, and Distribution. Journal of Eukaryotic Microbiology 65, 750–772. https://doi.org/10.1111/jeu.12518

Potvin, É., Rochon, A., Lovejoy, C., 2013. Cyst–theca relationship of the arctic dinoflagellate cyst *Islandinium minutum* (Dinophyceae) and phylogenetic position based on SSU rDNA and LSU rDNA. Journal of Phycology 49, 848–866. https://doi.org/10.1111/jpy.12089

Quaijtaal, W., Donders, T.H., Persico, D., Louwye, S., 2014. Characterising the middle Miocene Mi-events in the Eastern North Atlantic realm: A first high-resolution marine palynological record from the Porcupine Basin. Palaeogeography, Palaeoclimatology, Palaeoecology 399, 140–159. https://doi.org/10.1016/j.palaeo.2014.02.017

R Core Team, 2018. R: A Language and Environment for Statistical Computing.

Radi, T., Bonnet, S., Cormier, M.-A., de Vernal, A., Durantou, L., Faubert, É., Head, M.J., Henry, M., Pospelova, V., Rochon, A., Van Nieuwenhove, N., 2013. Operational taxonomy and (paleo-)autecology of round, brown, spiny dinoflagellate cysts from the Quaternary of high northern latitudes. Marine Micropaleontology 98, 41–57. https://doi.org/10.1016/j.marmicro.2012.11.001

Radi, T., de Vernal, A., 2008. Dinocysts as proxy of primary productivity in mid–high latitudes of the Northern Hemisphere. Marine Micropaleontology, Dinocysts as tracers of hydrographical conditions and productivity along the ocean margins 68, 84–114. https://doi.org/10.1016/j.marmicro.2008.01.012

Rasmussen, T.A.S., Kliem, N., Kaas, E., 2010. Modelling the sea ice in the Nares Strait. Ocean Modelling 35, 161–172. https://doi.org/10.1016/j.ocemod.2010.07.003

Ribeiro S, Limoges A, Massé G, Colgan W, Jackson R, Mikkelsen N, Johannsen KL, Georgiadis E, Weckström K, Kuijpers A, Olsen J, Olsen SM, Nissen M, Strunk A, Wetterich S, Syvaranta J, Henderson ACG, Mackay H, Taipale S, Jeppesen E, Larsen NK, Crosta X, Giraudeau J, Holm L, Nuttall M, Gronnow, B, Mosbech A, Davidson TA.

Vulnerability of the North Water polynya ecosystem to climate change. In Review. Nature Climate Change

Ribeiro, S., Moros, M., Ellegaard, M., Kuijpers, A., 2012. Climate variability in West Greenland during the past 1500 years: evidence from a high-resolution marine palynological record from Disko Bay. Boreas 41, 68–83. https://doi.org/10.1111/j.1502-3885.2011.00216.x

Richerol, T., Rochon, A., Blasco, S., Scott, D.B., Schell, T.M., Bennett, R.J., 2008. Distribution of dinoflagellate cysts in surface sediments of the Mackenzie Shelf and Amundsen Gulf, Beaufort Sea (Canada). Journal of Marine Systems, Sea ice and life in a river-influenced arctic shelf ecosystem 74, 825–839. https://doi.org/10.1016/j.jmarsys.2007.11.003

Rignot, E. Kanagaratnam, P., 2006. Changes in the Velocity Structure of the Greenland Ice Sheet. Science, 311, 986-990. https://doi.org/10.1126/science.1121381

Rudels, B., Björk, G., Nilsson, J., Winsor, P., Lake, I., Nohr, C., 2005. The interaction between waters from the Arctic Ocean and the Nordic Seas north of Fram Strait and along the East Greenland Current: results from the Arctic Ocean-02 Oden expedition. Journal of Marine Systems 55, 1–30. https://doi.org/10.1016/j.jmarsys.2004.06.008

Rysgaard, S., Boone, W., Carlson, D., Sejr, M.K., Bendtsen, J., Juul-Pedersen, T., Lund, H., Meire, L., Mortensen, J., 2020. An Updated View on Water Masses on the pan-West Greenland Continental Shelf and Their Link to Proglacial Fjords. Journal of Geophysical Research: Oceans 125, e2019JC015564. https://doi.org/10.1029/2019JC015564

Schnepf, E., Elbrächter, M., 1992. Nutritional strategies in dinoflagellates: A review with emphasis on cell biological aspects. European Journal of Protistology 28, 3–24. https://doi.org/10.1016/S0932-4739(11)80315-9

Schumacher, J.D., Aagaard, K., Pease, C.H., Tripp, R.B., 1983. Effects of a shelf polynya on flow and water properties in the northern Bering Sea. Journal of Geophysical Research: Oceans 88, 2723–2732. https://doi.org/10.1029/JC088iC05p02723

Seidenkrantz, M.-S., Roncaglia, L., Fischel, A., Heilmann-Clausen, C., Kuijpers, A., Moros, M., 2008. Variable North Atlantic climate seesaw patterns documented by a late Holocene marine record from Disko Bugt, West Greenland. Marine Micropaleontology, Dinocysts as tracers of hydrographical conditions and productivity along the ocean margins 68, 66–83. https://doi.org/10.1016/j.marmicro.2008.01.006

Serreze, M.C., Holland, M.M., Stroeve, J., 2007. Perspectives on the Arctic's Shrinking Sea-Ice Cover. Science 315, 1533–1536. https://doi.org/10.1126/science.1139426

Sha, L., Jiang, H., Seidenkrantz, M.-S., Li, D., Andresen, C.S., Knudsen, K.L., Liu, Y., Zhao, M., 2017. A record of Holocene sea-ice variability off West Greenland and its potential forcing factors. Palaeogeography, Palaeoclimatology, Palaeoecology 475, 115–124. https://doi.org/10.1016/j.palaeo.2017.03.022

Smith, S.D., Muench, R.D., Pease, C.H., 1990. Polynyas and leads: An overview of physical processes and environment. Journal of Geophysical Research: Oceans 95, 9461–9479. https://doi.org/10.1029/JC095iC06p09461

Stirling, I., 1997. The importance of polynyas, ice edges, and leads to marine mammals and birds. Journal of Marine Systems 10, 9–21. https://doi.org/10.1016/S0924-7963(96)00054-1

Stockmarr, J., 1971. Tablets with spores used in absolute pollen analysis. Pollen et Spores 13, 615–621.

Stoecker, D.K., Gustafson, D.E., Baier, C.T., Black, M.M.D., 2000. Primary production in the upper sea ice. Aquatic Microbial Ecology 21, 275–287. https://doi.org/10.3354/ame021275

St-Onge, M.-P., St-Onge, G., 2014. Environmental changes in Baffin Bay during the Holocene based on the physical and magnetic properties of sediment cores. Journal of Quaternary Science 29, 41–56. https://doi.org/10.1002/jqs.2674

Tang, C.C.L., Ross, C.K., Yao, T., Petrie, B., DeTracey, B.M., Dunlap, E., 2004. The circulation, water masses and sea-ice of Baffin Bay. Progress in Oceanography 63, 183–228. https://doi.org/10.1016/j.pocean.2004.09.005

Van Nieuwenhove, N., Head, M.J., Limoges, A., Pospelova, V., Mertens, K.N., Matthiessen, J., De Schepper, S., de Vernal, A., Eynaud, F., Londeix, L., Marret, F., Penaud, A., Radi, T., Rochon, A., 2020. An overview and brief description of common marine organic-walled dinoflagellate cyst taxa occurring in surface sediments of the Northern Hemisphere. Marine Micropaleontology 101814. https://doi.org/10.1016/j.marmicro.2019.101814

Versteegh, G.J.M., Blokker, P., 2004. Resistant macromolecules of extant and fossil microalgae. Phycological Research 52, 325–339. https://doi.org/10.1111/j.1440-183.2004.00361.x

Vincent, R.F., 2019. A Study of the North Water Polynya Ice Arch using Four Decades of Satellite Data. Scientific Reports 9. https://doi.org/10.1038/s41598-019-56780-6

Wall, D., Dale, B., 1966. "Living Fossils" in Western Atlantic Plankton. Nature 211, 1025–1026. https://doi.org/10.1038/2111025a0

Worldview: Explore Your Dynamic Planet [WWW Document], https://worldview.earthdata.nasa.gov/ (accessed 6.28.20).

Yao, T., Tang, C.L., 2003. The formation and maintenance of the North Water Polynya. Atmosphere Ocean 41, 187–201. https://doi.org/10.3137/ao.410301

Chapter 3. Discussion and Conclusions

3.1 Discussion

The main objective of this study was to understand the evolution of sea-surface conditions in the NOW polynya over the last ca. 3800 years in response to climate variations. This study was successful in inferring important changes in the polynya conditions during the late Holocene and in comparing the recent (last half a century) changes to the long-term variation.

The results of this study reveal intervals of increased freshwater input associated with Arctic Ocean throughflows and glacial runoff in the NOW polynya during the late Holocene. This is evidenced by increasing abundances of the cold-water dinocyst taxa *lslandinium minutum, Islandinium*? *cezare* and *Echinidinium karaense* a concurrent decrease in the autotrophic taxa *Operculodinium centrocarpum* and *Spiniferites elongatus* and a general increase in the NEW index values. The last ca. 60 years were marked by enhanced contribution of the autotrophic taxa *Operculodinium centrocarpum, Spiniferites elongatus* and cyst of *Pentapharsodinium dalei* to the assemblages. The latter taxon is associated with stratified and productive spring waters, indicating a shift to more stratified waters. Overall, the results indicate that 1) changes in the dinocyst abundances and fluxes between ca. 3800 to 156 years BP were relatively progressive, indicating gradual changes to the NOW polynya during this interval and 2) the polynya is highly sensitive to the recent Arctic climate amplification.

Importantly, this study is the first of its kind to use an approach based on MAT indices. This tool proved to be useful in understanding changing polynya dynamics within the NOW over time.

Finally, this study is also one of the few to report the preservation of cysts of *Polarella glacialis* in sediment cores spanning several millennia. This species is the only dinoflagellate that is known to go through encystment in the sea-ice matrix (e.g., Stoecker et al., 2000) and for which cysts have a potential of preservation in the sediment, and therefore has a particular significance for paleo-climate interpretations.

3.2 Issues and Future Work

An important feature of the NOW polynya is the contrasted oceanography between its western (fresher, cooler water masses) and the eastern (WGC influenced) sectors (Bâcle et al., 2002). However, during the writing of this thesis, the central and northern sectors (i.e., northern Baffin Bay and Smith Sound) of the polynya are the only areas where long-term high-resolution studies have been conducted (Jackson et al., In Review; Georgiadis et al., 2018, 2020). Understanding the changes to the water column, both at the surface and at depth in the western portion of the polynya is needed to better understand interactions between changes in the Arctic outflow, glacier dynamics, and polynya functioning/ecosystem services.

Future work could contribute to developing the MAT indices and extend their use as complementary tools for paleoenvironmental reconstructions. In the future, this type of approach would be favored by an increase in the number of sites included in the Northern Hemisphere surface database. The NEW polynya has a total of 24 sites and analyzing more sites within other polynya settings could help with future MAT index use.

Additionally, the resolving power of the MAT itself would be improved if more dinocyst taxa could be included. The cyst of *Polarella glacialis* and *Islandinium minutum* subsp. *barbatum* are currently not included and may carry an important environmental signature. Including more taxa could improve the variation in environmental conditions in the northern hemisphere.

3.3 References

Bâcle, J., Carmack, E.C., Ingram, R.G., 2002. Water column structure and circulation under the North Water during spring transition: April–July 1998. Deep Sea Research Part II: Topical Studies in Oceanography, The International North Water Polynya Study 49, 4907–4925. https://doi.org/10.1016/S0967-0645(02)00170-4

Georgiadis, E., Giraudeau, J., Jennings, A., Limoges, A., Jackson, R., Ribeiro, S., Massé, G., 2020. Local and regional controls on Holocene sea ice dynamics and oceanography in Nares Strait, Northwest Greenland. Marine Geology 422, 106115. https://doi.org/10.1016/j.margeo.2020.106115

Georgiadis, E., Giraudeau, J., Martinez, P., Lajeunesse, P., St-Onge, G., Schmidt, S., Massé, G., 2018. Deglacial to postglacial history of Nares Strait, Northwest Greenland: a marine perspective from Kane Basin. Climate of the Past 14, 1991–2010. https://doi.org/10.5194/cp-14-1991-2018

Heikkilä, M., Pospelova, V., Hochheim, K.P., Kuzyk, Z.Z.A., Stern, G.A., Barber, D.G., Macdonald, R.W., 2014. Surface sediment dinoflagellate cysts from the Hudson Bay system and their relation to freshwater and nutrient cycling. Marine Micropaleontology 106, 79–109. https://doi.org/10.1016/j.marmicro.2013.12.002

Jackson, R., Bang, A., Limoges, A., Georgiadis, E., Olsen, S., Tallberg, P., Andersen, T., Mikkelsen, N., Giraudeau, J., Massé, G., Ribeiro, S.,. North Water Polynya dynamics mediate Holocene Atlantic water influence in northern Baffin Bay. In Review. Scientific Reports.

Stoecker, D.K., Gustafson, D.E., Baier, C.T., Black, M.M.D., 2000. Primary production in the upper sea ice. Aquatic Microbial Ecology 21, 275–287. https://doi.org/10.3354/ame021275

Appendix I: Additional Statistical Analysis and Palynomorph Counts

I-I STATCOUNTS

STATCOUNTS was used to determine the sample size required to analyze representative dinocyst populations (Heslop et al., 2011). This Excel solver tool was adapted from the algorithms developed by Sison and Glaz (1995) and May and Johnson (2000). One of the solvers offered, ESCTCOUNTS, was used to evaluate the number of specimens that needed to be counted to reach pre-defined significance and error levels (Heslop et al., 2011). ESCTCOUNTS was used to determine the statistical significance of the counts from the different stratigraphic levels of the sediment archive; the associated significance (α) and error (%) are presented in Table I-2.

I-II Principal component analysis

Principal component analysis (PCA) was used in conjunction with the cluster analysis to help define the number of statistically significant ecozones. PCA is a multivariate statistical technique that reduces large multi-dimensional datasets down to smaller variables in linear space, called principal components, that represent the maximum variance between data (Jolliffe & Cadema, 2016). PCA allows for large datasets which may be complicated to interpret to be simplified while minimizing the information that is lost (Jolliffe & Cadema, 2016). The software Past4 was used to compute PCA eigenanalysis of the dataset, where the eigenvalues have a percent variance that is accounted for by the corresponding eigenvectors (Hammer et al., 2001). In our dataset,

the first two components accounted for ~41% (PC1) and ~19% (PC2) of the variation of the scatter of points, respectively (Table I-1).

Table I-1 The principal components (PC) and their associated eigenvalue and percent variance.

PC	Eigenvalue	% variance
1	0.285118	41.229
2	0.129964	18.793
3	0.0762957	11.033
4	0.0398262	5.759
5	0.038495	5.5666
6	0.0285336	4.1261
7	0.0158841	2.2969
8	0.0146304	2.1156
9	0.0124332	1.7979
10	0.0088612	1.2814

The broken-stick model plots the variance divided randomly against each component (i.e. 1,2,3, etc.) to form what looks like a broken stick graph (Fig. I-1; Frontier, 1976). A component is considered significant if its eigenvalue is larger than the broken stick distribution (Frontier, 1976). In studies comparing different PCA correlations it was found that the broken stick model accurately calculates the number of significant components (Jackson, 1993). As such, in this study five significant components were identified in our dataset and defined the most important ecozones (Fig. I-1).

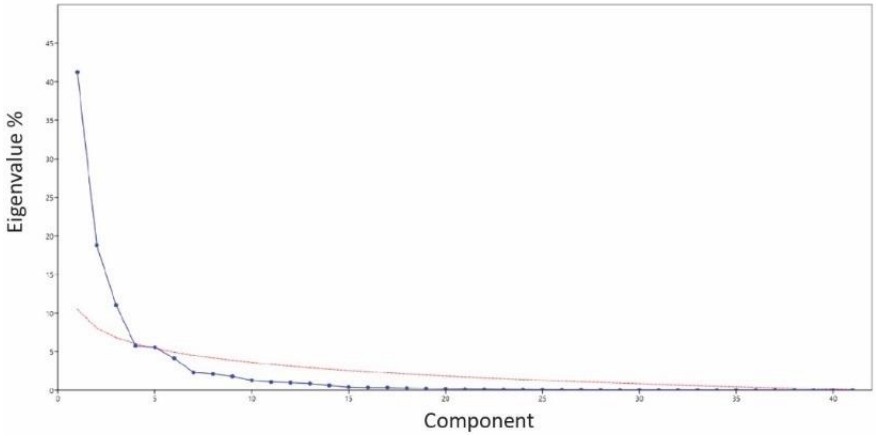


Figure I-1 The broken stick model, where the intersection between the red and blue curves indicates the number of meaningful components.

I-III Dinocyst Counts

Table I-2 Raw Dinocyst Counts from AMD15-Casq1-BC4 and AMD15-Casq1. All ages are in Years BP.

AGE	Total Dinocysts	α	Error (%)	*Brigantedinium* spp.	*Brigantedinium cariacoense*	*Brigantedinium simplex*
-65.0	1286	0.05	2.50	204	13	63
-64.6	895	0.05	3.10	130	4	18
-63.6	818	0.05	3.40	112	9	19
-62.6	807	0.05	3.50	109	2	9
-61.6	755	0.05	3.60	230	4	7
-60.6	601	0.05	3.90	124	0	11
-59.5	1019	0.05	3.10	185	1	13
-58.4	1038	0.05	3.00	162	2	14
-57.3	1513	0.05	2.60	373	2	16
-56.1	790	0.05	3.70	229	0	5
-55.0	862	0.05	3.20	137	4	7
-54.0	856	0.05	3.30	149	2	12
-53.0	1055	0.05	3.20	261	0	15
-51.9	751	0.05	3.80	224	0	7
-50.9	822	0.05	3.50	186	0	16
-49.7	659	0.05	3.90	169	0	4
-48.6	1022	0.05	3.10	200	0	5
-47.4	1153	0.05	2.90	237	0	15
-46.4	875	0.05	3.50	234	0	12
-45.4	893	0.05	3.30	198	0	4
-44.4	1133	0.05	2.80	158	0	19
-41.2	838	0.05	3.60	245	2	14
-38.2	1191	0.05	3.10	412	0	8
-35.9	926	0.05	3.10	149	1	5
-29.9	1408	0.05	2.80	424	0	5
-25.6	1446	0.05	2.60	358	0	7
-21.4	1305	0.05	2.60	214	0	13
-17.5	1513	0.05	2.50	328	0	4
-15.7	958	0.05	3.10	180	0	2
156.3	309	0.05	4.20	18	0	0
199.2	500	0.05	3.40	18	0	3
240.9	309	0.05	4.60	4	0	2
283.8	499	0.05	4.00	58	0	14
326.3	361	0.05	4.30	17	0	1
368.7	605	0.05	3.50	80	1	12
413.0	505	0.05	3.60	9	0	8
455.6	494	0.05	3.30	7	0	8
498.3	896	0.05	3.00	109	3	12
540.2	303	0.05	4.80	8	0	2

Table I-2 Continued

AGE	Total Dinocysts	α	Error (%)	*Brigantedinium* spp.	*Brigantedinium cariacoense*	*Brigantedinium simplex*
581.7	305	0.05	4.90	29	0	2
623.7	351	0.05	4.50	22	0	0
665.1	301	0.05	4.60	30	0	3
706.8	305	0.05	4.60	29	0	1
724.0	303	0.05	5.30	50	0	2
766.6	301	0.05	5.40	23	0	1
808.6	723	0.05	3.50	93	0	22
852.0	499	0.05	4.00	56	0	4
893.7	302	0.05	3.90	6	0	1
926.9	479	0.05	3.50	13	0	9
957.6	306	0.05	4.70	13	0	1
988.8	306	0.05	4.30	10	0	0
1019.3	307	0.05	4.60	25	0	2
1050.9	308	0.05	4.90	17	0	1
1082.1	305	0.05	4.60	26	0	4
1113.9	338	0.05	4.30	30	0	5
1145.0	344	0.05	3.80	10	0	4
1176.5	314	0.05	4.20	6	0	1
1208.1	302	0.05	4.20	12	0	2
1240.0	309	0.05	4.10	19	0	3
1272.1	506	0.05	3.40	18	0	0
1303.0	317	0.05	4.60	39	0	0
1333.1	307	0.05	4.50	25	0	1
1364.1	307	0.05	4.30	18	0	1
1395.5	493	0.05	3.50	12	0	8
1427.1	645	0.05	3.20	42	0	8
1458.8	313	0.05	4.30	22	0	3
1489.8	303	0.05	4.80	20	0	1
1521.7	333	0.05	4.20	14	0	3
1554.1	309	0.05	4.90	28	0	1
1585.7	311	0.05	4.30	21	0	0
1618.5	353	0.05	3.90	4	0	1
1650.1	329	0.05	3.70	10	0	1
1682.2	306	0.05	4.60	11	0	1
1713.9	325	0.05	4.40	12	0	0
1726.9	300	0.05	4.50	25	0	0
1757.6	301	0.05	3.70	6	0	0
1789.3	308	0.05	4.40	38	0	0
1821.4	310	0.05	4.90	40	0	2
1851.2	303	0.05	4.30	21	0	2
1881.4	610	0.05	2.80	19	0	3

Table I-2 Continued

AGE	Total Dinocysts	α	Error (%)	*Brigantedinium* spp.	*Brigantedinium cariacoense*	*Brigantedinium simplex*
1911.4	647	0.05	2.80	50	3	1
1941.4	320	0.05	4.60	31	0	4
1970.2	334	0.05	3.80	20	1	3
2000.2	326	0.05	4.00	6	0	0
2031.4	317	0.05	4.20	21	0	0
2062.5	309	0.05	4.30	29	0	2
2093.1	623	0.05	3.10	43	1	6
2123.7	312	0.05	4.50	27	0	3
2154.6	305	0.05	4.30	26	0	1
2185.1	307	0.05	4.50	30	0	0
2214.6	301	0.05	4.40	28	0	2
2246.1	639	0.05	3.30	67	0	10
2276.9	413	0.05	3.90	23	0	8
2310.1	305	0.05	4.30	13	0	4
2354.6	308	0.05	4.10	22	0	2
2385.8	305	0.05	4.50	14	0	1
2424.0	307	0.05	4.70	23	0	3
2462.1	306	0.05	4.60	41	0	3
2500.2	304	0.05	4.80	38	0	2
2538.7	318	0.05	3.60	10	0	4
2578.1	306	0.05	4.60	35	0	1
2617.3	307	0.05	5.10	56	0	4
2655.6	303	0.05	3.80	7	0	11
2692.5	306	0.05	4.90	57	0	1
2742.6	302	0.05	5.10	62	0	4
2763.7	1052	0.05	2.70	139	2	14
2814.4	307	0.05	4.80	49	0	4
2858.0	302	0.05	4.40	12	0	6
2893.5	312	0.05	4.80	38	0	1
2930.0	306	0.05	4.60	15	0	14
2967.0	621	0.05	3.10	34	0	18
3003.3	315	0.05	4.10	20	0	6
3040.3	363	0.05	4.20	26	0	1
3076.8	303	0.05	4.50	22	0	7
3113.2	305	0.05	4.80	31	0	7
3149.1	629	0.05	3.60	70	2	39
3185.6	609	0.05	3.70	91	0	14

Table I-2 Continued

AGE	Total Dinocysts	α	Error (%)	*Brigantedinium* spp.	*Brigantedinium cariacoense*	*Brigantedinium simplex*
3221.8	330	0.05	5.20	73	0	8
3257.8	306	0.05	5.50	79	0	6
3293.7	318	0.05	5.10	43	0	6
3325.0	611	0.05	3.60	118	0	6
3352.1	319	0.05	4.70	17	0	18
3379.4	310	0.05	4.90	40	0	1
3405.4	606	0.05	3.40	42	0	39
3430.6	404	0.05	4.10	56	0	10
3456.1	303	0.05	4.70	16	0	12
3486.9	302	0.05	5.50	69	0	10
3522.5	613	0.05	3.50	31	0	46
3558.7	304	0.05	5.00	53	0	2
3594.5	306	0.05	4.60	40	0	8
3630.4	635	0.05	3.70	101	0	20
3665.8	328	0.05	4.60	30	0	1
3703.3	352	0.05	4.20	16	0	13
3738.5	305	0.05	4.60	24	0	10
3776.1	306	0.05	4.30	13	0	6
3822.0	314	0.05	4.90	26	0	8

Table I-2 Continued

AGE	Round Brown	*Dubridinium* spp.	*Islandinium minutum* subsp. *minutum*	*Islandinium minutum* subsp. *barbatum*	*Islandinium*? *cezare*
-65.0	163	1	249	0	65
-64.6	106	0	146	0	72
-63.6	81	0	144	0	67
-62.6	59	0	159	0	58
-61.6	56	0	153	0	88
-60.6	61	0	166	0	44
-59.5	38	0	507	0	47
-58.4	7	0	631	1	18
-57.3	13	0	870	0	9
-56.1	6	0	433	0	11
-55.0	2	0	542	0	18
-54.0	2	0	522	0	10
-53.0	0	0	519	0	45
-51.9	10	0	365	0	21
-50.9	0	0	498	0	10
-49.7	0	0	375	0	11
-48.6	26	0	579	0	36
-47.4	0	0	662	0	47
-46.4	0	0	470	0	27
-45.4	0	0	535	0	24
-44.4	0	0	731	0	61
-41.2	0	0	426	0	30
-38.2	0	0	525	0	44
-35.9	0	0	601	0	40
-29.9	0	0	744	0	46
-25.6	0	0	852	0	50
-21.4	0	0	837	0	59
-17.5	0	0	924	0	31
-15.7	0	0	616	0	25
156.3	2	0	249	1	15
199.2	15	0	394	4	24
240.9	18	0	235	2	6
283.8	26	0	343	1	18
326.3	8	0	266	9	25
368.7	17	0	433	2	15
413.0	19	0	379	0	25
455.6	20	0	396	4	13
498.3	3	0	617	12	30
540.2	20	0	220	2	14
581.7	4	0	217	4	16

Table I-2 Continued

AGE	Round Brown	*Dubridinium* spp.	*Islandinium minutum* subsp. *minutum*	*Islandinium minutum* subsp. *barbatum*	*Islandinium*? *cezare*
623.7	12	0	256	5	9
665.1	4	0	229	2	13
706.8	2	0	232	1	8
724.0	11	0	191	5	14
766.6	39	0	186	1	4
808.6	22	2	456	3	31
852.0	30	0	344	3	16
893.7	11	0	254	3	3
926.9	25	0	375	1	21
957.6	22	0	224	1	7
988.8	19	0	241	2	8
1019.3	5	0	230	5	13
1050.9	27	0	215	4	2
1082.1	10	0	230	3	5
1113.9	5	0	260	2	8
1145.0	11	0	280	2	12
1176.5	15	0	248	3	11
1208.1	8	0	244	2	10
1240.0	4	0	249	4	10
1272.1	23	0	393	5	18
1303.0	8	0	239	3	5
1333.1	13	0	234	5	10
1364.1	6	0	240	2	5
1395.5	17	0	383	0	21
1427.1	1	0	489	5	28
1458.8	5	0	246	5	4
1489.8	16	0	216	3	9
1521.7	13	0	261	1	5
1554.1	15	0	220	2	9
1585.7	15	0	244	3	4
1618.5	23	0	283	1	8
1650.1	4	0	275	1	9
1682.2	20	0	230	2	7
1713.9	29	0	247	0	1
1726.9	3	0	231	1	7
1757.6	5	0	256	2	11
1789.3	2	0	242	4	1
1821.4	4	0	226	0	8
1851.2	7	0	242	1	3
1881.4	7	0	509	2	13
1911.4	5	0	533	6	9

Table I-2 Continued

AGE	Round Brown	*Dubridinium* spp.	*Islandinium minutum* subsp. *minutum*	*Islandinium minutum* subsp. *barbatum*	*Islandinium*? *cezare*
1941.4	9	0	240	1	3
1970.2	2	0	277	0	8
2000.2	18	0	266	1	6
2031.4	9	0	254	3	2
2062.5	7	0	247	2	0
2093.1	19	0	490	1	15
2123.7	13	0	235	4	4
2154.6	9	0	242	0	6
2185.1	10	0	236	0	6
2214.6	3	0	237	3	5
2246.1	14	0	464	2	12
2276.9	25	0	311	0	9
2310.1	12	0	243	1	9
2354.6	6	0	251	1	12
2385.8	28	0	237	0	4
2424.0	12	1	226	1	9
2462.1	4	0	234	0	4
2500.2	8	0	225	0	6
2538.7	14	0	271	0	3
2578.1	4	0	232	1	7
2617.3	4	0	213	3	4
2655.6	12	0	254	0	6
2692.5	1	0	227	0	7
2742.6	1	0	216	0	7
2763.7	36	0	752	2	15
2814.4	0	0	226	1	9
2858.0	17	0	236	0	5
2893.5	10	0	228	2	9
2930.0	0	0	233	0	19
2967.0	19	0	482	0	8
3003.3	10	0	254	0	11
3040.3	28	0	273	1	6
3076.8	0	0	242	0	8
3113.2	15	0	221	0	6
3149.1	23	0	413	0	13
3185.6	21	2	410	1	14
3221.8	3	0	215	1	11

Table I-2 Continued

AGE	Round Brown	*Dubridinium* spp.	*Islandinium minutum* subsp. *minutum*	*Islandinium minutum* subsp. *barbatum*	*Islandinium*? *cezare*
3221.8	3	0	215	1	11
3257.8	0	0	195	0	2
3293.7	24	0	211	1	5
3325.0	0	0	442	2	7
3352.1	16	0	232	0	8
3379.4	14	0	224	0	8
3405.4	12	0	447	0	9
3430.6	8	0	304	2	6
3456.1	16	0	229	1	9
3486.9	2	0	188	1	11
3522.5	23	0	435	1	6
3558.7	2	0	220	1	4
3594.5	6	0	231	1	4
3630.4	11	0	423	2	6
3665.8	26	0	238	1	4
3703.3	18	0	263	0	12
3738.5	16	0	228	0	8
3776.1	20	0	241	0	5
3822.0	26	0	215	0	3

Table I-2 Continued

AGE	cf. *Islandinium brevispinosum*?	*Echinidinium karaense*	*Echinidinium aculeatum*	*Echinidinium delicatum*	*Echinidinium transparantum*
-65.0	13	88	7	0	0
-64.6	10	71	0	0	0
-63.6	9	27	0	0	0
-62.6	9	36	0	0	0
-61.6	11	31	0	0	0
-60.6	11	34	0	0	0
-59.5	11	89	0	0	0
-58.4	12	94	0	0	0
-57.3	5	126	0	0	0
-56.1	7	48	0	0	0
-55.0	6	65	0	0	0
-54.0	7	65	0	0	0
-53.0	3	96	0	0	0
-51.9	11	36	0	0	0
-50.9	10	69	0	0	0
-49.7	4	68	0	0	0
-48.6	5	98	0	0	0
-47.4	17	87	0	0	0
-46.4	10	57	0	0	0
-45.4	11	64	0	0	0
-44.4	11	76	0	0	0
-41.2	8	57	0	0	0
-38.2	6	104	0	0	0
-35.9	8	66	0	0	0
-29.9	8	57	0	0	0
-25.6	13	96	0	0	0
-21.4	8	88	0	0	0
-17.5	23	109	0	0	0
-15.7	7	73	0	0	0
156.3	1	5	0	0	0
199.2	0	5	0	0	0
240.9	3	6	0	0	0
283.8	1	7	0	0	0
326.3	0	15	0	0	0
368.7	0	10	0	0	0
413.0	0	19	1	0	0
455.6	0	14	0	0	0
498.3	2	61	1	0	0
540.2	0	9	0	0	0
581.7	0	18	0	0	0

Table I-2 Continued

AGE	cf. *Islandinium brevispinosum*?	*Echinidinium karaense*	*Echinidinium aculeatum*	*Echinidinium delicatum*	*Echinidinium transparantum*
623.7	0	15	0	0	0
665.1	0	8	0	0	0
706.8	0	7	0	0	0
724.0	1	7	0	0	0
766.6	1	25	0	0	0
808.6	2	53	0	0	1
852.0	2	15	0	0	0
893.7	0	10	0	0	0
926.9	1	6	0	0	0
957.6	0	12	0	0	0
988.8	3	2	0	0	0
1019.3	2	11	0	0	0
1050.9	2	14	0	0	0
1082.1	0	11	0	0	0
1113.9	1	4	0	0	0
1145.0	1	5	0	0	0
1176.5	2	5	0	0	0
1208.1	1	5	0	0	0
1240.0	1	5	0	0	0
1272.1	1	10	0	0	0
1303.0	0	9	0	0	0
1333.1	0	4	0	0	0
1364.1	0	16	0	0	0
1395.5	0	19	0	1	0
1427.1	1	41	0	0	0
1458.8	1	12	0	0	0
1489.8	3	14	0	0	0
1521.7	4	2	0	0	0
1554.1	0	8	0	0	0
1585.7	1	11	0	0	0
1618.5	2	9	0	0	0
1650.1	3	4	0	0	0
1682.2	1	8	0	0	0
1713.9	0	10	0	0	0
1726.9	2	8	0	0	0
1757.6	0	6	0	0	0
1789.3	0	7	0	0	0
1821.4	1	6	0	0	0
1851.2	0	16	0	0	0
1881.4	3	12	0	2	0
1911.4	0	8	0	0	0

Table I-2 Continued

AGE	cf. *Islandinium brevispinosum*?	*Echinidinium karaense*	*Echinidinium aculeatum*	*Echinidinium delicatum*	*Echinidinium transparantum*
1941.4	0	10	0	0	0
1970.2	1	5	0	0	0
2000.2	2	8	0	0	0
2031.4	1	10	0	0	0
2062.5	2	9	0	0	0
2093.1	3	7	0	0	0
2123.7	2	5	0	0	0
2154.6	0	8	0	0	0
2185.1	2	7	0	0	0
2214.6	1	5	0	0	0
2246.1	0	32	0	0	0
2276.9	0	8	0	0	0
2310.1	1	3	0	0	0
2354.6	1	1	0	0	0
2385.8	1	9	0	0	0
2424.0	0	4	0	0	0
2462.1	0	4	0	0	0
2500.2	0	10	0	0	0
2538.7	1	3	0	0	0
2578.1	0	15	0	0	0
2617.3	2	7	0	0	0
2655.6	0	3	0	0	0
2692.5	1	5	0	0	0
2742.6	0	3	0	0	0
2763.7	3	27	1	0	0
2814.4	1	5	0	0	0
2858.0	1	5	0	0	0
2893.5	2	4	0	0	0
2930.0	0	6	0	0	0
2967.0	0	16	1	0	0
3003.3	1	1	0	0	0
3040.3	0	5	0	0	0
3076.8	0	6	0	0	0
3113.2	2	5	0	0	0
3149.1	1	15	0	0	0
3185.6	1	13	0	0	0

Table I-2 Continued

AGE	cf. *Islandinium brevispinosum*?	*Echinidinium karaense*	*Echinidinium aculeatum*	*Echinidinium delicatum*	*Echinidinium transparantum*
3221.8	1	5	0	0	0
3257.8	1	11	0	0	0
3293.7	1	6	0	0	0
3325.0	1	13	0	0	0
3352.1	0	8	0	0	0
3379.4	0	1	0	0	0
3405.4	0	12	0	0	0
3430.6	1	3	0	0	0
3456.1	0	2	0	0	0
3486.9	1	0	0	0	0
3522.5	0	9	1	0	0
3558.7	1	3	0	0	0
3594.5	1	2	0	0	0
3630.4	3	16	0	0	0
3665.8	1	4	0	0	0
3703.3	0	1	0	0	0
3738.5	0	1	0	0	0
3776.1	0	2	0	0	0
3822.0	2	7	0	0	0

Table I-2 Continued

AGE	*Echinidinium*? sp. B	Spiny Brown very long processes (*cezare* ?)	Spiny brown very long processes	Spiny Brown	*Polykrikos?* sp. of Kunz-Pirrung (1998)
-65.0	1	0	0	102	4
-64.6	0	0	0	57	2
-63.6	0	0	0	17	3
-62.6	0	0	0	27	0
-61.6	0	0	2	27	1
-60.6	0	0	1	55	1
-59.5	0	0	0	0	4
-58.4	0	0	0	20	0
-57.3	0	0	0	0	4
-56.1	0	0	0	0	2
-55.0	0	0	0	0	2
-54.0	0	0	0	0	0
-53.0	0	0	0	0	0
-51.9	0	0	0	35	6
-50.9	0	0	0	0	2
-49.7	0	0	0	0	0
-48.6	0	0	0	37	2
-47.4	0	0	0	0	7
-46.4	0	0	0	0	2
-45.4	0	0	0	0	0
-44.4	0	0	0	0	8
-41.2	0	0	0	0	12
-38.2	0	0	0	0	7
-35.9	0	0	0	0	3
-29.9	0	0	0	0	11
-25.6	0	0	0	0	10
-21.4	0	0	0	0	2
-17.5	0	0	0	0	4
-15.7	0	0	0	0	1
156.3	0	0	0	17	0
199.2	0	0	3	33	0
240.9	0	0	4	27	0
283.8	0	0	0	14	2
326.3	0	0	2	17	0
368.7	0	0	1	22	1
413.0	0	0	13	28	2
455.6	0	0	0	30	0
498.3	0	0	9	34	0
540.2	0	0	5	23	0
581.7	0	0	2	12	0

Table I-2 Continued

AGE	*Echinidinium*? sp. B	Spiny Brown very long processes (*cezare* ?)	Spiny brown very long processes	Spiny Brown	*Polykrikos?* sp. of Kunz-Pirrung (1998)
623.7	0	0	1	30	1
665.1	0	0	0	11	0
706.8	0	0	6	18	0
724.0	0	0	0	22	0
766.6	0	0	3	15	1
808.6	0	0	7	26	1
852.0	0	0	3	25	0
893.7	0	0	3	11	0
926.9	0	0	3	22	0
957.6	0	0	3	21	0
988.8	0	0	5	15	1
1019.3	0	0	1	10	0
1050.9	0	0	3	22	0
1082.1	0	0	0	12	0
1113.9	0	0	2	18	0
1145.0	0	0	5	11	1
1176.5	0	0	2	18	0
1208.1	0	0	4	11	0
1240.0	0	0	0	11	0
1272.1	0	0	4	29	0
1303.0	0	0	0	12	0
1333.1	0	0	0	10	0
1364.1	0	0	2	13	0
1395.5	0	0	12	17	0
1427.1	0	0	5	16	0
1458.8	0	0	0	9	0
1489.8	0	0	1	18	0
1521.7	0	0	12	12	0
1554.1	0	0	0	22	0
1585.7	0	0	1	9	0
1618.5	0	0	3	13	0
1650.1	0	0	4	11	1
1682.2	0	0	1	22	0
1713.9	0	0	2	24	0
1726.9	0	0	0	18	1
1757.6	0	0	4	8	0
1789.3	0	0	1	9	2
1821.4	0	0	0	21	0
1851.2	0	0	0	7	0
1881.4	0	0	7	24	0
1911.4	0	0	3	22	0

Table I-2 Continued

AGE	*Echinidinium*? sp. B	Spiny Brown very long processes (*cezare* ?)	Spiny brown very long processes	Spiny Brown	*Polykrikos?* sp. of Kunz-Pirrung (1998)
1941.4	0	0	2	13	1
1970.2	0	0	0	13	1
2000.2	0	0	2	11	1
2031.4	0	0	0	13	0
2062.5	0	0	1	6	0
2093.1	0	1	10	15	0
2123.7	0	0	3	12	0
2154.6	0	0	1	8	0
2185.1	0	0	1	11	0
2214.6	0	0	0	5	0
2246.1	0	0	4	20	0
2276.9	0	0	1	18	0
2310.1	0	0	4	7	0
2354.6	0	0	0	8	1
2385.8	0	0	1	7	0
2424.0	0	0	5	14	0
2462.1	0	0	1	7	0
2500.2	0	0	1	11	0
2538.7	0	0	1	5	1
2578.1	0	0	1	4	0
2617.3	0	0	0	7	0
2655.6	0	0	0	5	0
2692.5	0	0	0	2	0
2742.6	0	0	0	2	0
2763.7	0	0	4	22	1
2814.4	0	0	0	3	1
2858.0	0	0	1	11	0
2893.5	0	0	0	11	1
2930.0	0	0	3	7	0
2967.0	0	0	1	14	3
3003.3	0	0	1	8	0
3040.3	0	0	3	9	0
3076.8	0	0	4	8	0
3113.2	0	0	2	8	0
3149.1	0	0	3	23	3
3185.6	0	0	5	11	4

Table I-2 Continued

AGE	*Echinidinium*? sp. B	Spiny Brown very long processes (*cezare* ?)	Spiny brown very long processes	Spiny Brown	*Polykrikos?* sp. of Kunz-Pirrung (1998)
3221.8	0	0	0	7	0
3257.8	0	0	0	5	1
3293.7	0	0	0	6	1
3325.0	0	0	1	8	0
3352.1	0	0	0	7	0
3379.4	0	0	0	11	1
3405.4	0	0	1	24	1
3430.6	0	0	2	5	0
3456.1	0	0	0	2	0
3486.9	0	0	2	12	0
3522.5	0	0	3	26	3
3558.7	0	0	1	9	0
3594.5	0	0	0	3	0
3630.4	0	0	1	9	2
3665.8	0	0	2	7	0
3703.3	0	0	1	10	1
3738.5	0	0	1	3	1
3776.1	0	0	2	0	0
3822.0	0	0	2	4	2

Table I-2 Continued

AGE	*Polykrikos* spp.	*Protoperidinium* spp.	Cyst of *Polarella glacialis*	cf. *Biecheleria* sp.	*Operculodinium centrocarpum*
-65.0	0	3	0	0	66
-64.6	0	0	0	0	32
-63.6	0	0	0	0	9
-62.6	0	0	0	0	19
-61.6	0	0	0	0	20
-60.6	0	0	0	1	19
-59.5	0	0	0	0	15
-58.4	0	0	0	0	8
-57.3	0	0	0	0	25
-56.1	0	0	0	0	8
-55.0	0	0	0	0	13
-54.0	0	0	0	0	7
-53.0	0	0	0	0	18
-51.9	0	0	0	0	5
-50.9	0	0	0	0	4
-49.7	0	0	0	0	9
-48.6	0	0	0	2	1
-47.4	0	0	0	0	2
-46.4	0	0	0	0	7
-45.4	0	0	0	0	11
-44.4	0	0	0	0	3
-41.2	0	0	0	0	4
-38.2	0	0	0	0	6
-35.9	0	0	0	0	3
-29.9	0	0	0	0	7
-25.6	0	0	0	0	2
-21.4	0	0	0	0	4
-17.5	0	0	0	0	4
-15.7	0	0	0	0	5
156.3	0	0	0	1	0
199.2	1	0	0	0	0
240.9	0	0	1	0	1
283.8	0	0	0	0	10
326.3	0	0	0	0	0
368.7	0	0	0	0	4
413.0	0	0	1	0	1
455.6	0	0	0	0	2
498.3	0	0	0	0	1
540.2	0	0	0	0	0
581.7	0	0	0	1	0

Table I-2 Continued

AGE	*Polykrikos* spp.	*Protoperidinium* spp.	Cyst of *Polarella glacialis*	cf. *Biecheleria* sp.	*Operculodinium centrocarpum*
623.7	0	0	0	0	0
665.1	1	0	0	0	0
706.8	0	0	0	0	0
724.0	0	0	0	0	0
766.6	1	0	0	0	1
808.6	0	2	0	0	1
852.0	0	0	0	0	1
893.7	0	0	0	0	0
926.9	0	0	0	0	2
957.6	0	0	0	1	1
988.8	0	0	0	0	0
1019.3	0	0	0	0	1
1050.9	0	0	0	0	1
1082.1	0	0	1	0	1
1113.9	1	0	0	0	2
1145.0	0	0	0	0	1
1176.5	0	0	0	0	2
1208.1	1	0	0	0	1
1240.0	0	0	0	0	3
1272.1	0	0	0	0	3
1303.0	0	0	0	0	2
1333.1	0	0	0	0	4
1364.1	0	0	0	0	3
1395.5	0	0	1	0	1
1427.1	0	0	1	1	3
1458.8	0	0	0	0	5
1489.8	0	0	0	0	2
1521.7	0	0	0	0	5
1554.1	0	0	0	0	1
1585.7	0	0	0	0	1
1618.5	0	0	0	0	5
1650.1	0	0	0	0	2
1682.2	0	0	0	0	2
1713.9	0	0	0	0	0
1726.9	0	0	0	0	2
1757.6	0	0	0	0	3
1789.3	0	0	0	0	1
1821.4	0	0	0	0	1
1851.2	0	0	0	0	2
1881.4	0	0	1	0	2
1911.4	1	0	1	0	1

Table I-2 Continued

AGE	*Polykrikos* spp.	*Protoperidinium* spp.	Cyst of *Polarella glacialis*	cf. *Biecheleria* sp.	*Operculodinium centrocarpum*
1941.4	0	0	1	0	3
1970.2	0	0	1	0	1
2000.2	0	0	0	0	3
2031.4	0	0	0	0	2
2062.5	0	0	0	0	2
2093.1	0	0	1	0	2
2123.7	0	0	0	0	3
2154.6	0	0	1	0	3
2185.1	0	0	0	0	4
2214.6	0	0	1	0	8
2246.1	1	0	1	0	5
2276.9	0	0	1	0	3
2310.1	1	0	0	0	3
2354.6	0	0	0	0	2
2385.8	0	0	1	0	2
2424.0	2	0	2	0	4
2462.1	0	0	1	0	5
2500.2	1	0	0	0	1
2538.7	0	0	1	0	2
2578.1	0	0	0	0	3
2617.3	0	0	0	0	6
2655.6	0	0	0	0	2
2692.5	0	0	1	0	1
2742.6	1	0	1	0	2
2763.7	0	1	0	0	14
2814.4	0	0	0	0	2
2858.0	1	0	1	0	4
2893.5	0	0	0	1	4
2930.0	0	0	0	0	5
2967.0	0	0	0	0	12
3003.3	0	0	0	0	2
3040.3	0	0	1	0	7
3076.8	0	0	0	0	3
3113.2	2	0	0	0	2
3149.1	1	0	1	0	8
3185.6	0	2	2	0	13

Table I-2 Continued

AGE	*Polykrikos* spp.	*Protoperidinium* spp.	Cyst of *Polarella glacialis*	cf. *Biecheleria* sp.	*Operculodinium centrocarpum*
3221.8	0	0	0	0	3
3257.8	0	0	0	0	4
3293.7	0	0	1	0	9
3325.0	0	0	0	0	8
3352.1	0	0	0	0	8
3379.4	2	0	0	0	3
3405.4	0	0	0	0	8
3430.6	0	0	0	0	4
3456.1	0	0	0	0	10
3486.9	0	0	0	0	5
3522.5	0	1	0	0	17
3558.7	2	0	0	0	1
3594.5	0	0	0	0	4
3630.4	0	1	0	0	16
3665.8	0	0	1	0	8
3703.3	0	0	0	0	13
3738.5	0	0	0	0	9
3776.1	1	0	0	0	10
3822.0	0	0	0	0	4

Table I-2 Continued

AGE	*Operculodinium centrocarpum* Arctic morphotype	*Operculodinium centrocarpum* short processes	*Operculodinium centrocarpum* < 3µm	Cyst of *Pentapharsodinium dalei*
-65.0	43	8	2	169
-64.6	31	2	1	192
-63.6	42	2	0	264
-62.6	18	4	0	287
-61.6	16	2	0	98
-60.6	10	0	0	50
-59.5	8	4	0	76
-58.4	15	4	0	38
-57.3	17	6	0	38
-56.1	10	4	0	17
-55.0	7	2	0	46
-54.0	10	3	0	60
-53.0	9	3	0	72
-51.9	6	0	0	21
-50.9	4	0	0	20
-49.7	0	2	0	11
-48.6	5	0	0	22
-47.4	5	7	0	55
-46.4	2	0	0	50
-45.4	9	2	0	31
-44.4	1	0	0	61
-41.2	6	0	0	32
-38.2	19	0	0	56
-35.9	8	0	0	37
-29.9	15	0	0	74
-25.6	8	0	0	40
-21.4	13	0	0	46
-17.5	19	0	0	58
-15.7	2	5	0	41
156.3	0	0	0	0
199.2	0	0	0	0
240.9	0	0	0	0
283.8	0	1	0	0
326.3	0	1	0	0
368.7	0	0	0	1
413.0	0	0	0	0
455.6	0	0	0	0
498.3	0	0	0	0
540.2	0	0	0	0
581.7	0	0	0	0

Table I-2 Continued

AGE	*Operculodinium centrocarpum* Arctic morphotype	*Operculodinium centrocarpum* short processes	*Operculodinium centrocarpum* < 3µm	Cyst of *Pentapharsodinium dalei*
623.7	0	0	0	0
665.1	0	0	0	0
706.8	0	0	0	0
724.0	0	0	0	0
766.6	0	0	0	0
808.6	0	0	0	0
852.0	0	0	0	0
893.7	0	0	0	0
926.9	0	0	0	0
957.6	0	0	0	0
988.8	0	0	0	0
1019.3	0	0	0	1
1050.9	0	0	0	0
1082.1	0	1	0	0
1113.9	0	0	0	0
1145.0	0	0	0	1
1176.5	0	1	0	0
1208.1	0	0	0	0
1240.0	0	0	0	0
1272.1	0	0	0	0
1303.0	0	0	0	0
1333.1	0	0	0	1
1364.1	0	0	0	0
1395.5	1	0	0	0
1427.1	1	0	0	1
1458.8	0	0	0	0
1489.8	0	0	0	0
1521.7	0	0	0	0
1554.1	0	0	0	2
1585.7	0	0	0	1
1618.5	0	0	0	1
1650.1	0	0	0	3
1682.2	0	1	0	0
1713.9	0	0	0	0
1726.9	0	0	0	1
1757.6	0	0	0	0
1789.3	0	0	0	0
1821.4	0	0	0	0
1851.2	0	0	0	2
1881.4	4	0	0	1
1911.4	0	1	0	0

Table I-2 Continued

AGE	*Operculodinium centrocarpum* Arctic morphotype	*Operculodinium centrocarpum* short processes	*Operculodinium centrocarpum* < 3 µm	Cyst of *Pentapharsodinium dalei*
1941.4	0	0	0	1
1970.2	0	0	0	1
2000.2	0	1	0	0
2031.4	0	0	0	0
2062.5	0	1	0	0
2093.1	4	0	0	0
2123.7	0	0	0	0
2154.6	0	0	0	0
2185.1	0	0	0	0
2214.6	2	0	0	0
2246.1	0	0	0	1
2276.9	2	0	0	0
2310.1	2	0	0	0
2354.6	0	0	0	0
2385.8	0	0	0	0
2424.0	0	1	0	0
2462.1	0	0	0	0
2500.2	0	0	0	0
2538.7	0	0	0	0
2578.1	1	0	0	0
2617.3	1	0	0	0
2655.6	1	0	0	0
2692.5	0	0	0	1
2742.6	1	0	0	1
2763.7	8	1	0	2
2814.4	0	0	0	2
2858.0	0	0	0	1
2893.5	0	1	0	0
2930.0	1	0	0	2
2967.0	6	1	0	1
3003.3	0	0	0	1
3040.3	0	0	0	2
3076.8	1	0	0	0
3113.2	1	0	0	2
3149.1	5	4	0	3
3185.6	1	1	0	0

Table I-2 Continued

AGE	*Operculodinium centrocarpum* Arctic morphotype	*Operculodinium centrocarpum* short processes	*Operculodinium centrocarpum* < 3µm	Cyst of *Pentapharsodinium dalei*
3221.8	1	0	0	1
3257.8	0	0	0	0
3293.7	1	1	0	0
3325.0	2	0	0	0
3352.1	4	0	0	0
3379.4	0	0	0	3
3405.4	5	0	0	1
3430.6	1	2	0	0
3456.1	0	0	0	0
3486.9	0	0	0	0
3522.5	5	0	0	2
3558.7	0	0	0	3
3594.5	0	1	0	1
3630.4	14	0	0	0
3665.8	1	0	0	1
3703.3	0	0	0	2
3738.5	0	0	0	0
3776.1	0	0	0	1
3822.0	1	1	0	3

Table I-2 Continued

AGE	*Spiniferites elongatus*	*Spiniferites elongatus* (Beaufort morphotype)	*Spiniferites* spp.	*Spiniferites ramosus*
-65.0	0	2	9	3
-64.6	2	2	1	1
-63.6	1	1	1	3
-62.6	2	4	0	5
-61.6	1	0	1	0
-60.6	2	3	2	0
-59.5	0	9	0	4
-58.4	0	0	1	0
-57.3	0	9	0	0
-56.1	0	6	0	0
-55.0	0	6	0	2
-54.0	0	5	0	0
-53.0	0	9	0	3
-51.9	1	2	0	0
-50.9	0	1	0	0
-49.7	0	4	0	0
-48.6	1	2	0	0
-47.4	0	12	0	0
-46.4	0	2	0	0
-45.4	0	4	0	0
-44.4	0	4	0	0
-41.2	0	2	0	0
-38.2	0	1	0	0
-35.9	0	5	0	0
-29.9	0	17	0	0
-25.6	0	10	0	0
-21.4	0	17	0	4
-17.5	0	5	0	0
-15.7	0	1	0	0
156.3	0	0	0	0
199.2	0	0	0	0
240.9	0	0	0	0
283.8	2	0	2	0
326.3	0	0	0	0
368.7	5	0	1	0
413.0	0	0	0	0
455.6	0	0	0	0
498.3	2	0	0	0
540.2	0	0	0	0
581.7	0	0	0	0

Table I-2 Continued

AGE	*Spiniferites elongatus*	*Spiniferites elongatus* (Beaufort morphotype)	*Spiniferites* spp.	*Spiniferites ramosus*
623.7	0	0	0	0
665.1	0	0	0	0
706.8	0	0	1	0
724.0	0	0	0	0
766.6	0	0	0	0
808.6	1	0	0	0
852.0	0	0	0	0
893.7	0	0	0	0
926.9	1	0	0	0
957.6	0	0	0	0
988.8	0	0	0	0
1019.3	1	0	0	0
1050.9	0	0	0	0
1082.1	0	0	1	0
1113.9	0	0	0	0
1145.0	0	0	0	0
1176.5	0	0	0	0
1208.1	1	0	0	0
1240.0	0	0	0	0
1272.1	1	0	0	0
1303.0	0	0	0	0
1333.1	0	0	0	0
1364.1	1	0	0	0
1395.5	0	0	0	0
1427.1	2	0	0	0
1458.8	1	0	0	0
1489.8	0	0	0	0
1521.7	0	0	1	0
1554.1	1	0	0	0
1585.7	0	0	0	0
1618.5	0	0	0	0
1650.1	0	0	1	0
1682.2	0	0	0	0
1713.9	0	0	0	0
1726.9	1	0	0	0
1757.6	0	0	0	0
1789.3	1	0	0	0
1821.4	1	0	0	0
1851.2	0	0	0	0
1881.4	1	0	0	0
1911.4	2	0	1	0

Table I-2 Continued

AGE	*Spiniferites elongatus*	*Spiniferites elongatus* (Beaufort morphotype)	*Spiniferites* spp.	*Spiniferites ramosus*
1941.4	1	0	0	0
1970.2	0	0	0	0
2000.2	1	0	0	0
2031.4	2	0	0	0
2062.5	1	0	0	0
2093.1	3	0	1	0
2123.7	1	0	0	0
2154.6	0	0	0	0
2185.1	0	0	0	0
2214.6	1	0	0	0
2246.1	5	0	0	0
2276.9	2	1	0	0
2310.1	0	0	2	0
2354.6	0	1	0	0
2385.8	0	0	0	0
2424.0	0	0	0	0
2462.1	0	0	2	0
2500.2	0	0	1	0
2538.7	1	0	1	0
2578.1	1	0	1	0
2617.3	0	0	0	0
2655.6	2	0	0	0
2692.5	2	0	0	0
2742.6	1	0	0	0
2763.7	5	0	2	0
2814.4	4	0	0	0
2858.0	1	0	0	0
2893.5	0	0	0	0
2930.0	0	0	1	0
2967.0	4	0	1	0
3003.3	0	0	0	0
3040.3	1	0	0	0
3076.8	2	0	0	0
3113.2	1	0	0	0
3149.1	0	0	1	0
3185.6	2	1	0	0

Table I-2 Continued

AGE	*Spiniferites elongatus*	*Spiniferites elongatus* (Beaufort morphotype)	*Spiniferites* spp.	*Spiniferites ramosus*
3221.8	1	0	0	0
3257.8	2	0	0	0
3293.7	1	0	1	0
3325.0	2	0	1	0
3352.1	1	0	0	0
3379.4	1	0	1	0
3405.4	2	2	1	0
3430.6	0	0	0	0
3456.1	5	0	1	0
3486.9	1	0	0	0
3522.5	3	0	1	0
3558.7	2	0	0	0
3594.5	4	0	0	0
3630.4	6	0	4	0
3665.8	2	0	1	0
3703.3	2	0	0	0
3738.5	3	0	1	0
3776.1	3	0	2	0
3822.0	4	2	4	0

Table I-2 Continued

AGE	*Diplopsalid* spp.	*Impagidinium pallidum*	*Ataxiodinium choane*	*Bitectatodinium tepikiense*
-65	0	1	0	4
-64.603	0	0	0	7
-63.602	0	0	0	0
-62.601	0	0	0	0
-61.599	0	0	0	7
-60.598	0	0	0	5
-59.53	0	0	6	0
-58.396	0	1	5	3
-57.262	0	0	0	0
-56.128	0	0	2	0
-55.039	0	0	0	1
-53.996	0	0	0	0
-52.952	0	0	0	0
-51.908	0	0	1	0
-50.854	0	0	2	0
-49.706	0	0	2	0
-48.558	0	0	1	0
-47.41	0	0	0	0
-46.357	0	0	0	0
-45.397	0	0	0	0
-44.438	0	0	0	0
-41.171	0	0	0	0
-38.206	0	0	0	3
-35.932	0	0	0	0
-29.888	0	0	0	0
-25.592	0	0	0	0
-21.423	0	0	0	0
-17.542	0	0	0	4
-15.673	0	0	0	0
156.3	0	0	0	0
199.2	0	0	0	0
240.9	0	0	0	0
283.8	0	0	0	0
326.3	0	0	0	0
368.7	0	0	0	0
413	0	0	0	0
455.6	0	0	0	0
498.3	0	0	0	0
540.2	0	0	0	0
581.7	0	0	0	0

Table I-2 Continued

AGE	*Diplopsalid* spp.	*Impagidinium pallidum*	*Ataxiodinium choane*	*Bitectatodinium tepikiense*
623.7	0	0	0	0
665.1	0	0	0	0
706.8	0	0	0	0
724	0	0	0	0
766.6	0	0	0	0
808.6	0	0	0	0
852	0	0	0	0
893.7	0	0	0	0
926.9	0	0	0	0
957.6	0	0	0	0
988.75	0	0	0	0
1019.3	0	0	0	0
1050.9	0	0	0	0
1082.1	0	0	0	0
1113.9	0	0	0	0
1145	0	0	0	0
1176.5	0	0	0	0
1208.1	0	0	0	0
1240	0	0	0	0
1272.1	1	0	0	0
1303	0	0	0	0
1333.1	0	0	0	0
1364.1	0	0	0	0
1395.5	0	0	0	0
1427.1	0	0	0	0
1458.8	0	0	0	0
1489.8	0	0	0	0
1521.7	0	0	0	0
1554.1	0	0	0	0
1585.7	0	0	0	0
1618.5	0	0	0	0
1650.1	0	0	0	0
1682.2	0	0	0	0
1713.9	0	0	0	0
1726.9	0	0	0	0
1757.6	0	0	0	0
1789.3	0	0	0	0
1821.4	0	0	0	0
1851.2	0	0	0	0
1881.4	0	0	0	0
1911.4	0	0	0	0

Table I-2 Continued

AGE	*Diplopsalid* spp.	*Impagidinium pallidum*	*Ataxiodinium choane*	*Bitectatodinium tepikiense*
1941.4	0	0	0	0
1970.2	0	0	0	0
2000.2	0	0	0	0
2031.4	0	0	0	0
2062.5	0	0	0	0
2093.1	1	0	0	0
2123.7	0	0	0	0
2154.6	0	0	0	0
2185.1	0	0	0	0
2214.6	0	0	0	0
2246.1	1	0	0	0
2276.9	1	0	0	0
2310.1	0	0	0	0
2354.6	0	0	0	0
2385.8	0	0	0	0
2424	0	0	0	0
2462.1	0	0	0	0
2500.2	0	0	0	0
2538.7	0	0	0	0
2578.1	0	0	0	0
2617.3	0	0	0	0
2655.6	0	0	0	0
2692.5	0	0	0	0
2742.6	0	0	0	0
2763.7	1	0	0	0
2814.4	0	0	0	0
2858	0	0	0	0
2893.5	0	0	0	0
2930	0	0	0	0
2967	0	0	0	0
3003.3	0	0	0	0
3040.3	0	0	0	0
3076.8	0	0	0	0
3113.2	0	0	0	0
3149.1	0	1	0	0
3185.6	0	0	0	0

Table I-2 Continued

AGE	*Diplopsalid* spp.	*Impagidinium pallidum*	*Ataxiodinium choane*	*Bitectatodinium tepikiense*
3221.8	0	0	0	0
3257.8	0	0	0	0
3293.7	0	0	0	0
3325	0	0	0	0
3352.1	0	0	0	0
3379.4	0	0	0	0
3405.4	0	0	0	0
3430.6	0	0	0	0
3456.1	0	0	0	0
3486.9	0	0	0	0
3522.5	0	0	0	0
3558.7	0	0	0	0
3594.5	0	0	0	0
3630.4	0	0	0	0
3665.8	0	0	0	0
3703.3	0	0	0	0
3738.5	0	0	0	0
3776.1	0	0	0	0
3822	0	0	0	0

Table I-2 Continued

AGE	*Nematosphaeropsis labyrinthus*	*Quinquecuspis concreta*	*Votadinium calvum*	*Selenopemphix quanta*
-65	0	3	0	0
-64.603	0	8	0	0
-63.602	0	7	0	0
-62.601	0	0	0	0
-61.599	0	0	0	0
-60.598	0	1	0	0
-59.53	0	1	1	0
-58.396	0	2	0	0
-57.262	0	0	0	0
-56.128	0	0	0	2
-55.039	0	2	0	0
-53.996	0	0	2	0
-52.952	0	2	0	0
-51.908	0	0	0	0
-50.854	0	0	0	0
-49.706	0	0	0	0
-48.558	0	0	0	0
-47.41	0	0	0	0
-46.357	0	2	0	0
-45.397	0	0	0	0
-44.438	0	0	0	0
-41.171	0	0	0	0
-38.206	0	0	0	0
-35.932	0	0	0	0
-29.888	0	0	0	0
-25.592	0	0	0	0
-21.423	0	0	0	0
-17.542	0	0	0	0
-15.673	0	0	0	0
156.3	0	0	0	0
199.2	0	0	0	0
240.9	0	0	0	0
283.8	0	0	0	0
326.3	0	0	0	0
368.7	0	0	0	0
413	0	0	0	0
455.6	0	0	0	0
498.3	0	0	0	0
540.2	0	0	0	0
581.7	0	0	0	0

Table I-2 Continued

AGE	*Nematosphaeropsis labyrinthus*	*Quinquecuspis concreta*	*Votadinium calvum*	*Selenopemphix quanta*
623.7	0	0	0	0
665.1	0	0	0	0
706.8	0	0	0	0
724	0	0	0	0
766.6	0	0	0	0
808.6	0	0	0	0
852	0	0	0	0
893.7	0	0	0	0
926.9	0	0	0	0
957.6	0	0	0	0
988.75	0	0	0	0
1019.3	0	0	0	0
1050.9	0	0	0	0
1082.1	0	0	0	0
1113.9	0	0	0	0
1145	0	0	0	0
1176.5	0	0	0	0
1208.1	0	0	0	0
1240	0	0	0	0
1272.1	0	0	0	0
1303	0	0	0	0
1333.1	0	0	0	0
1364.1	0	0	0	0
1395.5	0	0	0	0
1427.1	0	0	0	0
1458.8	0	0	0	0
1489.8	0	0	0	0
1521.7	0	0	0	0
1554.1	0	0	0	0
1585.7	0	0	0	0
1618.5	0	0	0	0
1650.1	0	0	0	0
1682.2	0	0	0	0
1713.9	0	0	0	0
1726.9	0	0	0	0
1757.6	0	0	0	0
1789.3	0	0	0	0
1821.4	0	0	0	0
1851.2	0	0	0	0
1881.4	0	0	0	0
1911.4	0	0	0	0

Table I-2 Continued

AGE	*Nematosphaeropsis labyrinthus*	*Quinquecuspis concreta*	*Votadinium calvum*	*Selenopemphix quanta*
1941.4	0	0	0	0
1970.2	0	0	0	0
2000.2	0	0	0	0
2031.4	0	0	0	0
2062.5	0	0	0	0
2093.1	0	0	0	0
2123.7	0	0	0	0
2154.6	0	0	0	0
2185.1	0	0	0	0
2214.6	0	0	0	0
2246.1	0	0	0	0
2276.9	0	0	0	0
2310.1	0	0	0	0
2354.6	0	0	0	0
2385.8	0	0	0	0
2424	0	0	0	0
2462.1	0	0	0	0
2500.2	0	0	0	0
2538.7	0	0	0	0
2578.1	0	0	0	0
2617.3	0	0	0	0
2655.6	0	0	0	0
2692.5	0	0	0	0
2742.6	0	0	0	0
2763.7	0	0	0	0
2814.4	0	0	0	0
2858	0	0	0	0
2893.5	0	0	0	0
2930	0	0	0	0
2967	0	0	0	0
3003.3	0	0	0	0
3040.3	0	0	0	0
3076.8	0	0	0	0
3113.2	0	0	0	0
3149.1	0	0	0	0
3185.6	0	0	0	0

Table I-2 Continued

AGE	*Nematosphaeropsis labyrinthus*	*Quinquecuspis concreta*	*Votadinium calvum*	*Selenopemphix quanta*
3221.8	0	0	0	0
3257.8	0	0	0	0
3293.7	0	0	0	0
3325	0	0	0	0
3352.1	0	0	0	0
3379.4	0	0	0	0
3405.4	0	0	0	0
3430.6	0	0	0	0
3456.1	0	0	0	0
3486.9	0	0	0	0
3522.5	0	0	0	0
3558.7	0	0	0	0
3594.5	0	0	0	0
3630.4	0	0	0	0
3665.8	0	0	0	0
3703.3	0	0	0	0
3738.5	0	0	0	0
3776.1	0	0	0	0
3822	0	0	0	0

I-IV Palynomorphs Counted

Table I-3 Counted Lycopodium clavatum *marker grains, foraminiferal linings and specimens of* Halodinium *spp. in BC4 and Casq1*

AGE	Foraminiferal Linings	*Halodinium* spp.	*Lycopodium clavatum*
-65	368	64	490
-64.603	473	26	191
-63.602	394	30	121
-62.601	309	54	113
-61.599	484	98	170
-60.598	248	48	138
-59.53	434	321	95
-58.396	383	529	160
-57.262	483	763	135
-56.128	459	260	102
-55.039	306	432	107
-53.996	291	375	101
-52.952	402	297	108
-51.908	213	142	142
-50.854	235	259	104
-49.706	169	156	101
-48.558	255	223	155
-47.41	262	275	105
-46.357	246	95	102
-45.397	206	73	111
-44.438	281	473	100
-41.171	241	104	115
-38.206	402	100	100
-35.932	385	268	109
-29.888	418	177	103
-25.592	623	434	116
-21.423	269	227	122
-17.542	296	460	117
-15.673	208	221	137
156.3	14	7	35
199.2	28	11	72
240.9	20	6	42
283.8	28	10	85
326.3	18	8	33
368.7	30	13	109
413	20	14	83
455.6	26	17	81
498.3	58	37	131
540.2	13	7	63
581.7	16	14	35
623.7	18	10	37

Table I-3 Continued

AGE	Foraminiferal Linings	*Halodinium* spp.	*Lycopodium clavatum*
665.1	16	7	61
706.8	12	13	56
724	16	10	38
766.6	15	5	63
808.6	52	22	107
852	27	20	64
893.7	15	4	42
926.9	32	15	84
957.6	10	11	51
988.75	33	16	39
1019.3	13	10	47
1050.9	14	5	44
1082.1	18	11	39
1113.9	23	13	47
1145	33	11	68
1176.5	14	9	64
1208.1	20	9	44
1240	14	9	57
1272.1	64	25	67
1303	17	3	43
1333.1	14	5	49
1364.1	11	19	39
1395.5	43	13	87
1427.1	35	15	84
1458.8	8	13	55
1489.8	18	12	51
1521.7	25	9	38
1554.1	22	16	71
1585.7	16	17	51
1618.5	22	12	54
1650.1	18	7	56
1713.9	15	9	34
1726.9	5	14	46
1757.6	10	12	55
1789.3	26	18	68
1821.4	27	12	52
1851.2	19	14	57
1881.4	57	32	115
1911.4	15	31	123
1941.4	16	8	69
1970.2	11	19	65
2000.2	22	10	66
2031.4	17	14	55

Table I-3 Continued

AGE	Foraminiferal Linings	*Halodinium* spp.	*Lycopodium clavatum*
2062.5	13	16	55
2093.1	44	34	169
2123.7	13	11	61
2154.6	9	20	41
2185.1	12	10	49
2214.6	10	7	41
2246.1	34	22	121
2276.9	35	13	108
2310.1	5	13	55
2354.6	10	10	66
2385.8	28	10	58
2424	20	13	58
2462.1	29	11	61
2500.2	19	11	70
2538.7	16	14	63
2578.1	9	13	43
2617.3	19	12	47
2655.6	16	5	70
2692.5	8	10	45
2742.6	15	4	44
2763.7	80	47	279
2814.4	16	17	65
2858	5	7	67
2930	27	6	103
2967	37	27	165
3003.3	12	6	58
3040.3	38	11	42
3076.8	16	6	82
3113.2	7	4	57
3149.1	48	33	120
3185.6	37	22	97
3221.8	10	10	45
3257.8	9	1	43
3293.7	19	5	50
3325	16	12	70
3352.1	22	14	55
3379.4	14	12	33
3405.4	45	23	134
455.6	26	17	81
3456.1	17	16	81
3486.9	10	13	39
3522.5	46	33	164

Table I-3 Continued

AGE	Foraminiferal Linings	*Halodinium* spp.	*Lycopodium clavatum*
3558.7	20	5	56
3594.5	11	8	58
3630.4	45	32	147
3665.8	23	10	41
3703.3	12	5	79
3738.5	13	8	65
3776.1	9	10	69
3822	21	11	63

I-V MAT Summer Reconstructions for Casq1 and BC4

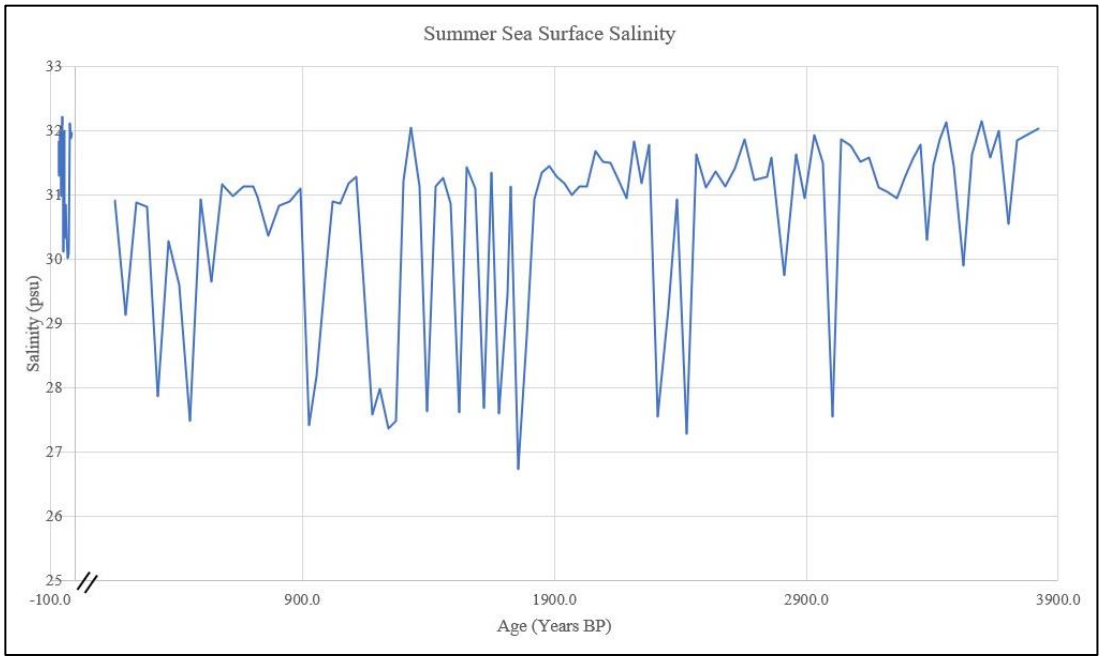


Figure I-2 MAT reconstructed sea-surface salinity through time, note the hiatus at ca. 156 years BP.

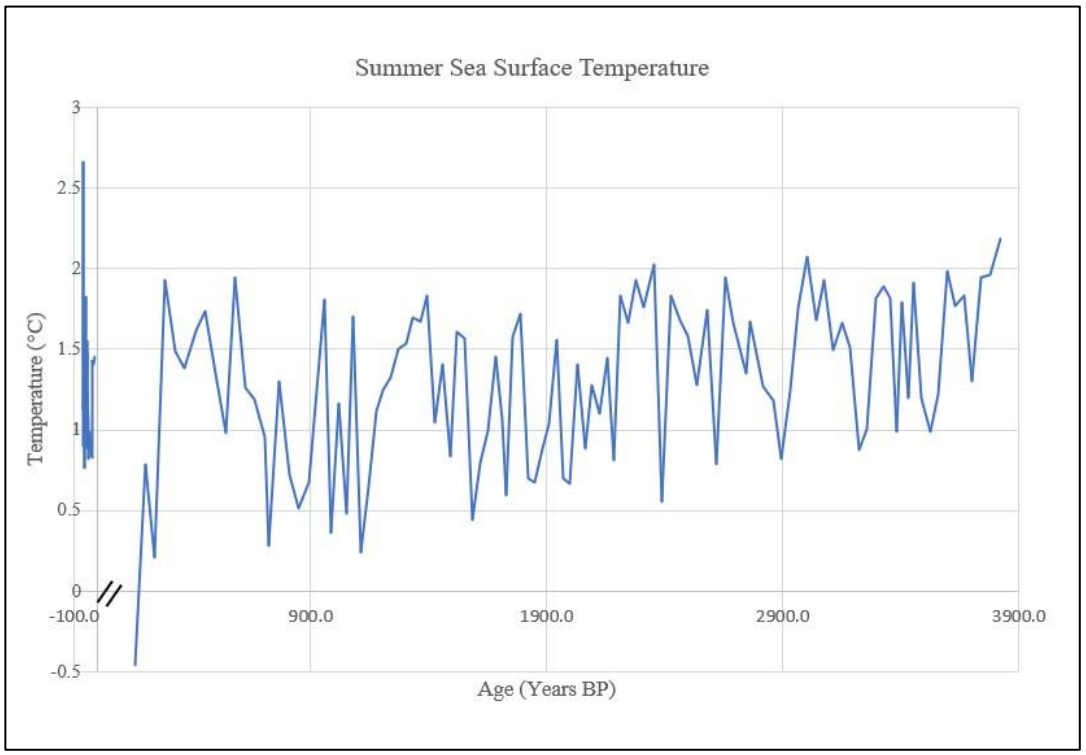


Figure I-3 MAT reconstructed sea-surface temperature through time, note the hiatus at ca. 156 years BP.

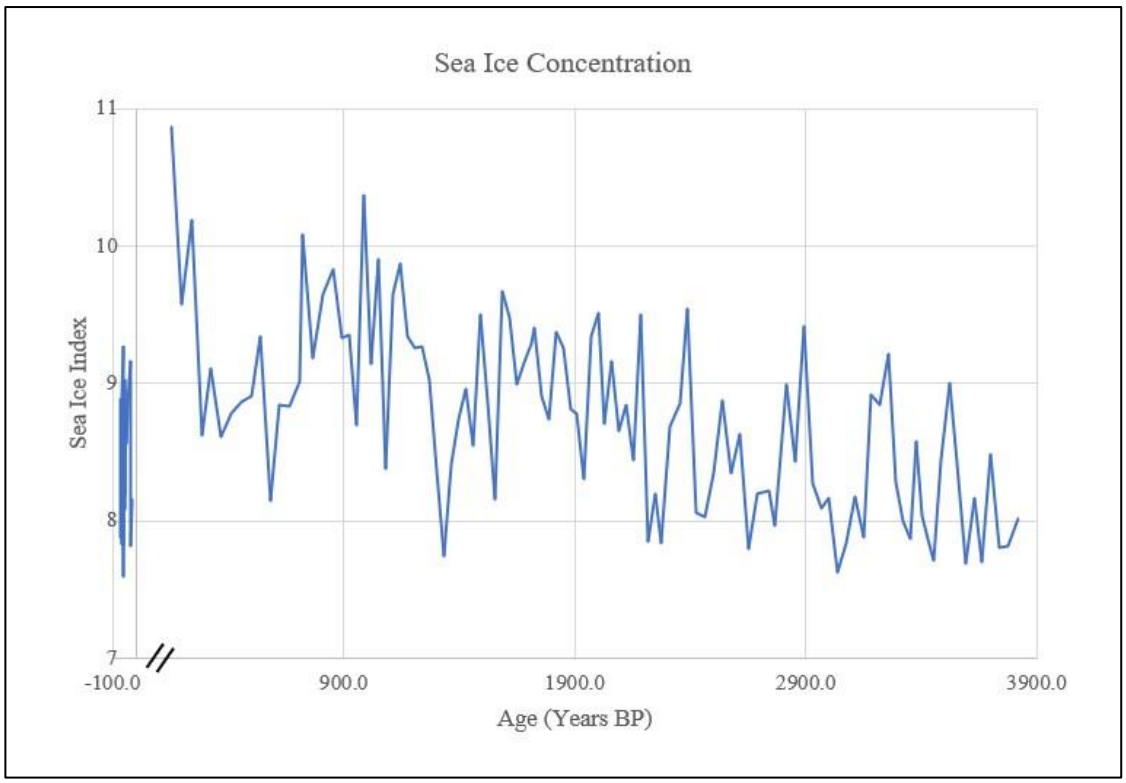


Figure I-4 MAT reconstructed sea ice concentration through time, where the sea ice index represents the number of months with > 50% sea ice cover. Note the hiatus at ca. 156 years BP.

I-VI References

Frontier, S. 1976. Decrease of eigenvalues in principal component analysis-comparison with broken stick model. Journal of Experimental Marine Biology and Ecology 25, 67-75.

Hammer, Ø., Harper, D.A.T., Ryan, P.D., 2001. Past: Paleontological Statistics Software Package for Education and Data Analysis 9.

Heslop, D., De Schepper, S., Proske, U., 2011. Diagnosing the uncertainty of taxa relative abundances derived from count data. Marine Micropaleontology 79, 114–120. https://doi.org/10.1016/j.marmicro.2011.01.007

Jackson, D.A., 1993. Multivariate analysis of benthic invertebrate communities: the implication of choosing particular data standardizations, measures of association, and ordination methods. Hydrobiologia 268, 9. https://doi.org/10.1007/BF00005737

Jolliffe, I.T., Cadima, J., 2016. Principal component analysis: a review and recent developments. Philosophical Transactions of the Royal Society A: Mathematical, Physical and Engineering Sciences 374, 20150202. https://doi.org/10.1098/rsta.2015.0202

May, W.L., Johnson, W.D., 2000. Constructing two-sided simultaneous confidence intervals for multinomial proportions for small counts in a large number of cells. Journal of Statistical Software 005.

Sison, C.P., Glaz, J., 1995. Simultaneous Confidence Intervals and Sample Size Determination for Multinomial Proportions. Journal of the American Statistical Association 90, 366–369. https://doi.org/10.1080/01621459.1995.10476521

Curriculum Vitae

Candidate's full name: Kelsey Amber Koerner

Universities attended:

University of New Brunswick (2018-2020): MSc. Earth Sciences

University of New Brunswick (2014-2018): BSc. Earth Sciences, Honours

Simon Fraser University (2012-2013)

Awards:

2020: Bourse d'excellence de doctorat – Institut des sciences de la mer – Université du Québec à Rimouski

2020: American Association of Stratigraphic Palynologists -The Palynological Society (AASP-TPS) Student Research Award

2020: Rodney M. Feldmann Student Research Award – The Paleontological Society

2020: Honorable Mention – Sandra Barr Award for Best Graduate Oral Presentation – Atlantic Geoscience Society 46th Colloquium

2020: Dr. W.J. Wright Graduate Fellowship

2019: 2nd Best Poster Award – Girls STEM UP: Discovery

2019: Northern Scientific Training Program

2018: CIM Award of Excellence

2018: NBIF STEM & Social Innovation Award

2018: Mineralogical Association of Canada Undergraduate Student Award

2017: Edwin Jacob Special University Scholarship

2017: Gerry Govett Geoscience Scholarship

2017: CSPG Undergraduate Student Scholarship

2016: Lowell Trembath Memorial Award

Publications & Presentations:

Atlantic Geoscience Society 46th Colloquium – Oral Presentation: *Late Holocene sea surface cooling in the North Water region, northern Baffin Bay* – Truro, NS – Feb. 7th to 8th, 2020

Girls STEM Up: Discovery – Poster Presentation: *Changes in sea surface conditions and dinoflagellate cyst productivity in the North Water (NOW) polynya over the last ca. 4000 years* – Fredericton, NB – Nov. 23rd, 2019

ArcTrain Annual Student Meeting – Poster/ Oral Presentation: *Changes in sea surface conditions and dinoflagellate cyst productivity in the North Water (NOW) polynya over the last ca. 4000 years* – Rimouski, QC – Sept. 16th to 20th, 2019

Annual Geotop Student Meeting – Poster Presentation: *Changements dans la productivité des kystes de dinoflagellés dans la polynie des eaux du Nord, au cours des derniers 4000 ans* – Orford, QC – March 22nd to 24th, 2019

Atlantic Geoscience Society 45th Colloquium – Oral Presentation: *Changes in dinoflagellate cyst productivity in the North Water (NOW) polynya during the past ca. 4000 years* – Fredericton, NB– Feb. 7th to 9th, 2018

Atlantic Geoscience Society 44th Colloquium – Poster Presentation: *Changes in sedimentation and primary productivity in the North Water (NOW) Polynya in the last ca. 3500 years* – Truro, NS – Feb. 2nd to 3rd, 2018

Atlantic Universities Geoscience Conference – Oral Presentation: *Changes in primary production and sedimentation in the North Water (NOW) Polynya during the past ca. 3500 years* – St. John's, NL – Oct. 26th to 28th, 2017